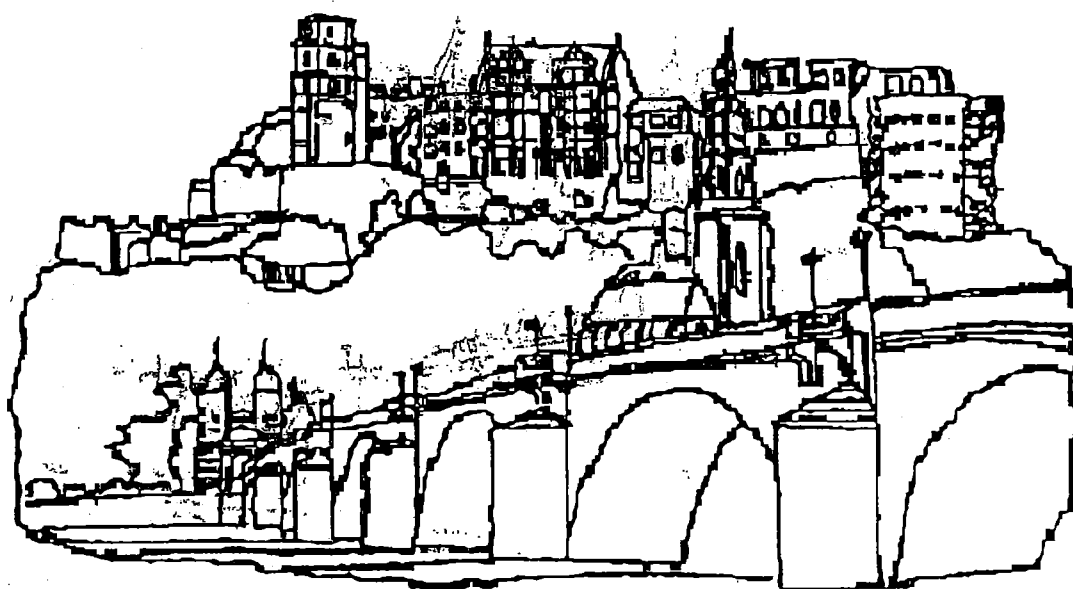


**2nd International Conference on
Magnetic Resonance Microscopy**
(The Heidelberg Conference)



**September 6 - 9, 1993
Heidelberg, Germany**

2nd International Conference on Magnetic Resonance Microscopy

The Heidelberg Conference

Heidelberg, September 6 - 9, 1993

Welcome to the 2nd International Conference on Magnetic Resonance Microscopy in Heidelberg. Essential features of this conference are:

- **Registration and conference activities take place at the Max-Planck-Haus, D-69120 Heidelberg, Berliner Str. 10 (300 m North of the Ernst-Walz bridge across the Neckar river).**
- **The registration desk is open during the entire conference: Sunday, Sept. 6: 16.00 - 20.00 o'clock, Mon. - Wed.: 9.00 - 18.00 o'clock, Thurs.: 8.30 - 13.00 o'clock.**
- **The posters are on display during the entire conference. There is an informal poster viewing on Sunday evening from 20.00 to 22.00 o'clock.**
- **A welcome cocktail party is given on Sunday from 19.00 to 20.00 o'clock in the mensa of the Max-Planck-Haus.**
- **Companies will exhibit their products in the Max-Planck-Haus during the meeting.**
- **The financial support of the vendors and industrial companies is gratefully acknowledged. It enables the participation of many students and colleagues in this conference who could not participate without financial support.**

Winfried Kuhn and Bernhard Blümich

Sponsors of the 2nd International Conference on Magnetic Resonance Microscopy

The organizers of the 2nd International Conference on Magnetic Resonance Microscopy would like to thank the following sponsors for their support

Deutsche Forschungsgemeinschaft (DFG), Bonn, Germany

Bruker Analytische Meßtechnik GmbH, Rheinstetten, Germany

Varian GmbH, Darmstadt, Germany

Otsuka Electronics Europe SARL, Strasbourg, France

Fraunhofer Institut für Biomedizinische Technik, St. Ingbert, Germany

Max-Planck-Institut für Polymerforschung, Mainz, Germany

Max-Planck-Institut für Medizinische Forschung, Heidelberg, Germany

SMIS, Guildford, United Kingdom

Tecmag, Houston, USA

Promochem, Wesel, Germany

Wemhöner & Popp, Aachen, Germany

SmithKline Beecham, King of Prussia, USA

Spintec, Remshalden, Germany

Boehringer Ingelheim KG, Ingelheim, Germany

JWC Scientific, Gateshead, England

BASF, Ludwigshafen, Germany

Verlag Chemie VCH, Weinheim, Germany

Springer Verlag, Heidelberg, Germany

Transportation in Heidelberg

Heidelberg has an excellent public transportation system. The Max-Planck-Haus is located about 300 m North of the Ernst-Walz-Bridge across the Neckar river. Most hotels are South of the river. The Max-Planck-Haus can be reached by

- Bus 12, passing "Bismarck-Platz". Exit bus at "Bunsen-Gymnasium", at the corner of Berliner Strasse / Mönchhofstrasse. Turn South to the Max-Planck-Haus.
- Bus 33 passing "Bismarck-Platz" and "Hauptbahnhof". Exit bus at first stop after the bridge ("Chirurgische Klinik").
- Tram 1, passing "Bismarck-Platz" and "Hauptbahnhof". Exit at first stop after the bridge ("Chirurgische Klinik"). Continue North to the Max-Planck-Haus.
- Tram 4, passing "Hauptbahnhof". Exit at first stop after the bridge ("Chirurgische Klinik"). Continue North to the Max-Planck-Haus.

If your hotel is not close to any of these lines, connect to bus 12 or tram 1 at "Bismarck-Platz" or to buses 12, 33 or trams 1, 4 at "Hauptbahnhof". Tickets are available from the conductor in the bus or tram and from ticket machines located at "Bismarck-Platz" and "Hauptbahnhof".

Eating and Drinking

Heidelberg has many restaurants, especially in the old part of the town. They tend to be very crowded in the evenings. The conference participants are encouraged to have lunch and dinner in the cafeteria of the Max-Planck-Haus. Tickets are available at the registration desk. Prices are DM 8.- for lunch and DM 10.- for dinner.

Conference Guide:

Notebook: Abstracts for talks and posters appear in two separate sections. The Author Index references the program code and the page on which the abstract appears. An update to the directory will be provided during the conference.

Location of Sessions: All talks are held in the lecture hall on the upper level. The posters are on display in the *Sitzungszimmer* on the same floor.

Speakers and Session Chairs: Please arrive 15 - 30 min. before your session to familiarize yourself with each other and with the audiovisual system. If using slides, please give them to the projectionist at least 30 minutes before the session begins.

Posters: All posters will be on display throughout the conference. Posters may be mounted beginning Sunday afternoon, 16.00 o'clock. Posters may be viewed informally on Sunday from 20.00 to 22.00 o'clock. All posters must be up by Monday noon. The poster abstracts are in the POSTERS section of this notebook. They are arranged in the same order as the session topics.

Conference Refreshments: There is one coffee break in the morning and one in the afternoon sessions. The refreshments are sponsored by the companies supporting the conference.

Welcome Cocktail: There is a welcome cocktail on Sunday from 19.00 to 20.00 o'clock in the mensa of the Max-Planck-Haus.

Conference Dinner: The conference dinner will be given in the Faßkeller of the Heidelberger Schloß (Castle) on Wednesday at 19.00 o'clock. Tickets can be purchased for DM 50.- at the registration desk.

Regulations:

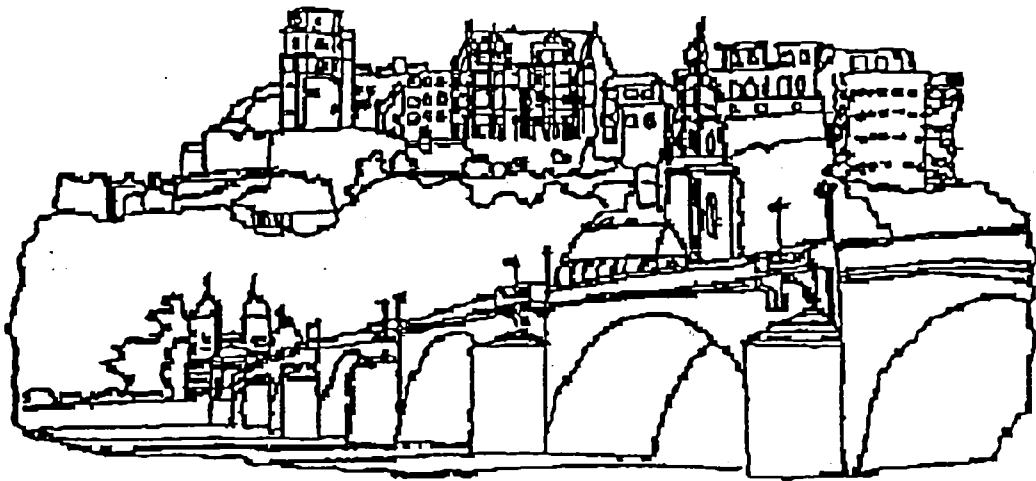
- No smoking in the lecture hall or in the posters room.
- Registration badges must be worn during all conference activities.



2nd International Conference on Magnetic Resonance Microscopy

(The Heidelberg Conference)

Program



September 6 - 9, 1993
Heidelberg, Germany

Sunday, Sept. 5, 1993

16.00 - 19.00 Registration

Educational Session (Chair: J. L. Ackerman)

- 13.00 **Basics of NMR**
R. Komoroski
- 14.00 **Solid State NMR I**
Multipulse NMR
U. Haeberlen
- 15.00 **Solid State NMR II**
Magic Angle Sample Spinning
R. Andrew
- 16.00-16.30 **Coffee Break**
- 16.30 **Imaging I (Basics, Methods)**
J. L. Ackerman
- 17.30 **Imaging II (Flow, Diffusion)**
P. T. Callaghan
- 18.30 **Electron Spin Resonance**
L. Berliner
- 19.30 **Welcome Cocktail**

Monday, Sept. 6, 1993

Opening (Chair: U. Haerberlen)

- 9.00 **Opening Remarks**
W. Kuhn
- 9.15 **Advances in NMR Microscopy at 500 MHz**
*Sir P. Mansfield, R. W. Bowtell, A. Peters, J. C. Sharp, P. M. Glover,
S. J. Blackband, Nottingham*

Methods I (Chair: B. Maraviglia)

- 10.00 **Technical Aspects of Microspectroscopy at High Fields**
*S. Crozier, Stephen Rose, Wolfgang Hoffmann, Paul Hockings, Stephen
Wilson, David M. Doddrell, Brisbane*
- 10.45 **Magnetic Resonance Detection and Imaging Using Force Microscope
Techniques**
Dan Rugar, San Jose
- 11.15 - 11.45 **Coffee Break**
- 11.45 **Toward Ultra Resolution NMR Microscopy**
Paul C. Lauterbur, W. Brian Hyslop and H. Douglas Morris, Urbana
- 12.00 **NMR Microscopy by Radio-Frequency Field Gradients**
D. Canet, P. Maffei, P. Mutzenhardt, R. Raulet and J. Brondeau, Nancy
- 12.15 **Methods for Reconstruction Slice Profiles in Magnetic Resonance Imaging;
Visualization of the Performance of Self-Refocusing Pulses**
*P. Devoulon, L. Emsley, P. Weber, R. Meuli, M. Decorps and G. Bodenhausen,
Lausanne*
- 12.30 **Spin Relaxation in the Vicinity of Susceptibility Boundaries**
Lucy C. Forde and Paul T. Callaghan, Palmerston North
- 12.45 **MR Microscopy of Electric Currents**
I. Sersa, O. Jarh, J. Seliger, and F. Demsar, Ljubljana
- 12.50 **Spatially Resolved One- and Two-Dimensional MAS-NMR Microscopy**
U. Scheler, B. Blümich and H. W. Spiess, Mainz
- 12.55 **Magic Echo Solid Imaging in Two and Three Dimensions**
Peter Barth, Siegfried Hafner and Winfried Kuhn, St. Ingbert
- 13.00 - 14.30 **Lunch**

Methods II (Chair: L. Berliner)

- 14.30 **High Resolution EPR Microscopy**
Sandra Eaton, Denver
- 15.15 **Radiofrequency FT-EPR Spectroscopy and Imaging**
*Sankaran Subramanian, John Bourg, Murali C. Krishna, and James B. Mitchell,
Bethesda*
- 15.30 **In Vivo ESR Studies of the Metabolic Fate of Nitrosobenzene in the Mouse**
H. Fujii, B. Zhao, J. Koscielniak and Lawrence J. Berliner, Columbus
- 15.45-16.15 **Coffee Break**

Materials I (Chair: H. W. Spiess)

- 16.15 **Broad-Line MRI and Fluid Ingress in Polymeric Materials**
M. R. Halse, H. J. Rahman and J. H. Strange, Canterbury
- 17.00 **Imaging of Elastomers and Ion Exchanging Systems**
W. M. Ritchey, L. Maylish, A. Wallner and P. Smith, Cleveland
- 17.30 **NMR Microimaging of Flow in Porous Materials**
J. Weis, H.-P. Müller and R. Kimmich, Ulm
- 17.45 **Spatially Resolved NMR for Materials Science**
B. Blümich, C. Fülber, U. Scheler, H. W. Spiess, F. Weigand, Mainz
- 18.00 **Micro-MRI as a tool for characterization of foams based on polyvinylalcohol-formaldehyde and phenol-formaldehyde resins**
Monique Ercken, I. Pollers, P. Adriaensens, R. Carleer, D. Vanderzande and Jan Gelan, Diepenbeek
- 18.15 **Fast Imaging of Porous Media**
J. M. Dereppe, C. Moreaux and R. Demeure, Louvain
- 18.20 **Improved Spatial Resolution in Lee-Goldburg Magic Angle Imaging of Solids**
F. de Luca, N. Luger, F. Di Nunzio, B. Maraviglia, Rom
- 18.25 **MR Microimaging Studies of the Imhibition of Miscible Liquids by Dense Polymers and Resin Matrix Composites**
S. N. Scrimgeour, C. H. Lloyd, J. A. Chudek and G. Hunter, Dundee
- 19.00 **Dinner**
- 20.00-21.00 **Poster Session**

Tuesday, Sept. 7, 1993

Materials II (Chair: E. R. Andrew)

- 9.00 **The Application of Gradient NMR Techniques to Wetting and Drying Processes in Porous Media**
G. Nesbitt, Amsterdam
- 9.30 **NMR Microscopy in Metals with sub- μ m Resolution**
G. Neue, Th. Geilke, Dortmund
- 9.45 **Solid State NMR Imaging Using Strong Gradients (STRAFI)**
Klaus Zick, Karlsruhe
- 10.00 **Molecular Dynamics of Polymer Networks as Studied by NMR Microscopy**
Winfried Kuhn, Siegfried Hafner, Peter Barth and Paul Denner, St. Ingbert & Erfurt
- 10.15 **Use of Magnetic Resonance Microimaging for the Measurement of the Depth of the Cure for VLC Dental Composite Filling Materials**
C. H. Lloyd, S. N. Scrimgeour, J. A. Chudek, R. L. Mackay, G. Hunter, D. Pananakis and W. Abel, Dundee
- 10.20 **Demonstration of the Linear Dependence of Magnetization Transfer on Polymer Concentration in Aqueous Solutions at Two Different Field Strength**
J. J. Tessier, T. A. Carpenter, J. A. Tyler and L. D. Hall, Cambridge
- 10.25 **Dynamical and Structural Parameters of Polymer Networks as Studied by Parameter-Selective NMR Microscopy**
G. Simon, H. Schneider*, P. Barth, S. Hafner and W. Kuhn, *Halle & St. Ingbert*
- 10.30-11.00 **Coffee Break**

Biomedicine I (Chair: W. E. Hull)

- 11.00 **NMR Microscopy in Biomedicine**
Laurel O. Sillerud, Los Alamos
- 11.45 **NMR Microscopy in Pharmaceutical Research**
Susanta Sarkar and Rasesh D. Kapadia, King of Prussia
- 12.15 **Spatial Heterogeneity of Macromolecular-Water Interactions in Human Articular Cartilage**
E. McFarland, M. Dunham and H. Dai, Santa Barbara
- 12.30 **NMR Microscopy on the Human Body**
J. C. Széles, M. Grabenwöger, M. Grimm, C. Leukauf, E. Feichtinger, S. Mészáros, Wien & Budapest
- 12.45 **Cyclocreatine Toxicity in Multicellular Tumor Spheroids: 31 P-NMR Spectroscopy and Diffusion NMR Microscopy**
Y. Steinfeld, G. Meir, C. Tempel, M. Neeman and M. Cohn, Rehovot & *Philadelphia*
- 13.00 **Lunch**

Biomedicine II (Chair: L. D. Hall)

- 14.30 **High Resolution NMR Microscopy of the Perfused Rat Kidney**
William E. Hull, Heidelberg
- 15.00 **Tumor Architecture and Physiology: a Chronological Approach using 19F 3D-NMR Microscopy of Perfluorocarbons**
Ralph P. Mason, Anca Constantinescu and Peter P. Antich, Houston, Peter Peschke and Eric W. Hahn, Heidelberg
- 15.15 **Magnetic Resonance Histology**
G. Allan Johnson, Robert D. Black, Gary P. Cofer, Xiaohong Zhou, Robert R. Maronpot, Durham
- 15.30 **¹H and ³¹P Spectroscopic Imaging Study of 9L Brain Tumor**
M. Szayna, P. Koszowski, J. K. Saunders and A. Jasinski, Ottawa & Cracow
- 15.45 **Self Diffusion of Water in Cartilage as Studied by NMR Microscopy**
C. Raible, F. Grinberg, Y. Morita and K. Gersonde, St. Ingbert
- 15.50 **Depiction of Dental Anatomy by Magnetic Resonance Microscopy**
Michael A. Baumann, Dieter Groß and Volker Lehmann, Mainz & Rheinstetten
- 15.55 **MR Microscopy Study of Honey Bee in vivo**
Z. Sulek, A. Jasinski, B. Tomanek, F. Hennel, J. Kibinski, T. Skorka, A. Krzyzak, P. Kulinowski and J. Muszynska, Krakow & Pulawy
- 16.00 **NMR Microscopy Detection of Different Grades of Hydration and Chemical Composition Inside of Degenerative Changed Articular Cartilage**
W. Gründer, M. Wagner, M. Biesold, Leipzig
- 16.05 **High-Field MRI of the Human Medulla Oblongata as a Research Method in Neuropathology**
M. Vandersteen, P. Adriaensens, E. Beuls, J. Gelan, L. Vanormelingen, Y. Palmers**, G. Freling**, Diepenbeek, *Maastricht, **Genk*
- 16.10 **Evaluation of the Spatial Distribution of Ethanol in the Human Brain by ¹H-NMR Spectroscopic Imaging**
G. Schauf, H. Schild, M. Thelen, Mainz
- 16.15 Coffee Break

Commercial Perspectives (Chair: J. H. Strange)

- 16.45 **NMR Spectrometer Design: Philosophy and Architecture**
Victor Bartuska, Chemagnetics, Strasbourg
- 17.10 **Title: Unknown**
Dieter Groß, Bruker, Rheinstetten
- 17.30 **Advances in High Gradient/Field Microimaging**
Evan Williams, Varian, Palo Alto
- 17.50 **Manipulation of Suszeptibility Effects in NMR Microscopy by Tailored RF**
Z. H. Cho, Irvine
- 19.00 Dinner
- 20.00 - 21.30 Poster Session

Wednesday, Sept. 8, 1993

Diffusion and Flow (Chair: P. T. Callaghan)

- 9.00 **Quantifying Mass Transport with Magnetic Resonance Imaging**
L. D. Hall, T. A. Carpenter, G. Amin, B. J. Balcom, J. A. Derbyshire, A. E. Fisher, S. J. Gibbs, A. D. Parker, K. Potter, D. Xing, Cambridge
- 9.45 **Patterns and Images of Flows and Vortices of Simple and Complex Fluids**
J. D. Grutzner, West Lafayette
- 10.15 **General Treatment of Diffusion in the Presence of Boundaries and Short or Long Gradient Pulses**
L. Z. Wang, A. Caprihan and Eüchi Fukushima, Albuquerque
- 10.30 **Quantification of Unrestricted Diffusion in NMR Microscopy**
M. Brandl, A. Link and A. Haase, Würzburg
- 10.45 **Diffusion and Suszeptibility Effects in NMR Microscopy**
Paul T. Callaghan, Palmerston
- 11.00 **Diffusion in Heterogeneous and Anisotropic Media as Studied by Pulsed Field Gradient NMR and Microimaging**
Farida Grinberg, Peter Barth, Siegfried Hafner and Winfried Kuhn, St. Ingbert
- 11.05 **Flow in Polymer Solutions Measured by Dynamic NMR Microscopy**
Craig J. Rofo, Rodney K. Lambert, Lourdes de Vargas and Paul T. Callaghan, Palmerston and *Mexico*
- 11.10 **Localized Diffusion Measurements with a Single B_1 Gradient**
E. Mischler, F. Humbert, and D. Canet, Nancy
- 11.15 Coffee Break

Progress in Medical Imaging (Chair: A. Haase)

- 11.45 **Short Overview**
Axel Haase, Würzburg
- 12.00 **MR Imaging and Spectroscopy at High Fields**
Kamil Ugurbil, Minneapolis
- 13.00 Lunch
- 19.00 **Conference Dinner in the *Faßkeller* of the Castle of Heidelberg (Faßkeller des Heidelberger Schlosses)**
- From Molecular Beams to Microimaging: Some Highlights in the Evolution of NMR**
 After Dinner Speaker: *Edwin D. Becker, Bethesda*

Thursday, Sept. 9, 1993

Plants and Agriculture (Chair: J. Pope)

- 9.00 **Functional NMR Imaging of Plants**
H. van As, Wageningen
- 9.45 **Molecular Motion and Nuclear Relaxation in Intact Biomaterials**
Thomas M. Eads, West Lafayette
- 10.15 **A Comparison of Water Self-Diffusion in Fresh and Stored Beans**
E. J. Kendall, D. W. Stanley and K. B. Chatson, Saskatoon
- 10.30 **In-Vivo Magnetic Resonance Microscopy for Non-Destructively Investigating Plants, Fruits, Vegetables and Small Animals**
S. Crestana, R. Kauten and D. R. Nielsen*, Sao Carlos & *Davis*
- 10.45 **NMR Microimaging in Meat Research**
J. M. Tingle, V. Sarafis, P. A. Baumgartner and J. M. Pope, Hawkesbury & *Kensington*
- 11.00 **Determination of the Vascular Architecture of the Raspberry Receptacle Through the Use of 3D Surface Rendering Techniques**
J. A. B. Lohman, J. A. Chudek, B. A. Goodman, G. Hunter and B. Williamson, *Coventry & Dundee*
- 11.05 **Development of Infection in a Strawberry Fruit by the Fungal Pathogen Botrytis cinerea**
B. Williamson, J. A. Chudek, G. Hunter, R. L. MacKay and B. A. Goodman, Dundee
- 11.10 **Axial- and Radial Water Transport in Ricinus Communis Seedlings Observed by Gradient Echo Deuterium Imaging**
A. Metzler, W. Köckenberger, E. Komor*, A. Haase, Würzburg & *Bayreuth*
- 11.15 Coffee Break

Rare Isotopes (Chair: G. D. Mateescu)

- 11.45 **Direct and Indirect Imaging Methods for the Isotopes of Boron, Nitrogen and ¹³C**
E. W. Randall, London
- 12.15 **Solid State NMR in Living Subjects**
J. L. Ackerman, L. Garrido, Martin J. Liszak, B. Pfeleiderer and Y. Wu, Boston
- 12.45 **Combined Oxygen-17/Phosphorus-31 MRI and MRS: A New Dimension in Cell Bioenergetics Research**
Gheorghe D. Mateescu, Cleveland
- 13.00 **Sensitive Detection of H₂¹⁷O via Proton MRI**
Itamar Ronen and Gil Navon, Tel Aviv
- 13.15 Lunch
- 14.30 Discussion
- 15.30 Conference End

Advances in NMR Microscopy at 500 MHz

P. Mansfield, R. W. Bowtell, A. Peters, J. C. Sharp, P. M. Glover, S. J. Blackband

Lectures and Postertalks

Methods

MET 1

Microvoxel Spectroscopy - Techniques, Technologies and Limitations

S. Crozier, D. Doddrell

MET 2

Magnetic Resonance Detection and Imaging Using Force Microscope Techniques

Dan Rugar

MET 3

Toward Ultra Resolution NMR Microscopy

Paul C. Lauterbur, W. Bryan Hyslop and H. Douglas Morris

MET 4

NMR Microscopy by Radio-Frequency Field Gradients

D. Canet, P. Maffei, P. Mutzenhardt, R. Raulet, J. Brondeau

MET 5

Methods for Reconstruction Slice Profiles in Magnetic Resonance Imaging; Visualisation of the Performance of Self-Refocusing Pulses

Philippe Devoulon, Lyndon Emsley, Peter Weber, Reto Meuli, Michel Decorps and Geoffrey Bodenhausen

MET 6

Spin Relaxation in the Vicinity of Susceptibility Boundaries

Lucy C. Forde and Paul T. Callaghan

MET 7

MR Microscopy of Electric Currents

I. Sersa, O. Jarh, J. Seliger, F. Demsar

MET 8

Spatially Resolved One- and Two-Dimensional MAS NMR-Spectroscopy

U. Scheler, B. Blümich and H. W. Spiess

MET 9

Magic Echo Solid Imaging in Two and Three Dimensions

S. Hafner, P. Barth, and W. Kuhn

EPR 1

High Resolution EPR Microscopy

*Sandra S. Eaton, Gareth R. Eaton, Minoru Sueki***EPR 2**

Radiofrequency FT-EPR Spectroscopy and Imaging

*Sankaran Subramanian, John Bourg, Murall C. Krishna, James B. Mitchell***EPR 3**

In Vivo ESR Studies of the Metabolic Fate of Nitrosobenzene in the Mouse

Hirotaada Fujii, Baolu Zhao, Janush Koscielniak, Lawrence Berliner

Materials

MAT 1

Broad Line MRI and Fluid Ingress in Polymeric Materials

*M. R. Halse, H. J. Rahman, J. H. Strange***MAT 2**

Imaging of Elastomers & Ion Exchange Resins

*W. M. Ritchey, L. Maylish, A. Wallner, P. Smith***MAT 3**

NMR Microimaging of Flow in Porous Materials

*J. Weis, H.-P. Müller and R. Kimmich***MAT 4**

Spatially Resolved NMR for Materials Science

*B. Blümich, C. Fulber, U. Scheler, H. W. Spiess, F. Weigand***MAT 5**

Micro-MRI as a Tool for Characterization of Foams Based on Phenol-Formaldehyde and Polyvinylalcohol-Formaldehyde Resins

*M. Ercken, P. Adriaensens, I. Pollers, D. Vanderzande, and J. Gelan***MAT 6**

Fast Imaging of Porous Media

*J. M. Dereppe, C. Moreaux, R. Demeure***MAT 7**

Improved Spatial Resolution in Lee-Goldburg Magic Angle Imaging of Solids

*F. De Luca, N. Luger, F. Di Nunzio, B. Maraviglia***MAT 8**

MR microimaging studies of the inhibition of miscible liquids by dense polymers and resin matrix composites

S. N. Scrimgeour, C. H. Lloyd, J. A. Chudek, G. Hunter

MAT 9

The Application of Gradient NMR Techniques to Wetting and Drying Processes in Porous Media

G. J. Nesbitt

MAT 10

NMR Microscopy in Metals with Sub-Micrometer Resolution

G. Neue, Th. Geilke, U. Skibbe

MAT 11

Solid State NMR Imaging Using Strong Gradients (STRAFI)

Klaus Zick

MAT 12

Spatially Resolved Investigations of the Molecular Dynamics of Elastomeric Networks

W. Kuhn, P. Denner, G. Simon, P. Barth, S. Hafner

MAT 13

Use of MR Microimaging for the Measurement of the Depth of Cure for VLC Dental Composite Filling Materials

C. H. Lloyd, S. N. Scrimgeour, J. A. Chudek, R. L. Mackay, G. Hunter, D. Pananakis, E. W. Abel

MAT 14

Demonstration of the linear dependence of magnetisation transfer on polymer concentration in aqueous solutions at two different field strengths

J. J. Tessier, T. A. Carpenter, J. A. Tyler and L. D. Hall

MAT 15

Dynamical and Structural Parameters of Polymer Networks - a Local Study by Parameter-Selective NMR Microimaging

G. Simon, H. Schneider, P. Barth, S. Hafner, W. Kuhn

Biomedicine

BIO 1

NMR-Microscopy in Biomedicine

Laurel O. Sillerud

BIO 2

NMR Microscopy in Pharmaceutical Research

Susanta K. Sarkar and Rasesh D. Kapadia

BIO 3

Spatial Heterogeneity of Macromolecular-Water Interactions in Human Articular Cartilage

E. McFarland, M. Dunham, H. Dai

BIO 4

NMR Microscopy on the Human Body

J. C. Szeles, M. Grabenwoger, M. Grimm, C. Leukauf, E. Feichtinger, S. Meszaros

BIO 5

Cyclocreatine toxicity in multicellular tumor spheroids: ³¹P NMR spectroscopy and diffusion NMR microscopy

Y. Steinfeld, G. Meir, C. Tempel, M. Neeman, M. Cohn

BIO 6

High-Resolution NMR Microscopy of the Perfused Rat Kidney

William E. Hull

BIO 7

Tumor Architecture and Physiology: a Chronological Approach using ¹⁹F 3D-NMR Microscopy of Perfluorocarbons

Ralph P. Mason, Anca Constantinescu, Peter P. Antich

BIO 8

Magnetic Resonance Histology

G. Allan Johnson, Robert D. Black, Gary P. Cofer, Xiaohong Zhou, Robert R. Maronpot

BIO 9

¹H and ³¹P Spectroscopic Imaging Study of 9L Brain Tumor

M. Szayna, P. Kozlowski, J. K. Saunders, A. Jasinski

BIO 10

Self-Diffusion of Water in Cartilage as Studied by NMR Microscopy

C. Raible, F. Grinberg, Y. Morita, K. Gersonde

BIO 11

Depiction of Dental Anatomy by Magnetic Resonance Microscopy

Michael A. Baumann, Dieter Groß and Volker Lehmann

BIO 12

MR Microscopy Study of Honey Bee in vivo

Z. Sulek, A. Jasinski, B. Tomanek, F. Hennel, J. Kibinski, T. Skorka, Krzyzak, P. Kulinowski, Muszynska

BIO 13

NMR Microscopic Detection of Different Grades of Hydration and Chemical Composition Inside of Degenerative Changed Articular Cartilage

W. Gründer, M. Wagner, M. Biesold

BIO 14

High Field MRI of the Human Medulla Oblongata as a Research Method in Neuropathology

M. Vandersteen, P. Adriaensens, E. Beuls, J. Gelan, L. Vanormelingen, and Y. Palmers

BIO 15

Evaluation of the Spatial Distribution of Ethanol in the Human Brain by ¹H-NMR Spectroscopic Imaging

G. Schauß, H. Schild, M. Thelen

Manipulation of Susceptibility Effects in NMR Microscopy by Tailored RF
Z. H. Cho

Diffusion and Flow

DIFF 1

Quantifying Mass Transport with Magnetic Resonance Imaging

L. D. Hall, T. A. Carpenter, G. Amin, B. J. Balcom, J. A. Derbyshire, A. E. Fisher, S. J. Gibbs, A. D. Parker, K. Potter, D. Xing

DIFF 2

Patterns and Images of Flows and Vortices of Simple and Complex Fluids

John B. Grutzner

DIFF 3

General Treatment of Diffusion in the Presence of Boundaries and Short or Long Gradient Pulses

L. Z. Wang, A. Caprihan, Eiichi Fukushima

DIFF 4

Quantification of Unrestricted Diffusion in NMR Microscopy

M. Brandl, A. Link and A. Haase

DIFF 5

Diffusion and Susceptibility Effects in NMR Microscopy

P. T. Callaghan

DIFF 6

Diffusion in Heterogeneous and Anisotropic Media as Studied by PFG NMR and Microimaging

Farida Grinberg, Peter Barth, Siegfried Hafner and Winfried Kuhn

DIFF 7

Flow in Polymer Solutions Measured by Dynamic NMR Microscopy

Craig J. Rofo, Rodney K. Lambert, Lourdes de Vargas, Paul T. Callaghan

DIFF 8

Localized Diffusion Measurements with a single B1 gradient

E. Mischler, F. Humbert, D. Canet

Progress in Medical Imaging

MED 1

MR Imaging and Spectroscopy at High Fields

Kamil Ugurbil

After Dinner Talk

From Molecular Beams to Microimaging: Some Highlights in the Evolution of NMR

Edwin D. Becker

Plants & Agriculture

PLA 1

Functional NMR Imaging of Plants

H. van As

PLA 2

Molecular Motion and Nuclear Relaxation in Intact Biomaterials

Thomas M. Eads

PLA 3

A Comparison of Water Self-Diffusion in Fresh and Stored Beans

E. J. Kendall, D. W. Stanley, K. B. Chatson

PLA 4

In Vivo Magnetic Resonance Microscopy for Non-Destructively Investigating Plants, Fruits, Vegetables and Small Animals

S. Crestana, R. Kauten, D. R. Nielsen

PLA 5

NMR Microimaging in Meat Research

J. M. Tingle, V. Sarafis, P. A. Baumgartner, J. M. Pope

PLA 6

Determination of the vascular architecture of the raspberry receptacle through the use of 3D surface rendering techniques

J. A. B. Lohman, J. A. Chudek, B. A. Goodman, G. Hunter, B. Williamson

PLA 7

Development of infection in a strawberry fruit by the fungal pathogen *Botrytis cinerea*

B. Williamson, J. A. Chudek, G. Hunter, R. L. MacKay, B. A. Goodman

PLA 8

Axial and Radial Water Transport in *Ricinus Communis* Seedlings observed by Gradient Echo Deuterium Imaging

A. Metzler, W. Köckenberger, E. Komor, A. Haase

Rare Isotopes

RAI 1

Direct and Indirect Imaging Methods for the Isotopes of Boron, Nitrogen and C-13

Edward W. Randall

RAI 2

Solid State NMR in Living Subjects

J. L. Ackerman, L. Garrido, M. J. Lyszak, B. Pfeleiderer, Y. Wu

RAI 3

Combined Oxygen-17 / Phosphorus-31 MRI and MRS: A New Dimension in Cell

Bioenergetics Research

Gheorghe D. Mateescu

Posters

MET 10

Stray Field Imaging - MRM of Hard Tissues

Michael A. Baumann and Klaus Zick

MET 11

MARIS - Software Package for Spectroscopy and Imaging

M. Rydzy, T. Jakubowski, F. Hennel, A. Jasinski, P. Kulinowski, Z. Sulek, B. Tomanek

MET 12

Modular System for Microimaging

Z. Sulek, A. Jasinski, B. Tomanek, T. Skaorka, S. Kwiecinski

MET 13

NMR Imaging as an Indicator of Chemical Potential

A. E. Fischer, B. J. Balcom, T. A. Carpenter, L. D. Hall

MET 14

Construction of Multiply Band-Selective 180 degree Refocusing RF Pulses for Simultaneous Multi-slice Spin-Echo Imaging

B. Newling, T. A. Carpenter, J. A. Derbyshire, L. D. Hall

MET 15

Fast Spin-Echo Techniques for High-Field Magnetic Resonance Microscopy

Xiaohong Zhou, Gary P. Cofer, Steve A. Suddarth, G. Allan Johnson

MET 16

MRI and Determination of T1 and T2 of Solid Polymers Using a 1.5 Tesla Whole Body Imager

S. Widmaier, W.-I. Jung, O. Lutz

MET 17

Optimization of RF Coil Parameters for Microimaging Applications

Knut Mehr, Peter Dejon and Winfried Kuhn

MET 18

Planar Microcoils Sensors for NMR Microscopy

T. L. Peck, L. La Valle, R. L. Magin, I. Adesida, P. C. Lauterbur

MET 19

Use of Different Propagators in the Measurement of Flow in the Presence of Stationary Fluid

Paul T. Callaghan, Walter Köckenberger, James M. Pope

MET 20

High Gradient PGSE Experiments in a Superconducting Magnet

Bertram Manz, Andrew Coy, Philip J. Back, Paul T. Callaghan

MET 21

Edge Enhancement Effects in Microcapillaries

Andrew Coy, Lucy C. Forde, Craig J. Rofo, Paul T. Callaghan

MET 22

VECSY: Velocity Correlation Spectroscopy Using q-space Encoding

*Bertram Manz, Paul T. Callaghan***MET 23**

The Low Field NMR-imaging of Small Objects

*V. Frolov***MET 24**

Low Power Slice Selection and NMR Imaging with Noise Excitation

*H. Nilgens, B. Blümich, J. Paff, P. Blümmler***MET 25**

Measurement of Water Permeability of Diffusion Barriers by NMR Signal Enhancement

*A. P. Kiefer, E. Kuchenbrod, A. Haase***MET 26**

Construction of Microimaging Gradient Coils Based on Target-Field-Approach

*B. Kalusche, A. Vath, H. Adolf, A. Haase***MET 27**

EPI Implementation with Conventional MRI Hardware

*J. A. Derbyshire, T. A. Carpenter, L. D. Hall***MET 28**

Rotating Frame NMR Microscopy

*Klaus Woelk, Jerome W. Rathke, Robert J. Klingler***MET 29**

Solid-State NMR Imaging with Magic Angle Spinning

*Herman Lock, Marian Buszko, Yahong Sun, Gary E. Maciel***MET 30**

NMR Force Microscopy: Development of Cantilevers and Polarized Samples for Nuclear Detection

*Gregory J. Moore and Laurel O. Sillerud***MAT 16**

3D-imaging of the Ingress of Water into Semiconductor Devices

*Siegfried Hafner and Winfried Kuhn***MAT 17**

Radial Distribution Function and other Statistical Evaluations of NMR Micrographs of Porous Media

*H.-P. Müller, J. Weis, R. Kimmich***MAT 18**

NMR Magic Sandwich Echo Imaging of Rigid Polymers

F. Weigand, B. Blümich, H. W. Spiess

MAT 19

Surface-Coil Parameter Imaging of Materials

*Carsten Fülber, Bernhard Blümich, H. W. Spiess***MAT 20**

Pore Geometry Information Via Pulsed Field Gradient NMR

*A. J. Lucas, S. J. Gibbs, M. Peyron, G. K. Pierens, L. D. Hall, R. C. Stewart, D. W. Phelps***MAT 21**

Ingress of Water into Zeolite 4A Powder Plugs

*B. Leone, M. R. Halse, J. H. Strange, A. R. Lonergan, P. J. McDonald, E. Smith***MAT 22**

Quantitative NMR Flow Measurement in Systems of Complex Geometry: Applications in Chemical and Petroleum Engineering

*S. Yao, V. Rajanayagam, J. M. Pope***MAT 23**

Methacrylic Acid Polymerization. Travelling Waves Observed by Nuclear Magnetic Resonance Imaging

*Bruce J. Balcom, T. Adrian Carpenter, Laurance D. Hall***MAT 24**

Micro-imaging by Magnetic Resonance on Flexible Polyurethane Foams

*R. Pirlot, B. Chauvaux, R. Huis and J. M. Dereppe***BIO 16**

Effect of Brine Injection on Water Dynamics in post mortem Muscle: Study of T2 and Diffusion Coefficients by MRI

*L. Foucat, G. Bielicki, J. P. Donnat, A. Traore, J. P. Renou***BIO 17**

NMR Microscopic Study of New Gadolinium Complexes

*M. Wagner, R. Ruloff, E. Hoyer, W. Gründer***BIO 18**

NMR Microscopic Representation of Joint Cartilage Degeneration by Liposome-Entrapped Ions

*W. Gründer, K.-H. Dannhauer, A. Werner, K. Gersonde***BIO 19**

High Spatial Resolution NMR Microscopy of Peripheral Joints of Man and Laboratory Animals

*T. A. Carpenter, L. D. Hall, R. J. Hodgson, B. D. J. P. Munasinghe, M. J. Nolan, J. A. Tyler, P. J. Watson***BIO 20**

A Comparison of the Early Development of Ischaemic Damage Following permanent Middle Cerebral Artery Occlusion as Assessed using Histology and Magnetic Resonance Imaging

N. G. Burdett, T. A. Carpenter, R. Gill, L. D. Hall, R. Hatfield, J. D. Pickard, E. Shervill, N. R. Sibson

BIO 21

Diffusion Anisotropy and Size Restriction in the Rat Brain

A. Berg, F. Grinberg, P. Mestres, W. Kuhn

BIO 22

2D- and 3D-Microimaging Studies of Spheroids

W. Gries, F. Grinberg, W. Kuhn, K. Gersonde

BIO 23

Visualization of Spinal Cord Damage by a T-Tube Drainage in Syringomyelia

E. Beuls, J. Gelan, P. Adriaensens, M. Vandersteen, L. Vanormeldingen, and Y. Palmers

BIO 24

Screening of Short Time Preservation Methods for Spinal Cord Specimens towards Optimal MRI Contrast

P. Adriaensens, M. Vandersteen, E. Beuls, J. Gelan, L. Vanormelingen, and Y. Palmers

BIO 25

Regional Ossification Differences in the Human Fetal Spine by High Field MRI

L. Vanormelingen, E. Beuls, J. Gelan, P. Adriaensens, M. Vandersteen, and Y. Palmers

BIO 26

High Resolution Imaging of Growth and Gene Therapy of Gliomas Injected into Rat Brain

R. Demeure, I. Mottet, J. F. Goudemant, A. Maron, T. Gustin, J. N. Octave

BIO 27

Deoxygenation following Sacrifice:

Effects on T2 - T2 and T1 in the Wistar Rat

B. Shuter and J. M. Pope

BIO 28

Interaction of Paramagnetic Metal Complexes With Intracellular Water: A Study of Cytoplasm and Nuclei of X. Oocytes by Spatially Resolved T1- and T2-Time Measurements

S. Päufer, K. Keller, C. Mügge, A. Zschunke

BIO 29

High resolution NMR imaging and microscopy of the ovarian cycle

Catherine Temple, Gila Meir, Yael Steinfeld, Michal Neeman

BIO 30

Preliminary Studies on Mollusc Shells by ¹³C-CP/MAS and IH-Microscopy

Teresa Nunes, Gabriel Feio, Rolanda Albuquerque de Matos

DIFF 9

Gum Rheology: NMR Flow Imaging of Aqueous Polysaccharide Solutions

S. J. Gibbs, S. Ablett, I. Evans, D. E. Haycock, T. A. Carpenter, L. D. Hall

DIFF 10

Diffusion Imaging in the Presence of Static Magnetic Field Gradients

A. J. Lucas, S. J. Gibbs, E. W. G. Jones, M. Peyron, J. A. Derbyshire, L. D. Hall

DIFF 11

Correlated Susceptibility and Diffusion Effects in NMR Microscopy Using Phase-Frequency Encoding

Lucy C. Forde and Paul T. Callaghan

DIFF 12

PGSE NMR and Diffraction Effects

Andrew Coy, Paul T. Callaghan

DIFF 13

Effect of Susceptibility Diffusion Under Pure Phase Encoding

Craig J. Rofo and Paul T. Callaghan

DIFF 14

Optimal Gradient Strength for Diffusion Experiments

S. T. Fricke, L. Landini, C. A. Veracini, A. Benassi, J. Nori

PLA 9

Application of Nuclear Magnetic Resonance Microscopy for Studies of Lepidopteran Metabolism

John T. Christeller, William A. Laing, Craig D. Eccles, Ute Skibbe, Paul T. Callaghan

PLA 10

Quantitative Imaging of NMR Relaxation in Plants

Hommel T. Edzes, D. van Dusschoten, H. van As

PLA 11

Exchange Studied by Combined Diffusion and T₂-Measurements

D. van Dusschoten, J. B. M. Goense, H. T. Edzes, P. A. de Jager, H. Van As

PLA 12

Senescence of Mushroom (*Agaricus Bisporus*) Studied by T₂ NMR Imaging

H. C. W. Donker, H. T. Edzes, H. van As

PLA 13

The Uptake of Water by the Mushroom (*Agaricus Bisporus*) Visualized by NMR Imaging with the Aid of Gd-DTPA Contrast Enhancement

H. C. W. Donker, H. J. Snijder, H. Van As, A. W. H. Jans

PLA 14

Development of fruits of blackcurrant (*Ribes nigrum*) revealed by NMR microscopy

B. Williamson, B. A. Goodman, G. Hunter, J. A. Chudek, J. A. B. Lohman

PLA 15

Development of grape (*Vitis vinifera* L.) fruits studied noninvasively by NMR microscopy

B. A. Goodman, B. Williamson, J. A. Chudek, G. Hunter

PLA 16

Identification of freezing damage to flower buds of blackcurrant (*Ribes nigrum*) by NMR microscopy

R. Brennan, J. A. Chudek, G. Hunter, B. A. Goodman

PLA 17

NMR Microimaging of Capsule Development in the Moss *Dawsonia*

V. Sarafis, J. M. Tingle

PLA 18

Axial Water Motion Within the Castor Bean Seedling Observed by Dynamic NMR Microscopy

Walter Köckenberger, James M. Pope, Paul T. Callaghan

PLA 19

Diffusion of cell-associated water in ripening barley seeds on NMR micro-imaging

N. Ishida, H. Kano, H. Ogawa

PLA 20

Magnetic Resonance Microscopy as a Non-invasive Technique for Investigating 3D Preferential Flow Occuring Within Stratified Soil Samples

Posadas, D. A., Tannus, A., Panepucci, H. C., Crestana, S.

PLA 21

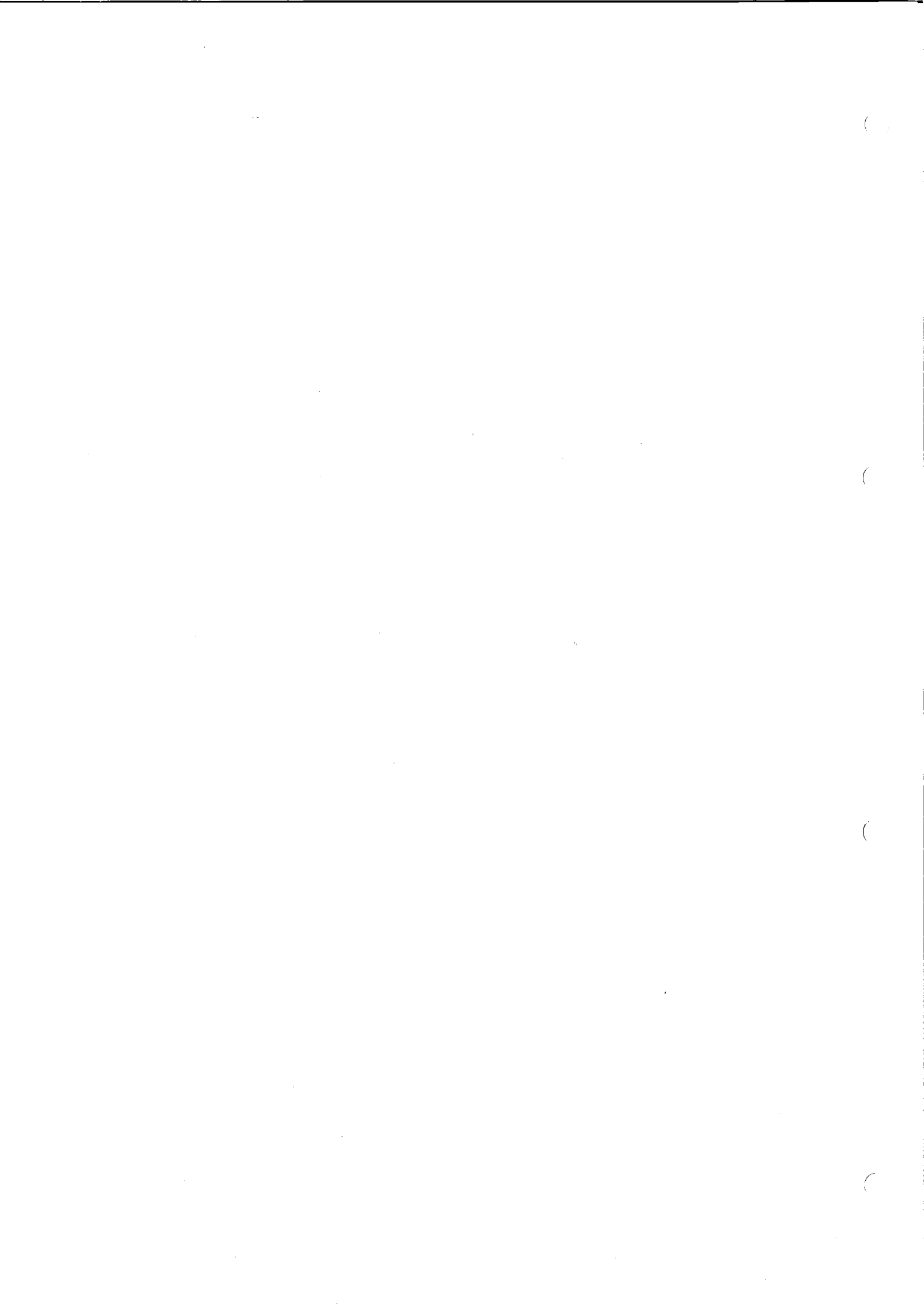
Sucrose Distribution in *Ricinus Communis* Seedling Observed by High Resolution Spectroscopic Imaging

A. Metzler, W. Köckenberger, M. von Kienlin, E. Komor, A. Haase



Lectures and Postertalks:

Abstracts



Advances in NMR Microscopy at 500 MHz

P. Mansfield, R.W. Bowtell, A. Peters, *J.C. Sharp, P.M.Glover
and †S.J. Blackband

Magnetic Resonance Centre. Department of Physics, University
of Nottingham, Nottingham, UK.

The principles of NMR microscopy (1,2) have allowed us to explore more broadly a range of microscopic applications using our in-house built NMR microscope. This has an 89 mm bore and operates at 11.7 T and incorporates active gradient screening (3). Although the system is basically capable of producing images with a resolution of $4.5 \mu\text{m}$, (see Ref. 4), the imaging time for 256×256 pixel arrays is typically 15 minutes. We have extended the range of application of the microscope by relaxing somewhat the spatial resolution in order to look very widely at potential applications.

This paper will therefore concern itself with a broader range of medium resolution applications. These include the study of restricted diffusion in rice plant calluses and the preliminary study of electric organs in skate tails. Other low resolution applications of considerable interest to the pharmaceutical industry are the design of slow drug release tablets based on hydrating hydrophilic matrix tablets. The rate and extent of swelling of the outer gel layer critically influences the drug release kinetics. The matrix comprises hydroxypropylmethylcellulose (HPMC). Typical values of in-plane resolution and slice thickness used in this work are $70 \mu\text{m}$ and $600 \mu\text{m}$.

Other areas of application at a preliminary stage are the study of single neurons from the abdominal ganglia of *Aplysia Californica* using line-narrowed 2DFT imaging. The line-narrowed sequence (5) has proved itself to be particularly robust at removing induced susceptibility artefacts which is a common problem at 500 MHz.

Echo-planar imaging (EPI) has also been investigated at 500 MHz. One of the main difficulties when applying high speed techniques is again the problem of induced susceptibility artefact. However, the so-called Pi-EPI or PEPI sequence (6) introduced originally to study water distribution and flow in mineral rock cores, has allowed us to obtain 64×64 and 128×128 snap-shot EP images with total acquisition times of 30 ms and 75 ms respectively. We feel therefore that PEPI will find increasing application for high field studies of insects and small animals *in vivo*.

References

1. P. Mansfield and P.K. Grannell, J. Phys. C. 6, L422 (1973); Phys. Rev. 12, 3618 (1975); Phys. Med. Biol. 20, 477 (1975).
2. J.B. Aguayo, S.J. Blackband, J. Schoeniger, M.A. Mattingly and M. Hintermann, Nature 322, 190 (1986).
3. R. Bowtell, G.D. Brown, P.M. Glover, M. McJury and P. Mansfield, Phil. Trans. Roy. Soc. Lond. A 333, 457 (1990).
4. R.W. Bowtell, P. Mansfield, J.C. Sharp, G.D. Brown, M. McJury and P.M. Glover, in Magnetic Resonance Microscopy (Ed: B. Blumich and W. Kuhn), VCH Verlag. Weinheim, 1992.
5. J.C. Sharp, R.W. Bowtell and P. Mansfield. MRM 29, 407-411 (1993).
6. D.N. Guilfoyle and P. Mansfield, J. Mag. Res. 97, 342-358 (1992).

Present Address: *National Research Council, Institute for Diagnostics, 435 Ellice Avenue, Winnipeg, Manitoba R3B 1Y6, Canada; †Magnetic Resonance Centre, Hull Royal Infirmary, Anlaby Road, Hull, HU3 2JZ.

Technical Aspects of Microspectroscopy at High Field

Stuart Crozier, Stephen Rose, Wolfgang Roffman, Paul Hockings,
Stephen Wilson and David M. Doddrell

Centre for Magnetic Resonance, Queensland University, St. Lucia,
Qld. 4072 , Australia

In vivo, cerebral ^1H Image-Directed-Spectroscopy (IDS) in small animal models has been performed routinely in our laboratory at proton frequencies from 100-500 MHz over the past four or so years (1). Two long term clinical trials are currently underway, studying neuronal damage caused by stroke in a gerbil model and Wernicke's encephalopathy in a rat model (2). Preliminary results from these studies will be presented. There are considerable difficulties in performing abdominal and thoracic imaging and IDS in small animal models at high field, particularly the influence of respiratory and cardiac motion and the effect of susceptibility differences at tissue boundaries, predominantly air cavity interfaces. A newly developed, non-invasive, optical respiratory trigger (3) and conventional cardiac monitoring were used to produce cardio-pulmonary gating signals for sequence triggering. High resolution thoracic and abdominal images and IDS from abdominal organs will be presented.

One of the most critical aspects to the use of *in vivo* IDS in vertical magnet systems is the design of shielded gradient coils. Residual fields, both spatially and non-spatially dependent, arising from gradient-transition induced eddy currents severely compromise the spectral resolution and signal-to-noise ratio of IDS experiments. The design of shielded gradient systems with parameters optimized for *in vivo* IDS experimentation will be detailed. In particular the extension of sheet designs to multilayer structures (4-6); effectively enhancing sensitivity while conserving radial space and minimizing inductance; and the use of Simulated Annealing (SA) optimization in real space for gradient design (7). SA has advantages of being able to easily trade performance characteristics, introduce real space constraints such as coil length and interconductor separation and locate the global minimum of an error function subject to the applied constraints.

References

- [1]. S. Crozier et al. *J. Magn. Reson.* 94, 123 (1991) (and references therein).
- [2]. S. Rose et al. *NMR in Biomed.*, in press, (1993).
- [3]. S. Wilson et al. *Magn. Reson. Imag.*, in press, (1993).
- [4]. C. Eccles et al. *ibid*, submitted (1993).
- [5]. P. Mansfield and B.Chapman, *J. Magn. Reson.*, 66, 573, (1986).
- [6]. R. Turner, *J. Phys. E.*, 21, 948, (1988).
- [7]. S. Crozier and D.M. Doddrell, *J. Magn. Reson.*, in press, (1993).

MAGNETIC RESONANCE DETECTION AND IMAGING USING FORCE MICROSCOPE TECHNIQUES

D. Rugar, O. Züger, C.S. Yannoni, H.M. Vieth,* and R.D. Kendrick,
IBM Research Division, Almaden Research Center, 650 Harry Rd.,
San Jose, CA 95120

We describe a new method for detecting magnetic resonance based on measuring a small oscillating magnetic force acting between the spins in a sample and a nearby ferromagnetic particle. The oscillating magnetic force is generated by polarizing the spins in the magnetic field and then modulating the sample magnetization using magnetic resonance techniques. The oscillating magnetic force is detected by sensing the angstrom-scale vibration of a micromechanical cantilever on which the sample is mounted. In an initial experimental demonstration,¹ we detected an oscillatory 10^{-14} N force generated while exciting and modulating electron paramagnetic resonance in a sub-30 ng sample of diphenylpicrylhydrazil (DPPH). The force detection technique is well suited for microscopic imaging applications. Using a magnetic field gradient of 4 Gauss/ μm , electron paramagnetic resonance images have been obtained that demonstrate axial resolution on the order of 1 μm and lateral resolution on the order of 5 μm . Possible extensions of the technique to atomic-scale nuclear magnetic resonance imaging will be discussed.

¹ D. Rugar, C.S. Yannoni and J.A. Sidles, Nature **360**, 563 (1992)

* permanent address: Freie Universität Berlin, Inst. für Experimentalphysik, D-1000 Berlin 33

TOWARD ULTRA-RESOLUTION NMR MICROSCOPY

Paul C. Lauterbur, W. Brian Hyslop and H. Douglas Morris
Biomedical Magnetic Resonance Laboratory, University of Illinois,
1307 West Park Street, Urbana, Illinois 61801

NMR microscopy is limited in resolution by the signal-to-noise ratio and by diffusional effects. We are developing a method, called DESIRE (Diffusional Enhancement of Signal Intensity and RESolution) that separates the spatial localization of features from signal detection. By confining the input function for magnetization change to a region smaller than the diffusional range, the magnetization change in that region can be transmitted by diffusion to a larger volume and stored for times of the order of relaxation times. The experiment is similar to those in which magnetization is transferred from rare spins to abundant spins in intimate contact, and can be described, for longitudinal magnetization, as heating of a large reservoir by energy supplied to a smaller one. The fundamental limits of DESIRE will be estimated, and experiments and simulations presented.

Acknowledgments

Partial support for this work was supplied by the National Institutes of Health-PHS 5 P41 RR05964, the National Science Foundation-DIR 89-20133, and the Servants United Foundation.

2nd International Conference on Magnetic Resonance Microscopy
(Heidelberg, September 6-9, 1993)

NMR Microscopy by Radio-Frequency Field Gradients.

D. Canet, P. Maffei, P. Mutzenhardt, R. Raulet and J. Brondeau

Laboratoire de Méthodologie RMN (U.R.A. CNRS n° 406 - LESOC)

Université de Nancy I

B.P. 239

54506 Vandœuvre lès Nancy Cedex

France

This communication will report on recent improvements of a NMR microimaging method which employs exclusively radio-frequency field gradients : one in the transverse direction created by a single turn coil, the other along the longitudinal direction generated by a specially devised saddle coil. The probe is designed to be used with wide-bore vertical superconducting magnets. The two coils are fed by two different transmitters operating at the same frequency and whose relative phase is set once and for all. The basic experiment involves a slice selection by means of the longitudinal gradient followed by the acquisition of the NMR signal in presence of the transverse gradient which is actually applied in the form of short pulses separated by acquisition windows. By rotating the object around the vertical axis in a stepped manner, a series of profiles is obtained whose analysis, including *inter alia* the filtered-back projection algorithm, provides a two-dimensional image. The experiment can be run routinely with a slightly modified conventional NMR spectrometer; the emphasis will be put on i) its relative immunity with regard to B_0 inhomogeneities and/or magnetic susceptibility variations across the object under investigation, ii) its ability to provide good quality images even when NMR lines are relatively broad (up to 2 KHz). Several examples, including solvent penetration in polymeric materials, will illustrate those features.

**Methods for Reconstruction Slice Profiles in
Magnetic Resonance Imaging;
Visualisation of the Performance of Self-Refocusing Pulses**

Philippe Devoulon¹, Lyndon Emsley^{2,3}, Peter Weber²,
Reto Meuli⁴, Michel Décorps¹ and Geoffrey Bodenhausen²

¹Institut National de la Santé et de la Recherche Médicale (INSERM), Grenoble, France; ²Section de Chimie, Université de Lausanne, Switzerland; ³Department of Chemistry, University of California, Berkeley, U.S.A.; ⁴Centre Hospitalier Universitaire Vaudois, Lausanne, Switzerland.

New methods are presented that allow one to obtain a phase-sensitive picture of the profile of a slice excited by applying a shaped radio-frequency pulse in the presence of a gradient. The relevant profile is defined during two distinct time periods. The first is the interval in which the selective pulse is applied. During this period one prepares a certain distribution of the magnitude M_{xy} and the phase φ as a function of offset, or equivalently, as a function of the spatial coordinate perpendicular to the plane of the slice. One of our objectives is to determine the distribution of the magnetization at the end of this period. This is what we refer to as the *excitation profile*. In the second period the gradients are being switched off or reversed for refocusing. If we neglect relaxation, no change in the amplitude occurs, but the phase φ undergoes important changes. Our second objective therefore is to determine the magnetization distribution at the end of this procedure (including the time required for all transients to settle down). This is what we refer to as the *slice profile*. It is this profile which determines the intensity of a pixel in an image. These definitions allow us to understand how different parts of the slice contribute to the signal. These methods were used to evaluate the performance of various self-refocusing pulses, such as 270° Gaussian pulses and various Gaussian cascades used without gradient reversal, which have been compared with traditional "sinc" pulses used in conjunction with gradient reversal.

Spin Relaxation in the Vicinity of Susceptibility Boundaries

Lucy C Forde and Paul T Callaghan

Department of Physics and Biophysics, Massey University,
Palmerston North, New Zealand.

Abstract

The local fields associated with boundaries in diamagnetic susceptibility are believed to be the cause of anomalous spin relaxation in plant tissue and other porous media⁽¹⁾. The precise nature of the relaxation depends on the rate of molecular self diffusion and, in particular, whether fast or slow exchange conditions prevail. One approach to understanding these effects is to apply a simple Anderson-Weiss depiction of exchange in which a Gaussian distribution of local fields is assumed. Experimentally, the relaxation may be elucidated by comparing images obtained using gradient echo, spin echo and Carr-Purcell-Meiboom-Gill echo pulse trains. We have carried out NMR microscopy experiments using a phantom consisting of fine glass rods packed inside a water-filled 1.4 mm diameter capillary. The natures of exchange conditions is elucidated and the resulting relaxation analysis of the local field distribution compared with calculations⁽²⁾. The same approach is used in an NMR microscopy study of a plant stem, *Stachys sylvatica*, and the resulting T_2 maps used to indicate cellular size on a scale finer than the pixel resolution.

1. P T Callaghan, *Principles of NMR Microscopy*, Oxford University Press, 1992.
2. P T Callaghan, *J Magn Reson* **87**, 304 (1990).

MR Microscopy of Electric Currents

I. Serša, O. Jarh, J. Seliger, and F. Demsar

Jožef Stefan Institute, Ljubljana University, Jamova 39, 61111 Ljubljana, Slovenia

Principles of electric current MR imaging

Imaging of electric currents flowing in conductive water samples is a new and encouraging development of MR techniques. The physical principle that enable this type of imaging is the following: electric currents that flow through the sample change the magnetic field in the sample. A small static component of order of magnitude μT is added to the static magnetic field, which causes its Larmor frequency shift. By measuring this frequency shift the change of magnetic field can be determined. Rotating the sample to all three perpendicular spatial orientations all components of the magnetic field can be measured. Finally, electric currents can be calculated using Maxwell equation $\vec{j} = 1/\mu_0 \nabla \times \vec{B}$.

Two different approaches are used for measuring the frequency shift caused by electric currents. In the first type of experiments currents are constantly flowing and frequency shift is measured directly [1], [2]. In the other type of experiments, currents are flowing through the sample in pulses which are synchronized with the imaging sequence. In the case of spin warp imaging sequence two pulses are used [3]. First starts after slice selection and ends before π pulse, and the second starts after π pulse, it has the same duration, equal strength, but the opposite direction. Since this two pulses have opposite direction, π pulse can not cancel the phase shift produced by electric current pulses, but it does just the opposite - it sums the phase shift effect of both pulses. By measuring this phase shift and knowing the duration of current pulses one can obtain the frequency shift.

Imaging of electric currents on a MR microimaging system

The capabilities of electric current imaging and theoretical considerations concerning signal to noise ratio (*SNR*) can be extensively studied on a microimaging system. The resolution of the method is determined by the experimental error in frequency shift measurements, or by the phase error for the method based on measuring frequency shift via phase shift. It can be shown, that phase error is approximately equal to noise to signal ratio ($1/$ *SNR*) of the magnitude image of the object. Therefore, the lowest measurable magnetic field is

$$B_{min} = \frac{1}{2 \gamma \tau SNR} \quad (1)$$

where γ is the proton gyromagnetic ratio and τ is the duration of one current pulse. Taking into account that the change of magnetic field between two neighbouring pixels should be at least B_{min} and considering electric currents constant in a vicinity of a pixel we can estimate that the lowest measurable current density is

$$j_{min} = \frac{N}{\mu_0 \gamma \tau SNR FOV} \quad (2)$$

where N is image matrix dimension and FOV is field of view. By dividing j/j_{min} signal to noise ratio in electric current MR image is obtained. For typical microimaging of electric currents with parameters: $N = 256$, $FOV = 10 \text{ mm}$, $SNR = 10$, $\tau = 50 \text{ ms}$, we obtain $B_{min} = 4 * 10^{-9} \text{ T}$ and $j_{min} = 150 \text{ A/m}^2$. Optimum conditions for electric current image are obtained when product τSNR is maximized, which is at $\tau = T_2/2$.

Theoretical calculations are compared with experiments on phantom samples. A number of applications can be found where knowing the pattern of the currents flowing through the sample is of major interest, such as imaging of electric current distribution in plant stalks and DC electric current tumour therapy.

References

- [1] A. A. Maudsley, H. E. Simon, S. K. Hilal, *J. Phys. E: Sci. Instrum.*, Vol 17, (216-220), 1983
- [2] Y. Manassen, E. Shalev, G. Navon, *J. Magn. Reson.*, Vol 76, (371-374), 1988
- [3] M. Joy, G. Scott, M. Henkelman, *Magn. Reson. Imag.*, Vol 7, (89-94), 1989

Spatially resolved one- and two-dimensional MAS NMR spectroscopy

U. Scheler, B. Blümich⁺, H.W. Spiess

Max-Planck-Institut für Polymerforschung, PF 3148 D-55021 Mainz

⁺Makromolekulare Chemie, RWTH, Worringer Weg 1, D-52074 Aachen

In NMR imaging spatial resolution and signal to noise ratio are determined by the linewidth in the NMR-spectrum and the gradient strength. Therefore, the wide lines encountered in NMR of solids should be narrowed. A useful technique is Magic Angle Sample Spinning (MAS). In combination with spatial resolution this requires a magnetic field gradient tensor which rotates simultaneously with the sample.^{1,2}

¹³C MAS imaging is of particular interest, because good *spatial resolution* can be achieved also in cases where ¹H MAS imaging fails and because the ¹³C NMR spectrum contains a variety of information on structure, order and dynamics of the system under study.

For high spinning speeds the ¹³C spectrum consists of only one narrow line at the position of the isotropic shift for each chemical side. At low spinning speeds the ¹³C MAS spectra are complicated by spinning sidebands resulting from insufficient averaging of the chemical shift anisotropy. These sidebands appear as artifacts in the images and disturb the spatial resolution. But it is known from solid state NMR spectroscopy, that spinning sidebands can be suppressed by suitable pulse sequences like TOSS (total suppression of spinning sidebands). We demonstrate the removal of spinning sidebands in spatially resolved ¹³C spectra and the corresponding artefacts from images.³

On the other hand the sideband intensities contain information about the anisotropy of the chemical shift. This information can be used to probe order parameters of macroscopically ordered samples. In a known two-dimensional experiment the spinning sidebands can be expanded in a second dimension. From the resulting two-dimensional sideband intensities the order parameters can be extracted. In a three-dimensional experiment we demonstrate the use of this method with spatial resolution. We call this Orientation Spectroscopy by Sideband Imaging (OSSI). From such a spatially resolved two-dimensional spectrum the spatial distribution of order parameters can be extracted.⁴

References:

- 1 D.G. Cory, J.W.M. van Os, W.S. Veeman, J. Magn. Reson. 76 (1988) 543
- 2 G. Schauss, B. Blümich, H. W. Spiess J. Magn. Reson. 95 (1991) 437
- 3 U. Scheler, B. Blümich, H. W. Spiess, Solid State NMR xx (1993) xx
- 4 U. Scheler, J. J. Titman, B. Blümich, H. W. Spiess J. Magn. Reson. xx (1993) xx

Magic Echo Solid Imaging of Rigid Solid Materials in two and three Dimensions

Peter Barth, Siegfried Hafner and Winfried Kuhn

Fraunhofer Institut für Biomedizinische Technik IBMT
Arbeitsgruppe Magnetische Resonanz
Ensheimer Str.48 66386 St. Ingbert, Germany

In the field of imaging of rigid solids several techniques have been developed and applied with some success to obtain 2D images of reasonable resolution. One of these techniques is the Magic Echo Phase-encoding Solid Imaging technique (MEPSI) (1,2) using pure phase-encoding in combination with the magic echo sequence to eliminate the evolution due to dipolar coupling. In this way a resolution of about 100 μm could be achieved in a real solid. In comparison with other solid imaging techniques, e.g. the techniques using multipulse sequences or MAS, MEPSI requires no special hardware and is easily implemented on any commercial NMR spectrometer equipped for imaging. Also, as a pure phase-encoding technique, MEPSI in principle gives access to spectroscopic information.

Dependent on the spectrometer performance the method can be applied to solids with line-width at half intensity of more than 40 kHz. This will be demonstrated in two and three dimensions for various materials. MEPSI is a very flexible method and can be combined with other sequences to determine special material properties. Parameter selective MEPSI imaging can be used to enhance contrast between different parts of the sample. The method also can be applied to rubber materials below glass transition temperature where the line-width at half intensity is in the range of 30 kHz. The temperature dependence of the magic echo is interesting itself because it is different for different materials and therefore gives information on material properties. In imaging this can be used to adjust optimal contrasts between the materials.

Literature:

1. D.E. Demco, S. Hafner and R. Kimmich
J. Magn. Reson. 96, 307 (1992)
2. S. Hafner, P. Barth and W. Kuhn
J. Magn. Reson., to be published (1993)

abstract for 2nd International Conference on Magnetic Resonance
Microscopy

High Resolution EPR Microscopy

Sandra S. Eaton, Gareth R. Eaton, and Minoru Sueki
Department of Chemistry, University of Denver, Denver,
Colorado, USA 80208

Spectral-spatial two-dimensional EPR imaging of the E' defects in irradiated fused silicon dioxide has been used to determine the depth profile of the radiation damage for a series of samples exposed to X-rays with different energies. The profiles reveal the effect of imperfect filtering of the X-rays and the impact of surface treatments.

The magnetic field modulation that is used for signal detection in continuous wave EPR induces eddy currents in conducting materials that are present in the resonator. Experiments and calculations were performed to examine the impact of these eddy currents on the spatial variation of the magnetic field modulation around 1 mm diameter copper, silver, and platinum wires. Two-dimensional spatial-spatial EPR images were in good agreement with calculations. The impact of the eddy currents on the modulation field decreased with decreasing conductivity of the wire and decreased with decreasing modulation frequency (100, 50, and 25 kHz), which is consistent with calculations.

The first-derivative CW EPR spectrum of polypyrrole deposited on gold wire, tungsten wire, platinum-coated tungsten wire or platinum foil is a singlet with a peak-to-peak linewidth of 0.2 to 0.4 G. However, when a film of polypyrrole is deposited on platinum or palladium wire (1.0 mm diameter), the X-band signal is an apparent doublet with a splitting of 0.6 G (Pt) or 2.2 G (Pd), which is attributed to the perturbation of the magnetic field by the relatively high magnetic susceptibility of the wire. The splitting of the polypyrrole signal on 0.25 mm diameter Pd or Pt wire increased as the external field was increased with S-band (1260 G) < X-band (3270 G) < Q-band (12550 G). The variation in magnetic field around the Pt and Pd wires was confirmed by spectral-spatial EPR imaging at X-band. The splitting of the EPR signals and the spatial variation of the magnetic field in the images are in good agreement with calculations of the effect of an infinitely long cylinder of magnetic material on a static magnetic field.

Radiofrequency FT-EPR Spectroscopy and Imaging

Sankaran Subramanian, John Bourg, Murali C. Krishna and James B. Mitchell

Radiation Biology Section, Radiation Oncology Branch, Clinical Oncology Program, Division of Cancer Treatment, National Cancer Institute, National Institutes of Health, Bethesda, Maryland 20892

For the first time radiofrequency Fourier transform EPR spectroscopy and imaging is demonstrated. We have obtained a good signal to noise ratio from samples at 300 MHz. The equipment consists of a Hewlett Packard 8644A signal generator whose output is pulse modulated using a 40 ns pulse from a Stanford Research System Model DG535 delay generator. The pulsed RF at 300 MHz is further amplified by an ENI 525LA amplifier (50 dB) and applied to a single four turn helical coil (AWG 20 Copper wire) tuned and matched to 300 MHz at 50 ohm impedance. The transmitter and receiver are isolated using the usual NMR type diode switch, and the signals are amplified by two cascaded MITEQ amplifiers with a total amplification factor of approximately 45 dB. The resulting signal is mixed with the synthesizer output, low pass filtered and recorded using a Tektronix TDS 540 500MHz digital Oscilloscope. The present system is a single channel spectrometer. At a loaded Q of 200, a 0.5 mg sample of lithium phthalocyanine with a filling factor of less than 5% gave a spectrum with a signal to noise ratio of 75 when 10,000 FID's were averaged (total time 50 seconds). The same coil with a loaded Q of 60 gave for a 0.4 ml solution of sodium in liquid ammonia containing 10^{18} electrons gave a spectrum with a signal to noise ratio of 6 with a single pulse followed by FT. We have also demonstrated the feasibility of 2D Fourier imaging by spatially resolving several tubes containing solvated electrons using a gradient of about 0.5 G/cm and processing the data using back projection techniques. We are in the process of measuring EPR spectra from ^{15}N nitroxides, construction of three dimensional gradient coils and ultra fast sampler and averager, so that EPR spectroscopy at ultra low concentrations and in vivo Fourier imaging will become a reality in the near future.

IN VIVO ESR STUDIES OF THE METABOLIC FATE OF NITROBENZENE IN THE MOUSE

Hirotsada Fujii, Baolu Zhao, Janusz Koscielniak and Lawrence J. Berliner
Laboratory of In-Vivo Electron Spin Resonance Spectroscopy, Department of
Chemistry, The Ohio State University
120 W. 18th Ave., Columbus, Ohio 43210 USA.

We report the first demonstration of ESR spectroscopy to study free radical reactions in live mice and excised muscle tissue resulting from the metabolism of nitrosobenzene. A broad three-line ESR spectrum ($a_N=11.6$ G) appeared in the buttocks region of a mouse placed in an L-band loop gap resonator after intramuscular or intraperitoneal injection of 0.2 mmol/kg nitrosobenzene. The signal intensity reached a maximum at 20-30 min and remained constant well beyond 2h. If muscle tissue was dosed with nitrosobenzene and excised within 5 min, a similar three-line X-band ESR spectrum was obtained which was preceded by the rapid growth and subsequent decay of an ESR spectrum identical to that of the phenylhydronitroxide radical, which was presumably generated from reactions between nitrosobenzene and reducing agents in the blood or tissue such as NADH or ascorbic acid. A model system containing nitrosobenzene and unsaturated fatty acids (olive oil or animal fat) yielded an identical three-line spectrum resulting from radical adducts of nitrosobenzene across the double bond. Overall, these results suggest that the most probable mechanism *in-vivo* was nitrosobenzene covalently adding ('binding') to polyunsaturated fatty acid clusters in fat or membranes. This work was supported, in part, by a grant from the U.S.P.H.S (RR03126).

Broad-line MRI and Fluid Ingress in Polymeric Materials

M.R. Halse, H.J. Rahman and J.H. Strange
Physics Laboratory, The University, Canterbury, Kent, U.K.

Abstract

The problem of ingress of fluid into solid materials is the subject of several investigations using MRI. Broad-line MRI techniques offer the possibility of studying both solid material and absorbed fluid. We have focussed attention on systems in which solvents penetrate organic polymers and have applied techniques that we have developed using large oscillating field gradients in order to study the diffusive behaviour of solvent and the modification to polymer molecular mobility that results from fluid ingress.

This paper describes in some detail the penetration of decane into lightly cross-linked peroxide vulcanizate of natural rubber (poly isoprene). The penetration studies allow measurement of a diffusion coefficient. We have also measured decane diffusion within rubber by the more traditional nmr methods (with both steady and pulsed field gradients). The studies require a concentration dependent diffusion coefficient for internal consistency.

Use of T₁ and T₂ filters allow us to distinguish clearly between absorbent and absorbate images. T₂ -weighted images of the rubber absorbate using gradient echo times that vary from 200 μ s to 1.8ms have been obtained. Signal intensity measurements from corresponding pixels in these images provide a T₂ profile of the rubber and establish an approximately linear relationship between the T₂ (and hence the motional correlation frequency) of the softened rubber and the local decane concentration.

APPLICATIONS OF NMR IMAGING TO STUDY MATERIALS. William M. Ritchey

Department of Chemistry, Case Western Reserve University, Cleveland, OH 44106-7078.

MRI [NMR Imaging] has been applied to various materials for use in nondestructive structural analysis. Ceramics in the green state may possess defects or voids that can create points of weakness upon further processing [i.e. firing]. MRI is used to detect these regions using solvent impregnation. Some defects may be below the digital resolution currently obtainable. These defects can often be observed by exploiting the magnetic susceptibility differences at solvent/air, solvent/ceramic, and solvent/organic material interfaces. This void "enhancement" is observed using a gradient-echo sequence.

Spin-echo and multi-slice proton imaging were employed to determine void and carbon black distribution throughout a sample of polyisoprene. The appearance of the images is determined by the spin-spin relaxation time, T_2 , of the sample and the echo time, TE, of the pulse program. Also the presence of carbon black affects signal intensity by decreasing T_2 and by reducing elastomer concentration. One advantage that multi-slice imaging has over single slice is that a number of images throughout the sample are acquired in the same time as one spin-echo image. Thus void and carbon black distribution can be followed and in addition, these data sets can be used to generate 3-D image files.

MRI has also been applied to study the non-uniformity of swelling of cation exchange beads (sulfonated styrene, divinylbenzene copolymers). Images of these resins show a variation in signal intensity within a bead due to a difference in water concentration. This variation in intensity could be due to a variation in cross-link density, degree of sulfonation, composition, sulfone bridging or a combination of these variables in different regions of the bead. A prototype of the Bruker Magnifier™ provided a better signal to noise in the copolymer images.

NMR Microimaging of Flow in Porous Materials

J. Weis, H.-P. Müller, R. Kimmich

Sekt. Kernresonanzspektroskopie, Universität Ulm, D-89069 Ulm, Germany

Introduction

Nuclear magnetic resonance is well suited for the study of flow in porous materials. The main objective of our work is to determine the influence of the microstructure on the three-dimensional flow distribution.

Method

The distribution of microscopic flow in porous media was studied by FEVI (Fourier Encoding Velocity Imaging). FEVI was used in a 4D version, where encoding with one velocity component was obtained by stepwise increasing a bipolar gradient in the direction of the component. A voxel size of $0.1 * 0.1 * 0.1 \text{ mm}^3$ was achieved by the usual 3D gradient echo technique using two phase encoding and one read out gradient. We improved the digital precision of the measurement matrix by a zero filling interpolation (ZFI) prior to Fourier transformation of the bipolar gradient encoded signal.

The quality of the proton spectrum evaluated for each voxel of the excited slice permits a reliable calculation of the local velocities (position of the maximum and the width at the half height of the spectrum).

Velocity maps in main flow direction (z-direction) and perpendicular to the main flow direction (x-direction) were obtained for pressed natural sponge, pure water and densely packed glass beads with a diameter of 1 mm. The digital resolution was $v = 0.08 \text{ mm/s}$.

Results

Laminar flow with a relatively flat parabolic profile was observed with water flowing in a tube (diameter 8 mm) in a range of $0 < v < 1 \text{ mm/s}$ without restriction by porous materials. With a plug of natural sponge, flow is characterized by the same amplitude range of velocities in z and x (y) directions. The relatively random distribution of velocities v_x, v_z indicates, that molecular motion in porous materials has an isotropic coherent character in a wide range of pore diameters.

Conclusion

FEVI in 4D version is a promising method for the measurement of all velocity components (v_x, v_y, v_z) in NMR flow microimaging. The distribution of flow can thus be correlated to the microstructure of the percolation network.

Spatially Resolved NMR for Materials Science

B. Blümich*, C. Fülber, U. Scheler, H.W. Spiess, F. Weigand

Max-Planck-Institut für Polymerforschung, Postfach 3148, D 55021 Mainz

* Makromolekulare Chemie, RWTH-Aachen, Worringer Weg 1, D 52074 Aachen

The interest of NMR imaging in materials science derives from the development of techniques with unsurpassed parameter contrast and adequate resolution of the space dimension. The progress in methodical development and applications of different techniques is reported:

1. **MAS imaging:** High spatial and spectral resolution is obtained by observation of ^{13}C . Sidebands from slow spinning can be suppressed by TOSS to simplify images and spatially resolved spectra¹. Under rotor synchronization 2D spectra have been recorded with spatial resolution from which the orientational distribution function can be derived as a function of space².
2. **Magic-Echo imaging:** Compared to multipulse line-narrowing, the interpulse spacing is larger enabling convenient gradient switching, and the technique appears to be more robust. This form of space encoding has been combined with magnetisation filters and spectroscopic resolution for contrast optimization. Applications to different polymers are reported³.
3. **Surface coils:** Surface coils are in need for localized investigations of large objects. The depth-dependent image contrast caused by spatial variation of the B_1 field strength can be overcome by imaging suitable parameters such as relaxation times, or in case of a spin-lock experiment, the correlation time of slow molecular motion⁴.

References:

1. U. Scheler, B. Blümich, H.W. Spiess, *Solid State NMR* xx (1993) xx
2. U. Scheler, J.J. Titman, B. Blümich, H.W. Spiess, *J. Magn. Reson* xx (1993) xx
3. F. Weigand, B. Blümich, H.W. Spiess, *Solid State NMR* xx (1993) xx
4. C. Fülber, B. Blümich, H.W. Spiess, *Macromolecules* xx (1993) xx

Micro-MRI as a tool for characterisation of foams based on polyvinylalcohol-formaldehyde and phenol-formaldehyde resins.

M. Ercken, I. Pollers, P. Adriaensens, R. Carleer, D. Vanderzande and J. Gelan.

Institute for Materials Research - Limburg University

B-3590 Diepenbeek - Belgium

NMR micro-imaging is a very promising non-invasive tool to characterise new and improved polymer materials. As an example, we investigated medical sponges based on polyvinylalcohol-formaldehyde (PVF) resins. The properties of those sponges rely on the formation of a physical network formed by linear polymer chains. In a second example, phenol-formaldehyde (PF) foams, with a closed cell structure, were examined. In this case, the resins are formed by a chemical, three-dimensional network.

The MRI images have been generated at 9.4 Tesla using a Unity 400 Varian spectrometer equipped with a 25mm diameter imaging probe. Most images were recorded under spin-density conditions with some T_2 -weighting by using the multislice spin-warp technique ($TE/TR=20/2000$).

The stability of the PVF-sponge structure could be evaluated by a thermal treatment at 90°C in water during one hour. Changes in the morphology could be observed depending on the production method of the sponges.

For the PF-foams, the degree of chemical networking, correlating with their isolating value, could be investigated by following the ingress of water in the foams and this was done under vacuum. The results of proton and carbon solid-state NMR spectroscopy, on the same closed cell foams, confirm their degree of networking. Further, the ingress of several solvents has been followed. From this, it was possible to set up a series of polarity.

Medical!

Fast imaging of porous media

J.M. Dereppe, C. Moreaux and R. Demeure
University of Louvain, Belgium.

The study of fluid displacements in porous media is of considerable interest for the oil industry in providing a better understanding of the oil recovery process. High speed imaging techniques are in principle required so that a steady state situation can be visualised as a fluid is forced through a porous solid.

Several methods of fast imaging have been described. Single shot imaging such as a modified version of echo planar imaging (EPI) (1) may be used. Nevertheless this approach imposes rather severe condition to the spectrometer hardware. Multiple shot technique such as the fast low angle shot (FLASH) method are not so demanding and may be used on many conventional imaging system (2).

It is well known that gradient refocused experiments are not well suited for the observation of fluids in porous media as the magnetic field inhomogenities induced by susceptibility differences at the solid liquid interface are not compensated as in a spin echo experiment. Nevertheless these methods can be applied in favorable case to obtain good quality images in very short time, 200 or 400 ms for a 128 x 128 image.

High quality proton density images of a water saturated chalk core were obtained in less than 400 ms by using the SNAP method. The images show the expected variation with the flip angle value for oil and water filled chalk samples. An apparent T1 was also measured by using a 180° inverting pulse followed by the acquisition of a series of image during the magnetization recovery process. The difference in the T1 value for oil and water saturated sample is larger at low flipping angle and largely sufficient to discriminate oil and water in partially saturated samples.

The restriction in the application of FLASH imaging is mainly due to short T2* value. Practically any sample having a T2*, defined as $1/\pi\Delta\nu_{1/2}$ larger than 0.5 ms i.e. $\Delta\nu_{1/2} < 500$ Hz may be imaged by FLASH-MRI.

1- GUIL FOYLE D.N. and MANSFIELD P. *Magn.Reson.Imaging* 9,775-777,1991

2- HAASE A. *Magn.Res.Med.* 13,77-89,1990

Improved spatial resolution in Lee-Goldburg Magic Angle Imaging of Solids

F. De Luca, B.C. De Simone, F. Di Nunzio, N. Lugerì, B. Maraviglia

Dipartimento di Fisica, Università "La Sapienza"

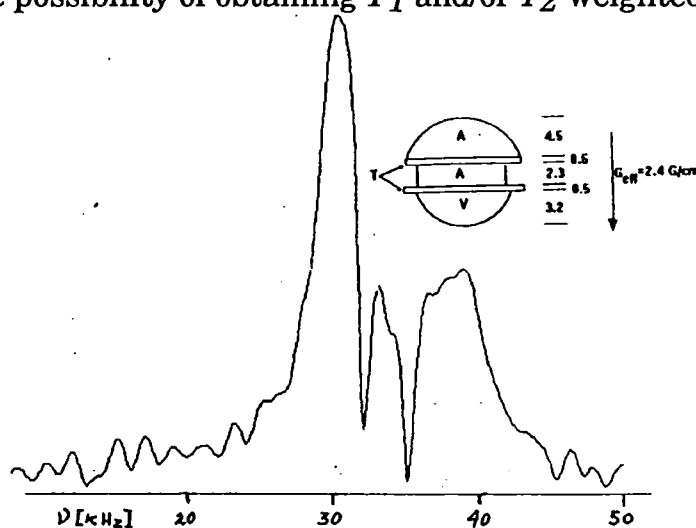
P.le Aldo Moro, 2 00185 ROMA, Italy

In recent years a new method of Solid State Imaging [1,2] based on the indirect detection (Lee-Goldburg experiments [3]) of the Magic Angle narrowed solid sample spectra in the Rotating Frame (RCF), has been presented, [4,5]. Spatial discrimination is provided by means of an effective field gradient, under the usual RCF "magic" condition as already proposed in the former version of Magic Angle SSI with direct detection [6].

With a new probe setting and improved sensitivity, a noticeable gain in spatial resolution has been obtained, with respect to the first experiments on Teflon samples ($\Delta\nu=10\text{kHz}$, $\Delta r=1\text{mm}$). The results of the experiments performed on Adamantane ($\Delta\nu=18\text{kHz}$), and on other intermediate bandwidth systems have shown a spatial resolution estimated on a few hundreds of μm , as show in fig. 1.

Experiments on such different samples (polycrystalline, amorphous, polymers) are in progress in order to confirm the wide range of applicability and the easiness of the method and, moreover, to show the possibility of obtaining T_1 and/or T_2 weighted images in a simple manner [7].

Fig.1: One-dimensional projection of the sample sketched in the figure (A=Adamantane; R=Vulcanized Rubber; T=Teflon). All dimensions in mm



References

- [1] *NMR Microscopy*. Edited by B. Blümich and W. Kuhn, VCH Verlagsgesellschaft (1992).
- [2] P. Blümli, B. Blümich *NMR Imaging of Solids* on "*NMR Basic Principles and Progress*" (1993)
- [3] M. Lee, W.I. Goldberg, *Phys. Rev.*, **140**, 1261 (1965)
- [4] F. De Luca, N. Lugerì, B.C. De Simone and B. Maraviglia, *Solid State Comm.* **82**, 151 (1992)
- [5] F. De Luca, B. C. De Simone, N. Lugerì and B. Maraviglia, *J. Magn. Reson.*, **102**, 287 (1993)
- [6] F. De Luca and B. Maraviglia, *J. Magn. Reson.*, **67**, 169 (1986)
- [7] F. De Luca, N. Lugerì, B.C. De Simone and B. Maraviglia, *Coll. and Surf.* (In press)

MR microimaging studies of the imbibition of miscible liquids by dense polymers and resin matrix composites

S.N. Scrimgeour^{1,2}, C.H. Lloyd¹, J.A. Chudek² and G. Hunter^{2*}

¹Department of Dental Prosthetics and Gerontology,

²Department of Chemistry,

The University of Dundee, Dundee DD1 4HN, Scotland, UK

Dense polymers and structural composites are frequently used in liquid environments. The selection of material for a particular purpose is usually made on the basis of low liquid absorption and the retention of structural integrity. Traditionally, imbibition studies have been restricted to diffusion of a single liquid. The simultaneous absorption of more than one liquid has largely been ignored due to the extreme difficulty of differentiating between diffusing species. We have found that the absorption of multicomponent single phase liquids can be ideally studied by MR microimaging. As exposure to pure liquids in reality is the exception rather than the rule the application of this technique has widespread potential.

Our studies have included MR microimaging of diffusion of binary liquid mixtures into dental PMMA and the effect of multi-component liquid mixtures and their individual constituents on commercial polyester resins, both pure and laminated.

Cylinders of dental PMMA were soaked in binary liquid mixtures of differing ratios for periods of up to three days. Both normal and deuterated solvents were used. 3D MR microimages (XY3DSE) were acquired simultaneously for one-, two- and three-day specimens and again 24 h later to assess the effects of drying out and solvent exchange. CSS imaging was also carried out. Surface reconstruction of the 3D data sets showed the progress of the solvents into the PMMA. We have found that in, for example, an acetone/water mixture there is a synergistic effect with *both* liquid components being rapidly absorbed into PMMA. Normally water uptake is only 2% by weight after several weeks immersion in pure water. The kinetics of replacement of H₂O by D₂O have also been studied.

Samples of five different polyester resins were soaked in single organic solvents and in binary and quaternary liquid mixtures for various lengths of time. MR microimages were obtained for all samples where detectable diffusion had occurred. 3D MR microimages of a sample of a laminated resin which had been soaked in a binary mixture for 18 months were also obtained. Each component of the liquid mixture was imaged selectively. The polymeric materials showed a wide variation in their resistance to the liquids and liquid mixtures. In general the behaviour of the polymers in pure liquids was as anticipated. Immersion in particular binary mixtures had catastrophic consequences in a relatively short time for some polymers. Surprisingly, this was not the case for quaternary mixtures - there was greater resistance, with performance resembling that in the pure liquids.

ABSTRACT

The 2nd International Conference on
Magnetic Resonance Microscopy; The Heidelberg Conference.

September 6-9, 1993

THE APPLICATION OF GRADIENT NMR TECHNIQUES
TO WETTING AND DRYING PROCESSES IN POROUS MEDIA.

G.J.Nesbitt

Koninklijke/Shell Laboratorium, Amsterdam

Models describing the transport of fluids through porous beds incorporate certain assumptions with respect to mass transfer at a particle interface. The nature of the adsorption/desorption profile drives the intraparticle mass transfer which in turn can be controlled by local conditions to be surface or pore diffusion sensitive. Validation of the models in this respect has been limited, however it is known that drying conditions influence the deposition of adsorbate onto support material.

For this reason NMR gradient techniques have been used to investigate drying and wetting processes in silica extrudate. The results show conclusively that deviations from theory can be detected and investigated more fully. Quantitative determination of the local transport coefficients allows the interpretation of bulk processes.

NMR Microscopy in Metals with sub- μ m Resolution

G. NEUE, TH. GEILKE

Physikalische Chemie, Universität Dortmund,
44221 Dortmund, Germany

and

U. SKIBBE

Department of Physics and Biophysics, Massey University,
Palmerston North, New Zealand

To examine metals by NMR spectroscopy is complicated by the action of the skin effect. As useful as it is for shielding probe heads from unwanted external radiation so troublesome is it if the sample itself is a metal. According to Maxwell's equations the magnitude of B_1 fields as well as their phases are non-uniform throughout the sample. Thus NMR was considered to be impossible in thick conductors and fine powders were used instead.

But the same effect can be used to obtain spatial resolution as it produces a magnetic field gradient (of the B_1 field)[1]. Thus it is a potential basis for an imaging method. It is demonstrated that for a great variety of sample geometries images can be reconstructed. Due to strong attenuation of the rf within the metal, gradients of the order of 1000 T/m are the rule. These extraordinarily large values translate into a spatial resolution that no other NMR imaging method can provide. SEEING-NMR (Skin Effect Enhanced Imaging) is shown to be able to resolve structures down to 100 nm. Technically, it belongs to the class of rotating frame imaging[2]. But in contrast to rotating frame imaging by surface coils the geometry of the gradients is much simpler, especially for thick¹ conductors.

Examples are given for the application of SEEING-NMR to layered materials. It is shown that it is a rather general technique to study the chemistry and spatial homogeneity in metals.

References

- [1] U.Skibbe, G.Neue
Colloids and Surfaces, **45** (1990) 235
- [2] D.I. Hoult
J. Magn. Reson., **33** (1979) 183

¹ As compared to the skin depth, typ. 10 μ m.

Solid State NMR Imaging using strong Gradients (STRAFI)

K. Zick, Bruker Analytische Meßtechnik, Germany

STRAFI (STRay Field Imaging)^{1,2,3)} is a high gradient imaging method, using the static gradient outside of the centre of a superconducting NMR magnet. STRAFI is originally designed for imaging of solid state samples, but the advantage of this method was also shown for imaging of liquid samples in the presence of magnetic distortions⁴⁾ and for investigations of nonequilibrium slow diffusion⁵⁾.

The basic experiment, i. e. the acquisition of a projection is done as follows: A sequence of selective pulses is applied to the sample in the strong gradient and the amplitude of the echoes, representing the total magnetisation of the excited slice, is detected. The slice is defined by the local magnetic field strength and the applied frequency. This position is called sensitive plane. Then the sample is moved in order to bring the consequent slice into the sensitive plane. In this way a projection is acquired directly in the frequency domain. This is comparable to a cw NMR experiment, but instead of sweeping the magnetic field, the sample is moved in the field gradient. 3D spatial resolution is achieved by rotating the sample about two perpendicular axis.

The sensitive plane is a selected position in the stray field of the magnet, such that the magnetic field is constant across a plane surface perpendicular to the direction of the magnetic field. This allows to get flat slices thus facilitating the reconstruction of the data significantly.

Due to the unusual data acquisition the S/N is somewhat different compared to usual imaging methods. As a special advantage the required filter bandwidth is determined by the bandwidth which corresponds to one slice and not to the whole field of view. A short discussion of the signal to noise properties of STRAFI will be given in the talk.

The spatial resolution of STRAFI depends only on the mechanical motion as long as the echo time can be kept short compared to T_2 .

References:

1. A. A. Samoilenko, D. Yu. Artemov, and L. A. Sibeldina, Bruker Rep. 2, 30 (1987)
2. A. A. Samoilenko and K. Zick, Bruker Rep. 1, 40 (1990)
3. A. A. Samoilenko and K. Zick, in "Proceedings, 25th Congress Ampere on Magnetic Resonance and Related Phenomena, Extended Abstracts, Stuttgart 1990" (M. Mehring, J. U. von Schütz, and H. C. Wolf, Eds.), P. 92, Springer-Verlag Heidelberg, 1990
4. P. Kinchesch, E. W. Randall, and K. Zick, JMR 100, 411 (1992)
5. P. McDonald et al. to be published

Molecular Dynamics of Polymer Networks as Studied by NMR-Microscopy

W. Kuhn, P. Denner[#], P. Barth, S. Hafner, G. Simon^{*}, H. Schneider^{*}

Fraunhofer-Institut für Biomedizinische Technik, Ensheimer Str. 48, D-66386 St. Ingbert,
[#]Pädagogische Hochschule Erfurt, ^{*}Universität Halle, Germany

During the last few years it has been shown that spatially resolved NMR can be a valuable tool for the investigation of semirigid polymers. The spatially resolved measurement of relaxation parameters can allow the identification of regions of aging and different crosslink densities within a polymer sample.

The transformation of NMR parameters such as relaxation times to the corresponding molecular motional parameters are a challenging task, since appropriate models of molecular motions must be applied.

Based on our spatially resolved measurements of T_1 , T_2 and $T_{1\rho}$ at several B_1 -field strengths a first attempt was made to correlate molecular properties such as crosslink densities, crosslink density inhomogeneities and the diffusion length of molecular entanglements in sulfur cured carbon black filled natural rubbers with NMR parameters derived from parameter selective images.

The interpretation of the measurements is based on calculations according to the "Limited Translational Defect Diffusion Model" and a mixed "BPP-Anderson-Weiss" theory.

Use of MR microimaging for the measurement of the depth of cure for VLC dental composite filling materials

C.H. Lloyd¹, S.N. Scrimgeour^{1*}, J.A. Chudek², R.L. Mackay², G. Hunter², D. Pananakis³ and E.W. Abel³

¹Department of Dental Prosthetics and Gerontology, Dental School,

²Department of Chemistry,

³Department of Biomedical Engineering

University of Dundee, Dundee DD1 4HN, Scotland, UK

Biocompatible resin containing up to 80% micron size glass particles is widely used now as filling material for the restoration of decayed teeth. The plastic mass which is packed into the prepared cavity is converted to a rigid, durable and aesthetic solid by the presence of an initiator activated by blue light. When setting is required an intense light source is applied to the surface of the restoration. The intensity of this light falls with depth into the restoration, thereby restricting effective hardening to a limited depth, 'the depth of cure'. Controversy surrounds this important parameter due to its arbitrary definition, a consequence of existing measurement methods.

Cylinders of a commercial product (Occlusin, ICI Dental) were cured from one end for clinically realistic exposure times. MR microimages of 2 mm longitudinal sections (ie parallel to the direction of the light beam) were obtained using a standard Bruker spin-echo pulse sequence. Following this the images were captured using a video acquisition card and stored in a PC. The vertical (20% image width) central strip was divided into 80 (averaged) segments and intensity/depth profiles built up.

A second series of specimens (subjected to identical curing) was used to determine Vickers (Micro)hardness as a function of distance from the light source. Following these measurements uncured and soft partly cured material was scraped away and the remaining hard polymerised material measured with a micrometer. Both methods, which are currently used, have deficiencies which cause uncertainties in the value.

For the MR microimages, there is a difference in contrast sufficient to enable the monomer to be differentiated from the polymer. For a wide range of curing times, good agreement exists between micrometer and MR microimaging measurement of depth of cure. Both give consistently greater values than microhardness measurement (to the last practical indentation). Such differences are explicable through the relationship between the geometry of the curefront and the particular method of measurement.

Demonstration of the linear dependence of magnetisation transfer on polymer concentration in aqueous solutions at two different field strengths.

J. J. Tessier[†], T. A. Carpenter[†], J. A. Tyler[†] and L. D. Hall[†]

[†] *Herchel Smith Laboratory for Medicinal Chemistry,
University of Cambridge School of Clinical Medicine,
University Forvie Site, Robinson Way,
Cambridge, CB2 2PZ United Kingdom*

[‡] *Strangeways Research Laboratory,
Worts Causeway,
Cambridge, CB1 4RN United Kingdom*

Saturation transfer experiments were performed at 85 MHz and 300 MHz to measure the magnetisation transfer (MT) rate as a function of macromolecular content. For this purpose calcium alginate gels with an internal concentration gradient were prepared from aqueous sodium alginic acid and calcium ions. Sodium alginate produces solutions whose viscosity increases with concentration. In contrast, calcium alginate is a solid gel even at low concentrations and hence provides a matrix with a long motional correlation time and a variable proportion of polymer-based hydroxyl protons.

Although aqueous sodium alginate did not exhibit any MT, the proton magnetisation transfer rate in calcium alginate gels was found to depend linearly on the concentration of polysaccharide. Since this rate did not depend on the field strength, the dominant mechanism for MT in these systems is either chemical exchange or a highly efficient intermolecular cross-relaxation process.

The high sensitivity of the MT ratio observed for low gel concentrations suggests that Magnetisation Transfer Contrast Imaging will be an excellent tool to monitor changes in chemistry, mobility and concentration of slow-moving polymer occurring at low macromolecular content.

Dynamical and structural parameters of polymer networks - a local study by parameter-selective NMR microimaging

by G. Simon, H. Schneider, Barth^{*)} and W. Kuhn^{*)}

Martin Luther University Halle, Department of Physics
Fraunhofer Institute St. Ingbert^{*)}

Abstract:

We demonstrate the possibilities of NMR relaxation and spectroscopy for obtaining dynamical and structural parameters of polymer networks such as (i) crosslink density, (ii) correlation times and (iii) molecular order under uniaxial stress.

A main tool for the determination of (i) and (ii) is the transversal ^1H -NMR relaxation which can be understood in the framework of chain models with anisotropic segmental motion. This anisotropy is sensitive to the dynamical and structural state of the network and leads to a residual dipolar interaction of protons which is reflected in the relaxation curves in a characteristic way.

The parameters can be extracted from the transversal relaxation curve of each voxel by NMR-microscopy and enable parameterselective pictures.

The molecular order in uniaxial stressed networks (iii) and consequently the molecular interaction under stress can be studied by ^2H -NMR spectroscopy if the networks are deuterated or slightly swollen by deuterated solvents. Possibilities of use in NMR microimaging are discussed.

First ^1H -NMR results of parameter-selective microimaging are demonstrated for crosslinked natural rubber.

NMR Microscopy in Biomedicine

Laurel O. Sillerud

Biomedical NMR Facility, Division of Life Sciences,
Los Alamos National Laboratory
Los Alamos, New Mexico 87545 USA.

NMR microscopy refers to the generation of NMR images with resolutions on the order of 1-10 microns. At this resolution NMR microscopy does not directly compete with other microscopy methods for the elucidation of tissue structure; rather it is uniquely sensitive to details of molecular structure, chemical dynamics and intermediary metabolism, which are inaccessible by other means. The high in-plane resolution provided by NMR microscopy is possible because samples are observed with NMR instruments operating at fields far above those used for routine clinical NMR imaging. These high-field systems also offer markedly greater sensitivity over clinical imagers and since resolution is strongly dependent on signal to noise ratio the length scales observable are consequently much smaller. The fact that the length scales characteristic of NMR microscopy are on the order of microns renders this method sensitive to dynamic details of molecular and bulk sample motion. The intensity of the NMR signal from a given voxel depends on a number of physical factors, in addition to the spin density. Contrast is generated by motion, differences in spin-lattice (T1), and spin-spin (T2) relaxation times, and by spatial differences in diffusion, since the mean free path for water in biological samples is often on the order of a few microns. For these reasons, NMR microscopy is an excellent method for measuring the diffusivity of molecules in situ, without destroying the sample. We have been pursuing NMR microscopy at 400 MHz for the last 7 years. This presentation will not serve as a general review of the subject, but will report studies of importance for evaluating possible directions for NMR microscopy in the future, as well as results from our own work in areas of particular interest in renal, tumor and neurobiology. We have concentrated on the examination of restricted diffusion in tumor spheroids and renal transplants, and on monitoring the progress of spinal cord injury and the development of methods for metabolic NMR microscopy.

NMR MICROSCOPY IN PHARMACEUTICAL RESEARCH

Susanta K. Sarkar and Rasesh D. Kapadia

**SmithKline Beecham Pharmaceuticals
709 Swedeland Road, King of Prussia, PA 19406, USA**

NMR microscopy provides an important method to monitor diseased states and its response to novel therapeutics in animal models *in vivo*. We have extended the 2- and 3- dimensional NMR microscopy techniques to several areas of pharmacological research including cardiovascular, cerebrovascular and inflammation therapeutics. An *in vivo* resolution of 40 x 40 x 250 μm is now routinely being observed at 9.4 T in our laboratory.

Examples from following disease processes in animal models will be presented: a) Stroke; b) Arthritis; c) Osteoporosis. The correlation between NMR microscopic images with histology (light microscopy) will be described and the utility of NMR microscopy in future drug discovery research will be discussed.

Spatial Heterogeneity of Macromolecular-Water Interactions in Human Articular Cartilage

E. McFarland, M. Dunham, and H. Dai, Department of Chemical and Nuclear Engineering, University of California, Santa Barbara (mcfar@engrhub.ucsb.edu)

Introduction: Cartilage is one of the few biological systems where the small scale (<1 μm) complexity of the system is tractable, however, there is sufficient large-scale (>10 μm) heterogeneity that magnetic resonance microscopy can be used for quantitative analysis. Additionally, it is a biomaterial of major importance medically. Considerable non-NMR biochemical work has been done in cartilage and the chemical constituents are well characterized. The matrix is approximately 75% water with dissolved NaCl. The dehydrated mass is 50% collagen and 15-30% strongly hydrophilic proteoglycans (PG) made up of several types of glycosaminoglycans (GAG) covalently bound to a protein core. Interlinked subsurface collagen arcades form mesh spaces with "pore" sizes ranging from 60-200 where proteoglycan aggregates reside. The small scale interactions can be thought to take place within the pores and are defined as water-collagen, water-PG, and restricted diffusion. These interactions take place in volumes well below the resolution limit of NMR. It is known that the concentration of PG and collagen vary across the cartilage thickness and possibly in response to pathological processes. Correlating these variations to changes in NMR variables was an objective of this research. Furthermore, we sought to improve our understanding of the dynamics of water cartilage interaction in cartilage and how it related to function in health and disease.

Methods: We studied cartilage obtained from patients immediately following total knee replacement surgery. The samples were imaged at 1.5T, 7T, and 11.6T and relaxation times, diffusion coefficients, and spin transfer coefficients (k_{mt}) were determined across the cartilage matrix under several selected perturbations including temperature and pH variations. $T_{1\rho}$ images were obtained using a spin lock time of 40 - 80ms with H_1 set for $\omega_1 = 1\text{kHz}$. The values were correlated to proteoglycan and collagen content determined biochemically.

Results: Images were obtained and analyzed at each field strength from samples from several patients. Excellent correlation between proteoglycan content and relaxation times was obtained indicating the importance of the water-PG interaction. Images will be presented showing marked contrast in the magnetization transfer images and not seen in T_1 and T_2 images. The table below gives values obtained at 7T from one patient.

REGION	[H / H ₂ O]	T ₁ (ms)	T ₂ (ms)	[D / D _{H₂O}]	k (s ⁻¹)
<i>Surface</i>	0.92	1437	38 ± 2	0.76	0.37
<i>Subsurface</i>	0.99	1306	34 ± 2	0.67	0.56
<i>Central Matrix</i>	0.83	1004	28 ± 2	0.52	0.77
<i>Prolif. Zone</i>	0.35	439	25 ± 1	0.32	1.73
<i>Fat</i>	0.46	276	26 ± 3	0.03	2.94
<i>Saline</i>	1.00	1554	89 ± 12	1.00	0

Conclusions: Resolution obtainable with magnetic resonance microscopy is sufficient to study spatial variations in water interactions with cartilage matrix. Significant diffusion, T_1 , $T_{1\rho}$ and T_2 differences are observed corresponding to histologically and biochemically definable zones. The $T_{1\rho}$ and k_{mt} results indicate that exchange processes occurring with correlation times smaller than 1 kHz also vary significantly within the cartilage matrix.

NMR Microscopy on the human body

J. C. Széles, M. Grabenwöger, M. Grimm, C. Leukauf, E. Feichtinger, U. Losert¹, E. Wolner
II. Chir. Univ. Klinik Wien und ¹Zentrum für Biomedizinische Forschung der Univ. Wien

S. Mészáros

Institute of Nuclear Research of the Hungarian Academy of Sciences

Nuclear Magnetic Resonance (NMR) Microscopy has advanced rapidly over the past years, but nevertheless, the restrictions still limit its use for clinical, in vivo experiment. A conceptual method that is currently in the testing process, approaches the possibilities of application of NMR microscopy on small areas and extremities of the human body as well as the technical solutions to perform NMR microscopy in these applications.

The following applications will be presented:

- ♦ NMR detection of the human extremities with specially devised equipment for the requirements of in vivo, and real time NMR,
- ♦ View of sensory receptors at the human ear and simultaneous detection of the sodium activity in order to see *the sensory receptors in action*,
- ♦ Non-destructive detection of small vessels and capillary structures at the finger and toe,
- ♦ Image of endothelial cells at the inner wall of blood vessels.

Spatial resolution in NMR microscopy can be improved by applying high magnetic field gradients, tightly coupled pick-up coils and low-noise detection arrangements, but have not yet been adapted for in vivo investigations. Therefore, two proposed solutions are analysed in this project.

Technical solutions to observe small size objects which have been worked out up to this time include the development of putting the object into the bore of high-field magnets. NMR Microscopy has been used for in vivo experiments on small animals and therefore the small size bore of these coils (100 to 150 millimeters) could be adapted for NMR application on the human body, specifically for viewing the human ear, finger, and toe. A special magnet system could be constructed where the necessary field profile for NMR could be implemented with, for instance, earphone-like pick up coils and using conventional NMR detection.

The object could be to directly detect the change in the static magnetic moment by using a SQUID (super-conducting quantum interference device) biomagnetic device with low-field magnetic system of conventional air-core copper coils. The coupling of the SQUID is performed with a third order superconductive gradiometer to eliminate external magnetic disturbances. Initial testing has proved that signals can indeed be obtained by using the SQUID.

Calculations and initial experimental results regarding these technical solutions will be presented.

Cyclocreatine toxicity in multicellular tumor spheroids: 31P NMR spectroscopy and diffusion NMR Microscopy

*Y. Steinfeld, *G. Meir, *C. Tempel, *M. Neeman and #M. Cohn

*Department of Hormone Research, Weizmann Institute of Science, Rehovot 76100, ISRAEL
and #Department of Biochemistry and Biophysics, University of Pennsylvania,
Philadelphia PA 19104-6089 USA

Multicellular spheroids are spherical cellular aggregates that provide an excellent model for the study of micro-environmental heterogeneity in tumors. We are interested in the transport mechanism of creatine and its analog cyclocreatine in multicellular tumor spheroids since we found that cyclocreatine inhibits in some cases cell proliferation and destroys cellular integrity throughout the viable rim of the spheroid.

Creatine is accumulated in many cell types and phosphorylated by creatine kinase to form phosphocreatine (Pcr). Cyclocreatine, an analog of creatine, is phosphorylated by creatine kinase as is presumably transported by the same mechanism as creatine. Our goal is the elucidation of the transport mechanism for cyclocreatine and its cytotoxicity. Here we report ³¹P NMR spectroscopy and diffusion NMR microscopy studies of cyclocreatine uptake in multicellular spheroids of two cell lines: C6 glioma and OC238 human ovarian cancer. Cyclocreatine inhibited cell growth for both cell lines. Swelling and destruction of cellular integrity was most prominent for C6 glioma cells but no membrane rupture was observed by propidium iodide staining. The other line showed no histologically obvious cell damage.

³¹P NMR spectra of spheroids derived from C6 glioma cells showed intrinsic signal due to PCr. The ovarian cancer cell line showed no phosphocreatine signal. Following addition of 5mM cyclocreatine, a rapid uptake of cyclocreatine was observed for C6 glioma cells but not for the OC238 ovarian cancer cells. Iso-osmotic replacement of NaCl by KCl or choline chloride ([Na⁺]=155mM and 45mM respectively) resulted in a markedly reduced rate of uptake that could be induced by replacement of sodium for the three cell lines that accumulated cyclocreatine. The spectra was taken in a 500 MHz AM Bruker spectrometer.

Diffusion weighted images of C6 glioma spheroids, taken in a 400 MHz AMX Bruker spectrometer, resolve the viable rim appearing as a bright region and the dark necrotic center. The diffusion coefficients for water were $2.44 (\pm 0.18) \times 10^{-5}$ cm²/s for the medium, $0.48 (\pm 0.13) \times 10^{-5}$ cm²/s for the viable rim and $0.62 (\pm 0.08) \times 10^{-5}$ cm²/s for the necrotic center. A time course of cyclocreatine uptake was obtained by accumulating sequential sets of diffusion images. Using the slow diffusion filter to attenuate extracellular water, we observed increasing self diffusion coefficients of the intracellular water in the viable rim of C6 spheroids after cyclocreatine treatment: $0.62 (\pm 0.02) \times 10^{-5}$ cm²/s after 48 hours in 20mM cyclocreatine. This fact correlates with the swelling of cells observed in histological sections.

Projections of the intracellular cyclocreatine of a perfused C6 spheroid were taken with a one dimensional chemical shift imaging pulse sequence which takes advantage of the chemical shift difference between water and cyclocreatine and the slower diffusion of the intracellular metabolites.

Cyclocreatine shows unusual interference with cell proliferation. One mechanism of its toxicity to tumor cells appears to be related to the control of cellular osmotic pressure rather than to a direct effect on energetics. The cotransport of sodium with cyclocreatine presents the cells with an increased osmotic stress which will affect quiescent cells that are energetically compromised at least to the same extent that it will affect the outer proliferating cell layer. This swelling is observed by light microscopy and is also apparent in the diffusion NMR microscopy studies. Another, yet unknown mechanism must be invoked to explain the effect of cyclocreatine on cell proliferation in the ovarian cancer cells, which showed no accumulation of phosphocyclocreatine. Despite the obvious cytotoxicity of cyclocreatine the cellular NTP content remains unchanged, and is probably buffered by the high PCCr content.

HIGH RESOLUTION NMR MICROSCOPY OF THE PERFUSED RAT KIDNEY

William E. Hull, DKFZ Heidelberg, Germany

**Tumor Architecture and Physiology:
a Chronological Approach using ^{19}F 3D NMR Microscopy of Perfluorocarbons**

Ralph P. Mason, Anca Constantinescu & Peter P. Antich,
Department of Radiology, UT Southwestern Medical Center, Dallas, TX and
Peter Peschke & Eric W. Hahn,
Schwerpunkt Radiologie, DKFZ, Heidelberg, Germany.

^1H MRI is used extensively to determine the location and extent of tumors and paramagnetic contrast agents such as Gd-DTPA may indicate regional perfusion. We have been exploring the use of perfluorocarbon blood substitute emulsions (PFCE) to probe tumor physiology. We report a novel approach to investigating tumor architecture using combined ^{19}F and ^1H MRI. Following IV infusion to animals a significant portion remains sequestered in tumors for many weeks facilitating longterm investigations during growth.

Tumor Growth: We have examined the Dunning prostate adenocarcinoma AT1 grown in a skin pedicle on the fore-back of a Copenhagen rat. This is a relatively slow growing tumor (volume doubling time ~ 5 days) and appears histologically homogeneous. The tumor was allowed to grow to ~ 1 cm diameter, then 4 x 4 ml Oxypherol (20% w/v emulsion of perfluorotributylamine) was infused IV in the tail over 2 days. The tumor was examined by NMR over the next 16 days with submillimeter in-plane resolution ($\sim 470 \times 300 \mu\text{m}$ with 5 mm slice thickness). ^1H MRI at 4.7 Tesla disclosed no anatomical heterogeneities in the tumor. ^{19}F MRI was used to reveal the distribution of perfluorocarbon in the tumor: immediately after administration of the emulsion the PFC was vascular and extensively distributed throughout the tumor with an intensity related to differential blood flow. After 2 days vascular clearance was complete and ^{19}F MRI revealed the enhanced peripheral distribution of sequestered PFC. Over the next 16 days the tumor doubled in diameter. Comparison of sequential images indicated that the PFC largely retained its form and extent and did not redistribute, indicating preferential growth from the periphery outwards.

Tumor regression: We have examined the Novikoff hepatoma in the thigh of the Wistar rat. Once the tumor had grown to ~ 1 cm Oxypherol was administered as described above. ^{19}F MRI indicated that the tumor had a multi-nodular structure with peripheral PFC. Over a period of weeks the tumor regressed spontaneously and the outline of the PFC was observed to shrink, but essentially maintain a constant pattern.

Conclusion: Tumor growth and response to therapy has largely been judged on the basis of tumor volume. Sequestered PFC provides architectural landmarks by which growth and regression are readily perceived. Not only is tumor volume apparent but the pattern of change, *e.g.*, peripheral growth and shrinkage is delineated. The longterm retention of PFCs makes them particularly appropriate for the assessment of relatively slow tissue remodelling processes. In future studies PFCs will be used to probe tissue physiology, *e.g.*, regional pO_2 , on the basis of ^{19}F spin lattice relaxation rate, thus, contributing to an understanding of the relationship between tumor size and vascular competence. Whilst contrast agents may be used to assess acute changes in tumor perfusion, they are cleared rapidly and cannot provide longterm landmarks. We believe this approach may be valuable in assessing changes in tumor anatomy in response to therapy. We envision the sequential application of multiple PFCs with individually unique spectra to define changes in tumor anatomy. Given the current use of PFCs in the clinical environment we envisage application to human studies in the near future.

MAGNETIC RESONANCE HISTOLOGY

G. Allan Johnson , Ph.D.¹, Robert D. Black, Ph.D.¹, Gary P. Cofer , M.S.¹,
Xiaohong Zhou, Ph.D.¹, Robert R. Maronpot, D.V.M.²

¹Center for *In Vivo* Microscopy, Duke University, Durham, North Carolina 27710

²National Institute of Environmental Health Sciences,
Research Triangle Park, North Carolina 27709

Magnetic resonance microscopy (MRM) has now advanced to the stage where it rivals conventional optical techniques in delineating tissue structure. It offers three distinct advantages over optical sectioning: a) it is nondestructive; b) it is inherently three-dimensional; c) it allows one to use "proton stains," i.e., T1, T2, diffusion, etc. Acceptance of MRM as a tool in histology is dependent on a) development of acquisition techniques that are efficient and, b) an understanding of the contrast mechanisms underlying the tissue differentiation. This paper addresses both of these issues.

Sensitivity and acquisition time continue to define the resolution limits in MRM. We have increased the available SNR by more than 50 X through the development of a high-temperature superconducting probe operating at 300 MHz with a Q > 40,000. The resulting improvement in SNR translates to a decrease in acquisition time of more than 2000 [Black RD, et al., Science 259:793-795, 1993].

The second barrier, i.e., acquisition time imposed by a large number of views used in 3DFT encoding, has been reduced through the use of fast spin echo (FSE) pulse sequences. FSE has been extended to MRM through a series of innovations that address the shorter T2 encountered at the high fields of MRM, diffusion losses encountered with stronger gradients, and phase errors from cumulative eddy currents arising from strong gradients.

We have applied these techniques in phantoms and specimens at 2.0 T, 7.1 T, and 9.4 T. We routinely acquire image arrays up to 512³ with isotropic resolution < 10 μ m. Correlation with conventional optical sections has been accomplished with registration using local tissue landmarks, e.g., vessels. Different cell types are clearly distinguishable in "T2" weighted images, i.e., images in which the effective echo time is 25-30 ms. Spin lattice relaxation provides limited contrast in the several pathologies studied (small tumors, foci, inflammation, and necrosis). Contrast is driven by a combination of spin spin relaxation and diffusion. Diffusion differences arising from differences in cell nuclear density provides a starting point in relating more conventional stains (hemotoxylin and eosin) to the MR contrast.

This work supported in part by NIH Grant #1 P41 RR05959-03, NSF Grant #CDR-8622201, and NIH Grant #5 R01 ES04187-04A1.

H¹ and P³¹ Spectroscopic Imaging Study of 9L Brain Tumour.

*M. Szayna, * P.Kozłowski, J.K.Saunders, A.Jasiński**

*H.Niewodniczański Institute of Nuclear Physics in Cracow, Poland
Institute for Biodiagnostic, NRC of Canada , Ottawa

Although NMR imaging and spectroscopy separately have been widely applied in tumour investigations for many years , here we report the pilot study of 9L Rat Brain Tumour (classified by some authors as a gliosarcoma) performed using H¹ and P³¹ Spectroscopic Imaging (SI).

36 Fischer -344 rats (male) were used. Measurements were provided in 3 groups: untreated rats with 9L tumour, rats with 9L tumour subjected to radiotherapy and the group of control rats (healthy and radiated rats). MRI and SI were done on a Bruker 4,7T Medspec system using home built rf probe.

Proton images, required for tumour localization were recorded using the standard multislice-multiecho sequence, when water suppression and lactate editing spectra were based on a specially designed ones.

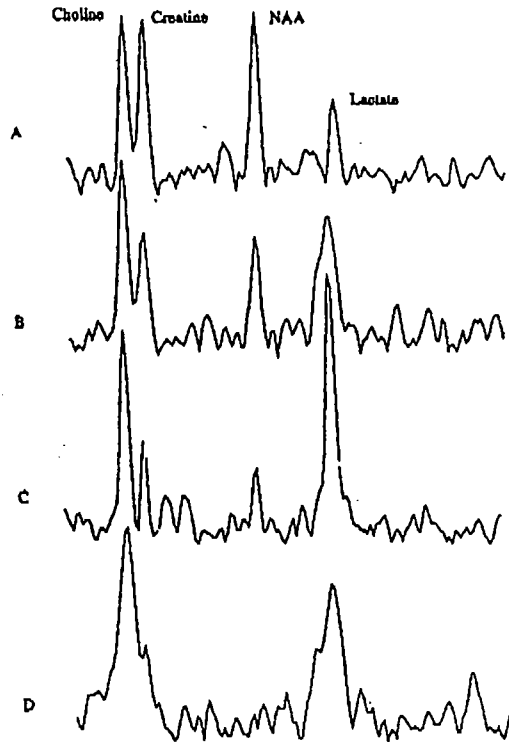
Voxel size, determined by the sensitivity profile of the surface coil and Field of View of the 2D imaging sequence was 1.5 x 1.5 x 1.5 mm for proton and 3.5 x 3.5 x 3.5 mm for phosphorus spectra.

Different intensities of 4 main peaks in proton spectra allow for early discrimination between healthy and tumour brain. This changes were intensified with time (fig.1, 2).

Phosphorus spectra showed the same trends as the proton . Considerable low lactate level was in full agreement with histopatological examinations and proved that 9L tumour do not reveal hypoxia fractions and its high radioresistivity can not be explain in this way. Successful radiation treatment of the tumour reverse trends in the spectra towards to normal ones characteristic for healthy brain.

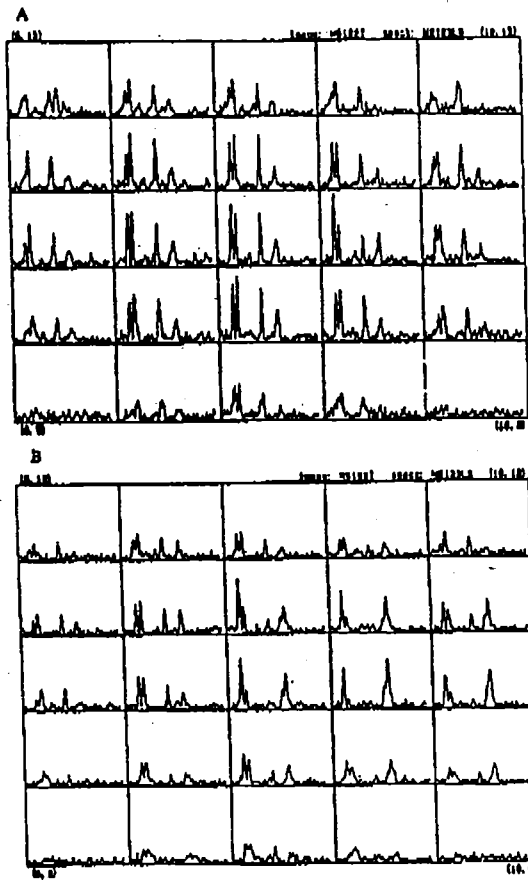
Achieved results have confirmed a possibilities to utilize SI to observe not only the changes in the metabolite concentration during tumour growth but to follow the effects of radiotherapy as well.

Moreover the choline to creatine ratio seems to be very sensitive indicator of cancer process.



LACTATE EDITED SPECTRA OF THE RAT BRAIN WITH UNTREATED 9L TUMOR
(the same voxel as a function of time)

A - 12 days after inoculation, B - 19 days after inoculation
C - 20 days after inoculation, D - 23 days after inoculation



LACTATE EDITING SPECTRA OF THE RAT BRAIN WITH 9L TUMOR

A - 20 days after inoculation
B - 24 days after inoculation

Self-Diffusion of Water in Cartilage

C. Raible, F. Grinberg, Y. Morita†, K. Gersonde

Fraunhofer-Institut für Biomedizinische Technik, and Fachrichtung Medizintechnik, Universität des Saarlandes, St. Ingbert, Germany, † Departement of Orthopaedics, Kyoto Prefectural University of Medicine, Japan

Introduction

Cartilage is a connective tissue with high water content (65 - 80%). The molecular extracellular components are collagen fibres and hydrophilic glycosaminoglycans (GAGs). The degeneration of cartilage is accompanied by a loss of proteoglycans and hence a change of the content and the mobility of water. It is the objective of this presentation to demonstrate that pulsed-field-gradient NMR (PFG-NMR) enhances the visual contrast between different zones of cartilage. In a first step the self-diffusion constant of water was assessed employing simple models of cartilage. In a second step bulk diffusion measurements of normal and degenerated articular cartilage were performed to investigate the molecular translational mobility of water in the weight-bearing zone of hyaline cartilage. In a third step diffusion imaging was performed under in vitro conditions to measure the diffusivities of water in cartilage as a parameter for the spatial mapping.

Materials and Methods

All measurements were performed on a 9.4 T NMR spectrometer (MSL 400, Bruker) equipped with a microimaging unit. The diffusivity of the water molecules was obtained by employing the stimulated echo technique. The diffusion magnetization decays have been measured as a function of the diffusion time (t_{diff}) with $22 \text{ ms} \leq t_{diff} \leq 990 \text{ ms}$. The duration of the gradient pulse (δ) varied in the range from 1 ms to 6 ms. Bulk diffusion measurements were performed with two polymer solutions of GAGs: (i) hyaluronic acid/H₂O, and (ii) chondroitin-4-sulfate/H₂O with concentrations varying between 10% and 70% (w/w). In cartilage of young chicken femoral condyles bulk diffusion measurements and diffusion imaging were performed. Degenerated cartilage was prepared from normal cartilage specimens by incubation in activated chymopapain.

Results and Discussion

Bulk Measurements of Cartilage Model Systems and Articular Cartilage

Articular cartilage and the above mentioned polymer solutions exhibit smaller diffusion coefficients, than free water. The apparent diffusion constants (D^{app}) slightly decreases for articular cartilage and for the polymer solutions at concentrations of $\geq 50\%$ (w/w) in the range of $t_{diff} \approx 100 \text{ ms}$ and does not depend on the diffusion times for values of $100 \text{ ms} \leq t_{diff} \leq 1000 \text{ ms}$. The experimental results qualitatively correlate with the model of diffusion in restrictive media with permeable barriers.

In vitro Imaging of Cartilage

In comparison to the diffusion constant of free water, the diffusion image of spongy bone and cartilage indicate a hindered motion of water molecules. The diffusion constants, measured in the cartilage zones, are at least a factor of two smaller than free water. The diffusion constants of the different zones of the fine structures differ remarkably. Growth cartilage exhibits the largest, hyaline cartilage a medium and spongy bone the smallest diffusion constant. Diffusion-weighted images also exhibit fine structures. Due to the short acquisition time, they are useful for clinical studies.

Conclusion

- PFG-NMR microscopy and spectroscopy offer detailed information about the state of water in cartilage.
- Diffusion imaging is an effective method for the non-invasive visualization of fine structures in joint cartilage.

DEPICTION OF DENTAL ANATOMY BY MAGNETIC RESONANCE MICROSCOPY

Michael A. Baumann, Dieter Groß* and Klaus Lehmann*

Policlinic of Operative Dentistry and Periodontology
Johannes Gutenberg-University, Augustusplatz 2, D - 6500 Mainz

* Bruker Analytische Meßtechnik, D - 7512 Rheinstetten

When a tooth is treated endodontically a dental radiograph and the experience of the dentist at the moment are the only support for getting a spatial imagination of the crown and especially root anatomy of the tooth. A lot of research in the past was done to exhibit variations in dental anatomy to have at least a statistical statement about the contour and form of the root canals. Nowadays magnetic resonance microscopy (MRM) seems to be an interesting technique which may be a new tool for endodontic diagnosis.

An extracted human central incisor was stored in a solution of 10% formaline and then given into a MRM. The experiments were performed in a BRUKER spectrometer AMX 300 WB with a microimaging attachment. The signal analysis was carried out by a 3D-Fourier-transformation. The following two or three dimensional reconstruction of the data set was done by a special software (UXNMR, Bruker). The edge length of the detected voxels reached 100 microns.

Using magnetic resonance microscopy totally new sights into dental anatomy could be reached. The outer contour of the hard substance as well as the soft tissue - the pulp - could be shown exactly opening the possibility to give the dentist a non-destructive diagnostic aid without using ionizing radiation as it is necessary within dental radiography.

MR Microscopy Study of Honey Bee *in vivo*

Z. Sułek, A. Jasiński, B. Tomanek, F. Hennel, J. Kibiński, T. Skórka,
A. Krzyżak, P. Kulinowski and J. Muszyńska*

Niewodniczanski Institute of Nuclear Physics, 31-342 Kraków, Poland

*Research Institute of Pomology and Floriculture, Division of Apiculture,
24-100 Puławy, Poland

Magnetic resonance (MR) microscopy may be a useful tool in studying morphology of small size animals and plants, transport and diffusion of water in living systems and materials containing protons interesting for technology. Honey bee is an interesting object for MR microscopy, which was not studied nondestructively so far.

A MR microscope based on a 6.4 T narrow bore vertical magnet, a broad band rf electronics, and an IBM PC controlling via CAMAC interface purpose build modules was constructed. The microscope operates under the control of MARIS-PC software system. The gradient system consisting of specially designed actively shielded gradient coils, gradient controller and Techron 7570 amplifiers delivers over 1 T/m gradient in 100 microsec with very little eddy currents. The temperature regulated probe is optimized for honey bee experiments. Gradient coils are mounted directly onto the probe. Honey bees are immobilized by cooling in air to the temperature where they stop moving but which is high enough for the insects to survive. The optimum cooling temperature was 10°C. Using typical multislice-multiecho imaging sequence images were recorded with in plane resolution of less than 40 microns with a slice thickness of 100 microns.

MR microimages of a honey bee queen, which has the diameter of less than 7 mm show detailed internal structure where most vital organs can be identified. Possible application of this technique to biological experiments will be discussed.

This work is supported by Committee of Scientific Research of Poland grant No. 2 2442 91 02.

NMR microscopic detection of different grades of hydration and chemical composition inside of degenerative changed articular cartilage

W.Gründer, M. Wagner, M. Biesold

Institut für Biophysik, Universität Leipzig, D-04103 Leipzig, Germany

Osteoarthritis is a degenerative process of joint characterized by increasing changes of the cartilage matrix and subsequent degradation of cartilage tissue.

Concerning new imaging techniques own studies showed that by magnetic resonance imaging applying special tissue specific contrast agents changes of the articular cartilage surface and to some extent cartilage structures can be visualized [1,2].

Water content and water binding are of great importance in nutrition and maintaining the resiliency and lubrication of joints. Therefore the detection of the decrease in water content and changes of water binding which can occur already in early stages of osteoarthritis could be of high diagnostic value in orthopaedics.

We have shown that NMR microscopy on in situ samples of normal and arthrotic sheep knee joints allow the visualization of calcification. Moreover by application of chemical shift resolved and parameter selective NMR microscopy we could show nonuniform changes of water content and water binding depending on stage of cartilage degeneration:

In contrast to the histology, which shows normal pictures of cartilage in the early stages of arthrotic degeneration, a rising calcification and a drastic decrease of T_2 from joint surface to subchondral bone was observed indicating decreasing water content and higher water binding to the cartilage matrix. So it could be shown that T_2 selective image analysis gives very valuable new informations about early processes of osteoarthritis.

Application of chemical shift imaging to arthrotic changed joint yielded additional information about regenerative tissue on the cartilage surface. In case of strong reduced arthrotic cartilage layer water image shows no closed cartilage layer. These nonvisible regions, which correlate with the main stressed joint regions are observable in the CH_2 image indicating zones of regenerative connective tissue. The experiments were performed on a Bruker AMX 300 spectrometer equipped with a microimaging accessory.

The noninvasive differentiation of tissue and the detection of different grades of hydrations can improve considerably the diagnosis of joint cartilage degeneration.

1. W.Gründer, K.-H.Dannhauer, K.Gersonde, Proc. SMRM New York, 881 (1991)
2. Y.Kusaka, W.Gründer, K.-H.Dannhauer et al., Magn.Reson.Med. 24 (1992) 137

***HIGH FIELD MRI OF THE HUMAN MEDULLA OBLONGATA AS A
RESEARCH METHOD IN NEUROPATHOLOGY***

M. Vandersteen (*), P. Adriaensens (**), E. Beuls (*/**), J. Gelan (**), L. Vanormelingen (*), Y. Palmers (*/**), G. Freling (***)

*Departement of Anatomy and ** Institute for Material Research at the Limburg University, B-3590 Diepenbeek (Belgium); ** Department of Neurosurgery, University Hospital, Maastricht (The Netherlands); ***Departement of Radiology, St. Jansziekenhuis, B-3600 Genk; Departement of Neuropathology, University Hospital, Maastricht (The Netherlands).

The purpose of this study is to investigate whether high field MRI is a reliable screening method in neuropathology, able to detect all the abnormalities which are found by light microscopy.

A human medulla oblongata specimen of a well documented case of Chiari malformation was fixed in 10% formalin and Proton Density images were made with a 9.4 Tesla vertical bore magnet in the three spatial dimensions. The obtained images were compared with reference images of normal specimens and the abnormal findings were inventoried. The specimen was then cut up for histopathologic control. Histopathologic examination confirmed all the MRI findings and, besides a discrete cellular loss in one of the nuclei, revealed no additional abnormalities. High field MRI may therefore be considered as a usefull neuropathologic screening method.

Evaluation of the Spatial Distribution of Ethanol in the Human Brain by ^1H -NMR Spectroscopic Imaging

G. Schauß, H. Schild, M. Thelen

Klinikum der Johannes-Gutenberg-Universität, Klinik für Radiologie,
55131 Mainz, Germany

Introduction and Purpose:

With ^1H localized spectroscopy it is possible to observe ethanol in the human brain (1). The goal of this work is to extract information about the spatial distribution of ethanol in the brain using ^1H magnetic resonance spectroscopic imaging (MRSI).

Methods and Materials:

All examinations were performed on a Philips S15/ACS system (1.5T). The spectroscopy head-coil (diameter: 30 cm) was used for both the MRI and MRSI investigations. The MR images were used to define the field of view (FOV) of the spectroscopic images. In all examinations the FOV was 250*250mm with a slice thickness of 20mm. The transversal spectroscopic images were tilted to get a cut through the cerebellum and the ventricle system. To compare the spectroscopic results with anatomic information, three T_1 -weighted images ($T_R/T_E = 300/15$) with a slice thickness of 6mm and a gap of 1mm were measured prior to the spectroscopic examinations.

To exclude lipid signals from the skull, a rectangular volume of interest (VOI) was defined with typical dimensions of 100*90*20mm (anteroposterior, left to right, craniocaudal). Because the suppression of the lipid signal was not perfect, lipid signal intensity was visible in the ethanol images but outside the VOI. The CH_3 resonance (1.2ppm) was used to calculate the ethanol distribution.

Water suppression was accomplished using two selective prepulses, each followed by a spoiling gradient. The flip angle of the first pulse was fixed at 85° , whereas the second was adjusted to get a minimum water signal. Typically, angles between 300° and 400° were achieved.

This water suppression and a double-spin-echo sequence for volume selection were combined with two phase-encoding gradients for ^1H -MRSI (2). In both phase directions, 32 steps were used; this means the in-plane resolution of the spectroscopic images is about 8 mm. The echo time (T_E) was chosen to be 270 ms since the CH_3 group has a J splitting of 7 Hz and Rose et. al. had found a large value (335 ms) for the T_2 relaxation time of ethanol in dog brain (3). Additionally, this T_E is longer than the T_2 of many other metabolites in the brain, which were then automatically suppressed.

The calculation of the spectroscopic images was done with the implemented procedure. As described in (2), a Lorentz-Gauss windowing (exponential narrowing of 3 Hz and Gaussian broadening of 5 Hz) in the time domain and a cosine window in the two-dimensional k -space were performed. In addition to (2), a B_0 correction was used to correct for the residual inhomogeneity (less than 10 Hz after shimming the VOI). This was done by first measuring a few voxels without water suppression and then calculating the B_0 shift via the shift of the water resonance.

The volunteers drank as much alcohol as each needed to reach a blood alcohol content (BAC) of about 1‰. This means they consumed 50 g to 80 g pure ethanol depending on their weight. They could choose the drink containing this amount. Before and after the MRSI examinations, the BAC was determined.

Results:

The spectroscopic images show high intensities of ethanol in the ventricle system and in the cerebellum. Besides this, the concentration in the cerebellum is even higher than in the occipital lobe. Images which were taken 2h after drinking show high concentrations of ethanol only in the ventricle system. Thus, there is a difference in ethanol concentration in the cerebellum depending on the time after consumption.

Discussion:

It is shown that the spatial distribution of ethanol in the human brain can be measured with MRSI. Furthermore, it is possible to extract a correlation between ethanol distribution and physiological effect: The higher concentration of ethanol in the cerebellum could be responsible for alcohol-induced motoric disorder which was observable by most of the volunteers at the beginning of the examination. In comparison, the low cerebellic ethanol level at the end of the examination correlates with clinical well-being.

References:

1. Hetherington, H.P., et. al., *SMRM*, 1989, p. 370
2. Luyten, P.R., et. al., *Radiology*, 176, 791-199 (1990).
3. Rose, S.E., et. al., *Magn. Reson. Med.*, 23, 333-345 (1992)

NMR SPECTROMETER DESIGN: PHILOSOPHY AND ARCHITECTURE

by

Victor J. Bartuska

OTSUKA Electronics Europe (Chemagnetics)

Parc d'Innovation

"Les Scientifiques"

Rue Tobias Stimmer

67400-Strasbourg FRANCE

Ph:33-88 66 82 00

A coherent and unified approach to NMR spectrometer design (and spectrometer evaluation) will be presented.

Experimental Parameters, Parameter Agility and Parameter Performance will be discussed along with their implementation in modern NMR spectrometers.

From the basic philosophies presented above, the development of future NMR instrumentation will be presented

Manipulation of Susceptibility Effects in NMR Microscopy by Tailored RF

- Z. H. Cho, University of California, Irvine

Advances in High Gradient / High Field Microimaging

Evan Williams, Varian, Palo Alto

QUANTIFYING MASS TRANSPORT WITH MAGNETIC RESONANCE IMAGING

L. D. Hall and T. A. Carpenter

G. Amin, B. J. Balcom, J. A. Derbyshire, A. E. Fisher,
S. J. Gibbs, A. D. Parker, K. Potter, D. Xing

Herchel Smith Laboratory for Medicinal Chemistry
Cambridge University School of Clinical Medicine
University Forvie Site, Robinson Way
Cambridge, CB2 2PZ United Kingdom

Magnetic Resonance techniques offer sensitivity to molecular motions over a vast range of length and time scales. Of interest here are two MR windows, serial MR imaging and pulsed field gradient spin-echo (PGSE) based techniques. Serial MR imaging permits observation of motions on a length scale of 0.01 – 10 cm and on a time scale of ms to hours. PGSE methods are sensitive to motions on a length scale of 0.1 – 100 μm and a time scale of ms to seconds. These MR methods thus provide a powerful means of studying both molecular diffusion and flow, especially when coupled with a fast imaging protocol such as echo planar imaging (EPI). This lecture will provide a summary of our recent areas of application for serial imaging of mutual diffusion, reaction, and flow; and PGSE imaging of both diffusion and flow. These include diffusion of paramagnetic species in gels, polymerization processes, diffusion of water in heterogeneous structures such as plant tissue, convective dispersion in soil, flow in packed beds of large beads and around obstructions, and the flow of fluids exhibiting complex rheology.

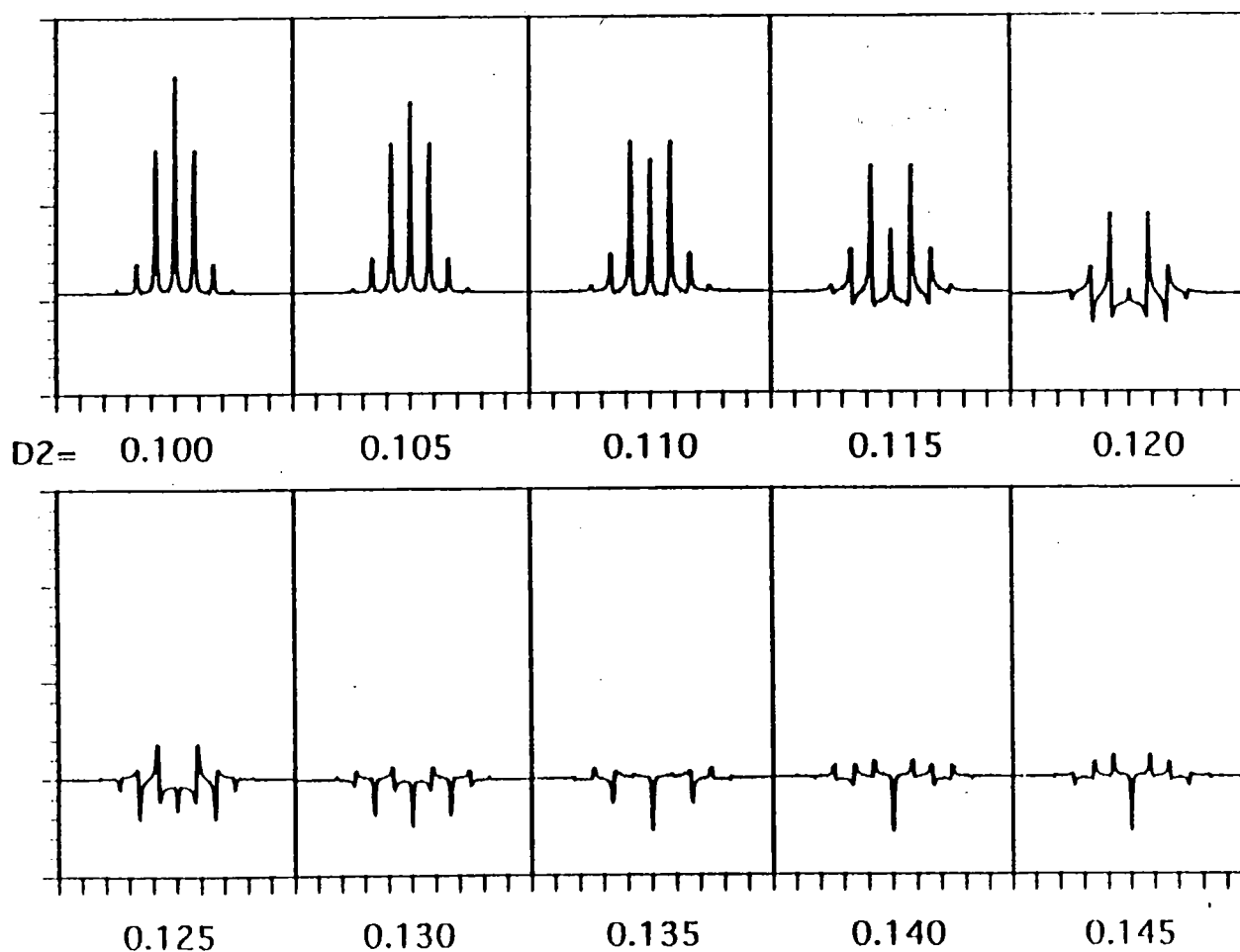
Patterns and Images of Flows and Vortices of Simple and Complex Fluids

John B. Grutzner and Jeff Hopkins

Department of Chemistry, Purdue University
West Lafayette, IN 47907-1393, USA

The Hahn spin-echo in the presence of a magnetic field gradient provides time and space separation of spectral information. Sample rotation across the field gradient provides a modulating field which generates a spinning sideband convoluted image of the spatial distribution. The sideband patterns generated by various fluid flows will be presented and analyzed. Examples will include Couette flow of simple and complex fluids and Taylor vortex flow images.

In order to analyze the observed patterns, a Fourier transform treatment of spinning sidebands has been developed. The classic Williams and Gutowsky (*Phys. Rev.* 1956, 104, 278) analysis gives the frequency spectrum following a single pulse. It is extended for multiple pulses by calculating the time domain response and Fourier transforming to obtain the spectrum. The additional phase modulation induced by the echo sequence for a uniformly spinning sample is shown below. Applications to stroboscopically selected slices in Couette flow will be presented.



General Treatment of Diffusion in the Presence of Boundaries and Short or Long Gradient Pulses

L. Z. Wang, A. Caprihan, and Eiichi Fukushima
The Lovelace Institutes
2425 Ridgecrest Dr., SE
Albuquerque, NM 87108 U.S.A.

We present a general formalism for the determination of the diffusion coefficient by the usual NMR echo attenuation experiment in the presence of a magnetic field gradient. An expression is derived which is valid for various diffusion distances with respect to the size of the region bounded by walls. Included is the usual restricted diffusion in which diffusion distances during the duration between gradient pulses are significant compared to the bounded region size. We discuss a subclass of the above in which the diffusion distance is significant within the bounded region even during a gradient pulse and examine the conditions under which the usual short pulse approximation for free diffusion holds. We find that the short pulse approximation is surprisingly poor for modest diffusion distances during the pulse. We also discuss the conditions under which the usual short pulse, restricted diffusion expression, which is often used to infer cell sizes, holds.

Abstract for 2nd Int'l Conference on MR Microscopy, Heidelberg, September 6-9, 1993.

QUANTIFICATION OF UNRESTRICTED DIFFUSION IN NMR MICROSCOPY

M. Brandl, A. Link, and A. Haase

Physikalisches Institut, Lehrstuhl für Biophysik, Am Hubland, 97074 Würzburg, Germany

PURPOSE

In NMR Microscopy strong imaging gradients are used to achieve high resolution. Due to molecular self diffusion of the imaged molecules, the gradient pulses lead to severe and irreversible signal attenuation. The purpose of this work is to quantify this signal loss for both imaging sequences, spin-echo and gradient-echo, and to derive the consequences for NMR Microscopy.

THEORY

In spin-echo or gradient-echo imaging sequences, the transverse magnetization is spatially encoded by three orthogonal gradients: read, phase, and slice. They cause a magnetization loss which can be calculated according to Torrey (1). Taking spin-spin relaxation T_2 into account, the signal decrease in dependence of time TE is described by a mono-exponential decay with an apparent T_2^{app} given by:

$$\frac{1}{T_2^{app}} = D \frac{C_1}{\Delta x^2} + D \frac{C_2}{\Delta s^2} + \frac{1}{T_2}$$

where D is the diffusion constant, Δx , Δs the spatial resolution, respectively the slice thickness, and C_1 and C_2 are parameters of the imaging sequence (2). The apparent T_2^{app} , describing the signal loss at echo time TE, has different consequences for NMR Microscopy:

- the measurement of spin-spin relaxation time T_2 in a series of images with increasing echo time TE is difficult to achieve since T_2^{app} is at least one order of magnitude smaller than T_2 . However, with the Magnetization Preparation Pulse Sequence, described by (3), we found a possibility for an accurate measure of T_2 and other parameters in NMR Microscopy (4).
- signal-to-noise ratio can be maximized by finding the optimum echo time TE by extending the acquisition time for noise reduction with respect to T_2^{app} .
- T_2^{app} offers the possibility for distinction of NMR Microscopy from NMR Macroscopy by the ratio T_2^{app} to T_2 .

EXPERIMENTS

Series of images of 1mm glass capillary filled with doped water were taken with an inplane resolution up to 9 μm . The experiments were performed on a BRUKER AMX-500 widebore magnet (89 mm inner diameter) at 11.75 T. The results of these measurements confirm our theoretical findings and show the advantage of Magnetization Preparation in NMR Microscopy.

CONCLUSION

Diffusion leads in NMR Microscopy to severe signal loss resulting in mainly diffusion weighted images. This loss can be used for optimizing the signal-to-noise ratio. However, an accurate measure of parameters like relaxation time T_2 is difficult to achieve. With Magnetization Preparation a correct quantification of this parameters is possible. Finally, our theoretical findings and experimental results confirm the thesis that molecular diffusion sets the ultimate limit to NMR Microscopy (5).

References:

1. H.C. Torrey, Phys.Rev. 104, 563 (1956)
2. M. Brandl, A. Haase, J.Magn.Reson, Series B (in press Dec. 1993)
3. A. Haase, Magn. Reson. Med. 13, 77 (1990)
4. A. Haase, M. Brandl, E. Kuchenbrod, A. Link, J. Magn. Reson, submitted
5. P. Mansfield, P.K. Grannell, Phys.Rev. B 12, 3618 (1975)

Diffusion and Susceptibility Effects in NMR Microscopy

Paul T. Callaghan, Massey University, New Zealand

Diffusion in heterogeneous and anisotropic media as studied by PFG NMR and microimaging

Farida Grinberg, Peter Barth, S. Hafner and Winfried Kuhn
Fraunhofer Institute for Biomedical Engineering,
Ensheimer Str. 48, D-6670 St. Ingbert, Germany

The method of PFG NMR provides the possibilities to measure the direct characteristics of the molecular translational mobility (self-diffusion constant or diffusivity) in the desired direction in accordance with the orientation of the applied magnetic gradients. Due to this PFG NMR is expected to be an effective tool for the investigation of the objects with the heterogeneous, particularly, anisotropic features or geometry. The further advantage of PFG NMR is connected with the possibilities to combine the studies of the anisotropic diffusion with the imaging methods, using the diffusivity as a parameter for the spatial mapping.

A detailed investigation of the anisotropic water diffusion via both bulk diffusion measurements and imaging has been reported for heterogeneous biological objects. Particularly, the wood branches with preferable orientation of the fibres in one direction have been used as samples.

Water diffusion in swollen wood materials (maple and birch) have been shown to display anisotropic features with lower molecular mobility and broader distribution of the diffusivities across wood fibres than that in the direction along the fibres. The analysis of the dependences of the water diffusion decays on the diffusion time has shown that water diffusion in woods is restricted by the permeable boundaries either along and across the fibres. Rough estimation of the linear sizes between the boundaries gives by the order of magnitude the value of about $10 \mu\text{m}$.

Diffusion images of woods have been measured with the diffusion gradients being oriented in the directions along and across the fibres. Typical values of diffusivities used for scaling the images were in the range of $6.0 \cdot 10^{-7} \text{ cm}^2/\text{s}$ to $6.0 \cdot 10^{-6} \text{ cm}^2/\text{s}$. Measured images give a strong evidence for the anisotropic water diffusion, correlating with the results of the bulk measurements, and display the peculiarities of the distribution of the molecular mobilities in spatial coordinates. The characteristics of the diffusivity distribution function have been suggested as the parameters for imaging weighting.

Some applications of PFG NMR for investigation of phase transitions in water emulsions and heterogeneous polymer systems have been discussed.

Flow in Polymer Solutions Measured by Dynamic NMR Microscopy

**Craig J Rofe, Rodney K Lambert, Lourdes de Vargas* and
Paul T Callaghan**

Department of Physics and Biophysics, Massey University,
Palmerston North, New Zealand; *Instituto Politecnico Nazionale,
CP 07300 Mexico DF, Mexico.

Abstract

The shear-thinning behaviour of polymer solutions and melts is a well known rheological phenomenon but one which is not well understood at a molecular level. Dynamic NMR microscopy enables shear-thinning to be studied via flow imaging while simultaneous diffusion and relaxation measurement^(1,2) can provide molecular insight.

Three separate flow systems have been examined, in each case by measuring the velocity and diffusion profiles of semi-dilute polymer solutions. These comprise polyethylene oxide/water and *Xanthan* gum/water solutions in both capillary and Couette geometries. Both superconducting and electromagnetic magnets were used to investigate steady and transient flow behaviour respectively.

1. P T Callaghan and Y Xia, *Die Makromolekular Chemie, Macromol Symp* **34**, 277 (1990).
2. Y Xia and P T Callaghan, *Macromolecules* **24**, 4777 (1991).

2nd International Conference on Magnetic Resonance Microscopy
(Heidelberg, September 6-9, 1993)

Localized Diffusion Measurements with a single B₁ gradient.

E. Mischler, F. Humbert and D. Canet

Laboratoire de Méthodologie RMN (U.R.A. CNRS n° 406 - LESOC)

Université de Nancy I

B.P. 239

54506 Vandœuvre lès Nancy Cedex

France

The simple pulse sequence

$$(g_1)_{\varphi_1} - \Delta - (g_1)_{\varphi_2} - (\pi/2) - \text{Acq.}$$

leads very easily to the determination of self-diffusion coefficients in multiline spectra. g_1 stands for a radio-frequency field gradient (B₁ gradient) which is applied in the form of two pulses of duration δ separated by the time interval Δ . In order to avoid echo formation and to rely upon longitudinal magnetization (so that the measurement is subjected to longitudinal relaxation in addition to the translational diffusion process), the following phase cycle is used

φ_1	φ_2
x	x
x	-x
-x	x
-x	-x

Varying either δ or Δ yields *global* self-diffusion coefficients (averaged on the whole sample).

Consider now an experiment in which the last $(\pi/2)$ pulse is replaced by a gradient pulse $(g_1)_y$ of incrementable duration t_1 . The resulting 2D map corresponds to the chemical shift in one dimension (f_2) and to the spatial coordinate of the gradient direction in the other dimension (f_1). In fact, because of interference effects associated with the value of δ , the trace along the f_1 dimension is not continuous but is made of separate peaks, each of them corresponding to a specific location along the gradient axis. Performing several 2D experiments of this kind with different Δ values yields in principle *local* self-diffusion coefficients. Thanks to a suitable experimental arrangement (vertical gradient direction), the investigation of a liquid-liquid interface can be envisaged.

MR Imaging and Spectroscopy at High Fields

Kamil Ugurbil, Minnesota

FUNCTIONAL NMR IMAGING OF PLANTS

H. Van As

Wageningen Agricultural University

Department of Molecular Physics and Wageningen Agricultural NMR Centre
Dreijenlaan 3, 6703 HA Wageningen, The Netherlands

Knowledge about the transport pathways in relation to the cell water balance in plants is essential for understanding important mechanisms such as elongation growth and growth inhibition by pathogen infection and drought stress. The advantage of NMR over any other method of analysis is its potential for the non-invasive and simultaneous measurement of this information at the whole organism, tissue and (sub)cellular level. The information content and the contrast of NMR images can be manipulated to represent parameters of physical or metabolic processes, such as proton density, (quantitative) spin relaxation values, flow, diffusion, exchange, or a combination of and correlation between these parameters. In this way MRI allows for a combination of anatomical and physiological information, referred to as functional imaging (1).

Functional images of plants have hardly been published. This is due to specific problems of plant NMR (compartmentation/microscopic heterogeneity and susceptibility artefacts due to air spaces). In addition, information about the tissue contrast or information content and relaxation mechanisms of plant tissue water has only very recently become available, based on accurate relaxation time and diffusion measurements (2-4). Applications of ^1H MRI to plant tissue will be presented, illustrating the potential use and limitations for functional plant imaging, and demonstrating the field strength dependence of the spatial resolution and the different information content of e.g. (quantitative) T_1 , T_2 and (restricted) diffusion images in discrimination cell sizes, water content and (tonoplast) membrane permeability.

The results show that low field NMR based on multi-echo sequences with short TE (in the order of a few ms) have some distinct advantages over its high field counterpart for functional (proton) imaging of plants.

References:

1. C.T.W. Moonen, P.C.M. van Zijl, J.A. Frank, D. LeBihan, and E.D. Becker, *Science* **250**, 53-61 (1990)
2. H. Van As, *Acta Horticulturea* **304**, 103-112 (1992).
3. J.E.M. Snaar, H. Van As, *Biophysical Journal* **63**, 1654-1658 (1992).
4. J.E.M. Snaar, H. Van As, *Journal of Magnetic Resonance* **A102**, 318-326 (1993).

Heidelberg Conference 1993

Molecular Motion and Nuclear Relaxation in Intact Biomaterials

Thomas M. Eads
Department of Food Science and
Whistler Center for Carbohydrate Research
Purdue University
1160 Smith Hall
West Lafayette, Indiana 47907-1160 U.S.A.

Upon removal by magic angle spinning of broadening due to magnetic susceptibility inhomogeneity in biomaterials, the nuclear relaxation of liquid-phase components with sharp resonances may be observed in ordinary experiments. Components in solid-like phases in the same sample may be observed indirectly in the "Z-spectrum" obtained in a proton cross-relaxation experiment [Grad and Bryant, *J. Magn. Reson.* **90**, 1 (1990)]. Nuclear relaxation parameters can be obtained by fitting the data to the theoretical expression, in which the number of adjustable parameters is reduced by obtaining some of their values in independent measurements during the same NMR session. The sensitivity of ^1H observation has clear implications for analytical devices. However, combined with additional information about microstructure, sometimes obtained by MRI, the compositional and nuclear relaxation data obtained non-destructively by NMR provides a dynamical picture for interpreting functional properties. Examples are provided from studies on fruit, cell walls of a transgenic vegetable, plant polysaccharides, and selected foods.

A comparison of water self-diffusion in fresh and stored beans

¹Kendall, E.J.; ²Stanley, D.W. and ¹Chatson, K.B. ¹National Research Council of Canada, 110 Gymnasium Place, Saskatoon, Canada S7N 0W9 and ²Department of Food Science, University of Guelph, Guelph, Canada N1G 2W1.

Prolonged storage of beans under relatively high humidity (85%) and temperature conditions (30°C) induces a hard to cook (HTC) defect. The impaired water uptake exhibited by (HTC) beans is attributed to a reduced osmotic gradient (Ψ) and to enhanced resistance to diffusive flow. This study measured the mobility of water molecules in fresh and HTC beans using the pulsed gradient spin echo (PGSE) method of Stejskal and Tanner and examined the regional heterogeneity of the diffusion statistic (D) at $60\mu\text{m}^2$ (in-plane) resolution by adding imaging gradients to the PGSE experiment.

The self-diffusion coefficient for water in control black beans ranged from $1.18 \times 10^{-10} \text{m}^2/\text{s}$ (after 2.5h imbibition) to $1.73 \times 10^{-10} \text{m}^2/\text{s}$ (after 48h imbibition). Storage for 1 year at 30 °C and 85% RH significantly enhanced the rate of diffusion to $1.35 \times 10^{-10} \text{m}^2/\text{s}$ at the 2.5h imbibition treatment. At 48h imbibition the value for D declined to $1.11 \times 10^{-10} \text{m}^2/\text{s}$. Similar trends were noted for white beans where the corresponding values $0.76 \times 10^{-10} \text{m}^2/\text{s}$ and $1.73 \times 10^{-10} \text{m}^2/\text{s}$ and $1.53 \times 10^{-10} \text{m}^2/\text{s}$ and $1.03 \times 10^{-10} \text{m}^2/\text{s}$ were obtained at 2.5h and 48h imbibition for control and stored beans respectively.

At 30 gauss/cm the diffusion gradient resulted in 20% - 40% signal attenuation depending on the treatment-related water mobility. An excellent linear relationship was obtained in the S-T plot over the 20 gauss/cm to 30 gauss/cm diffusion gradient range.

Diffusion weighted spin-echo microimaging was performed to determine localized values for D through the bean cavity, endosperm and embryo. Significant regional heterogeneity for water diffusion along a single orthogonal axis was observed in $500\mu\text{m}$ slices. Values obtained were generally larger than those averaged over the whole bean and ranged from $1 \times 10^{-10} \text{m}^2/\text{s}$ to $9.2 \times 10^{-10} \text{m}^2/\text{s}$.

IN-VIVO MAGNETIC RESONANCE MICROSCOPY FOR NON-DESTRUCTIVELY INVESTIGATING PLANTS, FRUITS, VEGETABLES AND SMALL ANIMALS.

S. Crestana (CNPDIA/EMBRAPA, P.O.Box 741, 13560-970 São Carlos/SP-Brazil); **Kauten, R.** and **Nielsen, D.R.** (University of California, 95616, Davis-CA - USA).

Presently, the non-invasive and local evaluation of the internal structure of porous and biological systems consists of a real scientific and technological challenge. Particularly, in the areas related to Agriculture, Food Science, Plant Physiology, Veterinary Medicine and related ones non-destructive studies of biological, physical and chemical processes occurring in the interior of fruits, vegetables, plant tissues and small animals are of great interest. The internal quality evaluation of fruits and vegetables is an important factor in the production and marketing selection. Also, diagnosis of in-vivo animals is highly desirable in Veterinary Medicine research. The results to be shown are demonstrating that Magnetic Resonance Imaging (MRI) performed at micrometric resolution is already an achievable and novel opportunity for characterizing and quantifying those processes and problems. The images were obtained by employing a non-medical NMR spectrometer commercially designed for in-vivo imaging small objects and animals (up to 20 cm internal diameter). High-resolution coils were used and set up in the centre of the magnetic cavity aiming the obtention of microscopic images with pixel resolution better than 50 microns. With the goal of testing the appropriateness of high-resolution MRI in investigation the presence of bruises, voids, seeds, pits, stage of maturity, dry regions and worm damage of several fruits and vegetables such as tomatoes, peaches, nectarines, apples, oranges and a bean seedling in a soil column were imaged. In-vivo MRI of small animals such as small dogs and a macaw (parrot) permitted the observation and diagnosis of knee and ear infections, hydrocephalic anomalies and brain lesions. The principal constraints and possibilities of obtaining MR images of porous and biological materials such as those studied, at high-resolution, will be discussed.

NMR Microimaging in Meat Research.

J.M. Tingle, V. Sarafis, P.A. Baumgartner and *J.M. Pope.

University of Western Sydney, Hawkesbury.
Bourke Street, Richmond, NSW 2753 Australia.

*University of New South Wales.
PO Box 1, Kensington, NSW 2033 Australia.

Despite many years of work in the field of meat research there is still a great deal that remains to be understood about the biochemical and physical processes that occur in the production and processing of meat and meat products. Important parameters which may affect meat quality between abattoir and the dinner table include method of slaughter, storage conditions and processing, aging, kitchen preparation and cooking. We are investigating the potential of NMR microimaging and relaxometry in studying changes which occur in meat during storage and processing. These techniques may assist in elucidating some of the variables which contribute to meat texture, taste and juiciness; parameters which are currently amenable to subjective assessment by tasting panels.

The Distribution of Intramuscular Fat.

Chemical shift selective imaging (1) can be used to generate separate images of the fat and water components in a meat sample. Fat images require long acquisition times to achieve an acceptable signal to noise ratio at microscopic resolution because the relatively long minimum echo time (TE) for this method leads to attenuation of the short T_2 fat signal. Three dimensional chemical shift imaging (3D-CSI) can generate similar fat and water images simultaneously, with reduced TE values, but the time penalty incurred is now due to the use of two (spatial) phase encoding dimensions (1). While these methods find application for static meat samples changes in water and fat distribution during cooking which occur over timescales of minutes, necessitate rapid imaging methods for fat/water discrimination. We have employed the STIR technique (2) to suppress the fat contribution, while simple T_1 weighting can provide a relatively quick image of fat distribution by attenuating most of the (longer T_1) water components in the sample.

Relaxometry.

NMR relaxometry has been employed for over 20 years in the study of skeletal muscle and a number of models of water structure in meat have been published (3-6). Standard saturation recovery or inversion recovery techniques for T_1 measurement are slow and do not discriminate between fat and water contributions. We have employed fast inversion recovery methods (7,8) for both bulk T_1 measurements and T_1 mapping or region of interest calculation and spectroscopic T_1 and T_2 determination to separate fat and water contributions in bulk measurements. These techniques have been applied to a number of experiments on meat processing including aging, cooking and freezing to monitor localised changes in relaxation times.

(1) H Rumpel and JM Pope. *Concepts in Magnetic Resonance* 5, 43-55 (1993).

(2) RJ Ordige and FL Van de Vyver. *Radiology* 157, 551-552 (1985).

(3) CF Hazlewood, BL Nichols and NF Chamberlain. *Nature* 222, 747-750 (1969).

(4) PS Belton, RR Jackson and KJ Packer. *Biochem et Biophys Acta* 286, 16-25 (1972).

(5) DC Chang, CF Hazlewood, BL Nichols and DE Woessner. *Biophys J* 14, 583-606 (1974).

(6) BM Fung and PS Puon. *Biophys J* 33, 27-37 (1981).

(7) R Graumann, H Barfuß, H Fischer, D Henschel, A Oppelt. *Electromedica* 55, 67-72 (1987).

(8) I Kay and RM Henkelman. *Mag.Res Med* 22, 414-424 (1991).

Determination of the vascular architecture of the raspberry receptacle through the use of 3D surface rendering techniques

J.A.B. Lohman^a, J.A. Chudek^b, B.A. Goodman^c, G. Hunter^b and B. Williamson^c

^a Bruker Spectrospin Ltd., Banner Lane, Coventry CV4 9GH, England, U.K.

^b Department of Chemistry, University of Dundee, Dundee DD1 4HN, Scotland, U.K.

^c Scottish Crop Research Institute, Invergowrie, Dundee DD2 5DA, Scotland, U.K.

The development of NMR microscopy in recent years has resulted in a technique that can perform rapid non-invasive investigations of plant histology without the artifacts associated with fixation, dehydration and embedding that are a feature of conventional destructive microscopic methods. NMR microscopy can routinely produce images of proton-containing samples with pixel dimensions of a few tens of micrometres or less and several *in vivo* investigations of botanical specimens have now been reported.

Conventionally, NMR images are produced as cross-sectional slices of the specimen, with the image intensity representing proton density, possibly weighted by one or more physical or chemical characteristics, such as T_1 or T_2 relaxation times or chemical shift. The resulting images are, however, often difficult to interpret in terms of 3-dimensional botanical structures. This problem can now be largely overcome through the use of 3D image reconstruction techniques. 3D surface rendered image reconstruction involves the recording of a 3-dimensional array of pixel intensities and then clustering together all pixels that have intensities of interest; clusters that do not have the selected properties are discarded. Projectional views are then calculated in any desired direction to yield a surface-rendered image of the selected component. Conversely, a maximum intensity projection of the data displays all gray levels as intensity bands within the 3D image.

This paper describes the use of projection and surface rendered 3D image reconstruction to investigate the vascular architecture of the raspberry receptacle. The results illustrate the departure of each vascular trace from the stele towards the point of attachment of the corresponding drupelet. The spiral phyllotaxis of the drupelet arrangement is seen clearly in the arrangement of the vascular traces, in which the xylem and phloem tissues can be resolved separately.

Development of infection in a strawberry fruit by the fungal pathogen *Botrytis cinerea*

B. Williamson^a, J.A. Chudek^b, G. Hunter^b, R.L. MacKay^b and B.A. Goodman^a

^a Scottish Crop Research Institute, Invergowrie, Dundee DD2 5DA, Scotland, U.K.

^b Department of Chemistry, University of Dundee, Dundee DD1 4HN, Scotland, U.K.

Strawberry represents one of the most important soft fruit crops of temperate regions of the world. It is, however, susceptible to infections by the grey mould fungus, *Botrytis cinerea*, the control of which involves the use of large quantities of fungicides prior to harvest. As part of a strategy for the breeding of cultivars resistant to *B. cinerea*, a greater understanding of the mechanisms of infection, disease development and host resistance in strawberry is desirable. This paper describes the use of NMR microscopy to obtain structural information on healthy and diseased strawberry fruit and to follow the development of *B. cinerea* infection.

In contrast to other soft fruits that we have investigated, the experimental conditions for imaging healthy strawberry fruits are critical. In particular, good quality images could only be achieved by using large sweep widths (c. 100,000 Hz) and consequently small values for TE (<4 ms) with a spin echo imaging sequence. So far we have failed to obtain structural information using gradient echo methods.

Regions of strawberry fruit infected with *B. cinerea* exhibit dramatically different imaging characteristics to those shown by healthy tissue. NMR microscopy, therefore, is a very convenient non-invasive technique for discriminating between healthy and diseased tissue. Examples of its use to follow the development of *B. cinerea* in a single fruit will be illustrated, both in the form of 2-dimensional slices and 3-dimensional reconstructions.

Axial- and Radial- Water Transport in Ricinus Communis Seedlings observed by Gradient Echo Deuterium Imaging

A. Metzler, W. Köckenberger[†], E. Komor Ph.D.[†], A. Haase Ph.D.

Physikalisches Institut V., Universität Würzburg, 8700 Würzburg, Germany; [†]Botanisches Institut, Universität Bayreuth, 8580 Bayreuth, Germany

INTRODUCTION: Deuterated water can be used as a contrast agent in deuterium MR- Imaging because of the low natural abundance (0.015 %) in biological organisms. Tracer- deuterium MRI of plants may give important information about water transport, especially in the regime of very low transport velocities (1).

METHODS AND MATERIALS: Castor bean seedlings were grown in special tubes, containing a 0.5 mM CaCl₂ solution aerated by a gentle flow of air bubbles through the bottom of the tube. In the experiment a seedling with it's root still in the tube was put in a special teflon insert fitting in a modified BRUKER microimaging probe. Just before the beginning of the experiment, the solution in the tube was exchanged with a 50% D₂O/50% H₂O 5mM CaCl₂ solution.

Short TE (1.1 ms) deuterium gradient echo imaging was accomplished using half-echo acquisition running on a BRUKER AMX 500 WB NMR spectrometer with actively shielded gradient coils. An acquisition window of 12.3 ms and 18 times oversampling for determination of the echo time origin was used. A data set with 6mm FOV consisting of 192- radial projections with 64 complex data points was acquired. The 3mm slice, excited by an self refocused E-BURP-2 Hf-Pulse (2), was transversely oriented. After automatic phase correction, maximizing the integral of the fourier transformed real data, 64 by 64 pixel images were reconstructed from the projection data by a ILST- iterative reconstruction algorithm (3).

RESULTS: The time course of the deuterium signal intensities in the images showed a exponential behavior asymptotically reaching an equilibrium level. In the xylem tissue of the plant this equilibrium was approached after 13 h. The signal for the inner and outer parenchyma adjusted only a short time delay after the signal detected for the xylem. Within the various layers of the parenchyma tissue there was no significant difference in the time course.

DISCUSSION AND CONCLUSION: The short delay between the approach of equilibrium within the xylem area and the parenchyma indicates that convectional transport contributes only weakly to the tracer movement. This agrees with the expected slow water uptake in the seedling since transpirational process is reduced by the protection of the cotyledons with the endosperm. Since the almost simultaneous appearance of the tracer within the transversal image, diffusion in axial and radial direction must be comparable.

REFERENCES:

- (1) J. Link and J. Seelig, *J. Magn. Reson.* **89**, 310-330 (1990)
- (2) H. Geen and R. Freeman, *J. Magn. Reson.* **93**, 93-141 (1991)
- (3) R. A. Brooks and G. di Chiro, *Phys. Med. Biol.* **21/5**, 689-732 (1976)

DIRECT AND INDIRECT IMAGING METHODS FOR THE ISOTOPES OF BORON AND NITROGEN, AND FOR ^{13}C

E. W. Randall .

Chemistry Department, Queen Mary & Westfield College, London E1 4NS, England

Images produced 'directly' for various samples containing ^{10}B , ^{11}B , ^{14}N , ^{15}N and ^{13}C will be presented. In the case of ^{15}N and ^{13}C (both $I = 1/2$) nOe enhanced images will be presented.

In all cases indirect detection techniques via protons will be illustrated and will include $^1\text{H}\{^{14}\text{N}\}$ decoupling, and for other nucleides $^1\text{H}\{\text{X}\}$ Spin Echo Double Resonance (SEDOR) methods.

The enhancements expected and obtained in each case will be presented and compared with alternative approaches.

Solid State NMR in Living Subjects

Jerome L. Ackerman, Leoncio Garrido, Martin J. Lizak,^a
Bettina Pflückerer, and Yaotang Wu,^b

NMR Center, Department of Radiology, Massachusetts General Hospital, Charlestown, MA,
and Harvard Medical School, Boston, MA, U.S.A.

Bone mineral is a complex and fascinating material whose chemistry is not fully understood. We are using solid state NMR to investigate several features of bone mineral chemistry. The most obvious and most biologically relevant place to study bone is in the living organism, and so we have endeavored to adapt techniques of conventional solid state NMR to the spectroscopy and imaging of live animals.

Solid state NMR of live animals carries great potential for obtaining information not available by any other means, because of its sensitivity to subtle aspects chemical structure. In contrast, conventional noninvasive modalities (plane film radiography, CT, DEXA, radioisotope scans) which are used to characterize bone are rather insensitive to chemical factors. However, solid state NMR on live subjects carries certain difficulties for the experimenter, and in some cases substantial risks to the subject.

The three nuclei of most interest to us in bone are ^1H , ^{19}F , and ^{31}P . We use ^{11}H - ^{31}P cross polarization to learn about phosphate chemistry in bone—in particular, what are the types of phosphate ions present, and how do their concentrations vary with the maturity of the mineral. We use ^{19}F NMR to detect fluoride ion in bone which has been incorporated as a tracer for the characterization of bone mineral deposition rate.

The main considerations in adapting conventional solid state NMR to the *in vivo* case are 1) the inability to spin the subject; 2) the need to use coils, such as surface coils, with poor RF homogeneity; and 3) the requirement to limit RF heating to safe levels.

Because magic angle spinning is inapplicable to living subjects, spectra are poorly resolved, and discrimination between resonances must rely on nonspectral parameters such as relaxation times or cross polarization rates. Although a surface coil may be double tuned just as can a solenoid, the RF field of a surface coil varies enormously with position. Thus, Hartmann-Hahn matching is maintained at all points in space. However, the B_1 variation makes the application of pulses of well defined flip angles essentially impossible for large volumes: pulse sequences which rely on specific flip angles fare poorly. In computer simulations, we have found that the familiar spinlocked cross polarization results in a signal loss, due primarily to the flip inhomogeneity, of as much as 75 percent. However, CP performed with adiabatic demagnetization is far more effective, because the ADRF process is rather insensitive to the size of B_1 . Finally, ADRF carries the advantage that the total RF dosage is greatly reduced over that from spinlocked CP.

We will discuss some of our applications, and present some schemes for addressing the problems inherent in solid state NMR of live subjects.

^aPresent address: National Institutes of Health, Bethesda, MD

^bPresent address: Children's Hospital, Boston, MA

From: G.D. Mateescu

**Re: TITLE FOR RARE ISOTOPES SESSION
2nd HEIDELBERG CONFERENCE**

**COMBINED OXYGEN-17 / PHOSPHORUS-31 MRI AND MRS:
A NEW DIMENSION IN CELL BIOENERGETICS RESEARCH**

**GHEORGHE D. MATEESCU
Case Western Reserve University
Cleveland, Ohio 44106, U.S.A**

Department of Chemistry

MAILING ADDRESS
Case Western Reserve University
10900 Euclid Avenue
Cleveland, Ohio 44106-7078

VISITORS AND DELIVERIES
102S Millis Science Center
2074 Adelbert Road

**Phone 216-368-3820
Fax 216-368-3006**

Sensitive Detection of H₂¹⁷O Via Proton MRI

Itamar Ronen and Gil Navon

School of chemistry, Tel Aviv University, Ramat Aviv, Tel Aviv 69978, Israel

During the last few years, various methods have been suggested for the measurement of ¹⁷O distribution, either by direct detection of the ¹⁷O NMR signal or by exploiting the effect of the unresolved ¹H-¹⁷O scalar coupling on the T₂ of the protons in H₂¹⁷O molecules in order to obtain contrast effect in proton MRI. In the present work we propose a new method imaging by reverse detection of ¹⁷O. The method is based on the increase of the T₂ of the protons in H₂¹⁷O molecules, produced by an irradiation of the ¹⁷O resonance during the echo time of a CPMG sequence applied on the protons. We show that in the limit of low concentration of H₂¹⁷O, the T₂ increase following the ¹⁷O decoupling is directly related to the ¹⁷O content of the sample, and so is the difference between the proton echo signal with irradiation of the ¹⁷O resonance and without it. The effect on T₂^{*}, as suggested by Kinchesh *et al.* [JMR, 100, 625 (1992)] for ¹⁴N was found to be negligible for this system. Since the increase in T₂ is significant, even at low concentrations of H₂¹⁷O, and since there are practically no SNR limitations due to the sensitivity of the proton signal, the time to echo may be optimized, leading to a significant difference between the echo signal with ¹⁷O irradiation and without it, still preserving a high SNR.

The method was demonstrated using a high resolution NMR (Bruker AMX 360-WB) equipped with a broad band variable frequency 20 mm probe. We used the Z-shim for a production of a gradient for one dimensional imaging. Figure 1 is a schematic representation of the phantom we used for the demonstration of the method: an 5mm NMR tube filled with small glass cylinders (4mm diameter, 5mm height), filled with a mixture of 20% H₂O and 80% D₂O with ¹⁷O concentrations as listed on the figure. Figure 2 shows the two images of the phantom, one obtained with irradiation of the ¹⁷O resonance with 10db attenuation on the maximum irradiation power (dotted line), and the other (solid line) is the image without irradiation of the ¹⁷O resonance. The time to echo was 320 msec and the CPMG included 8 180° pulses. Figure 3 shows the difference between the two images, divided by their sum (in order to compensate for non linearity of the Z gradient and inhomogeneities in B₁). It is seen that the intensity of the image is roughly proportional to the ¹⁷O content, except for the high concentration of 4.6%, where the decoupling power was not enough to fully decouple the broadening due to the ¹⁷O decoupling.

The method presented here may be useful for functional imaging of brain oxidative metabolic activity. This method is advantageous for several reasons: (a) It is highly sensitive even to minute amounts of ¹⁷O (lower than 0.2%) and hence may drastically reduce the cost of functional imaging experiments; (b) It reflects the amount of H₂¹⁷O in the tissue; (c) Since ¹⁷O resonance frequency in MRI instruments is relatively low, power deposition is relatively low; (d) Implementation of the pulse sequence to MRI is fairly straightforward, using interleaved sequences with and without ¹⁷O decoupling, hence minimizing the error due to all time dependent effects.

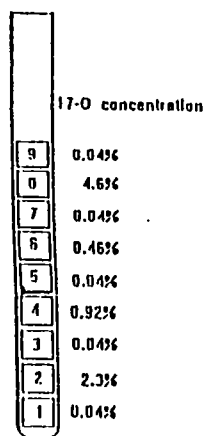


Fig. 1

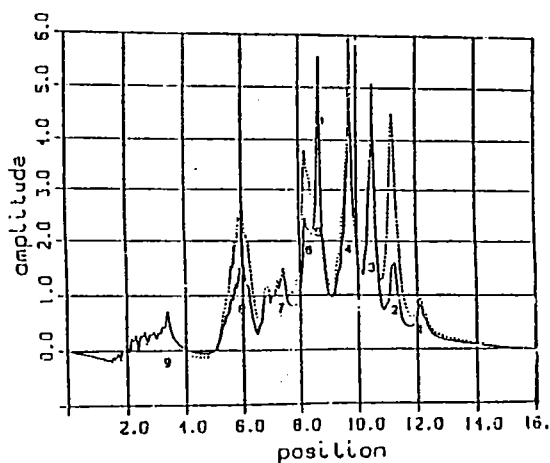


Fig. 2

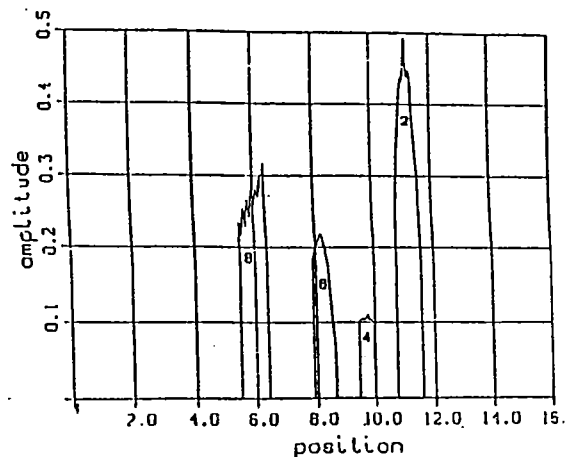


Fig. 3

Posters:

Abstracts

STRAY FIELD IMAGING - MRM OF HARD TISSUES

Michael A. Baumann and Klaus Zick*

Policlinic of Operative Dentistry and Periodontology
Johannes Gutenberg-University, Augustusplatz 2, D - 6500 Mainz

* Bruker Analytische Meßtechnik, D - 7512 Rheinstetten

Nowadays magnetic resonance tomography (MRT) is a common and useful tool in medical diagnostics. Up to now hard substances like bone and teeth are not depictable with conventional MRT devices. Therefore another method with the option for magnetic resonance microscopy (MRM) - the Stray Field Imaging (STRAFI), normally used for spectroscopy of solids - was chosen.

Extracted human teeth were stored in a formaline solution and given into a MRM. The experiments were performed in a BRUKER spectrometer MSL 400 WB with strayfield accessory. The excitation of the 128 slices was reached with a solid echo train. The signal analysis was carried out by a 3D-backprojection algorithm. The following two or three dimensional reconstruction of the data set was done by a special software (UXNMR, Bruker). The edge length of the detected voxels reached 300 microns.

Spatial images of the outer hard tissues representing the anatomy of the teeth as well as inner contours of the root canal system were found to give new interesting views with the possibility of sectioning in every plane of interest. Thereby views into the inside of solid materials like teeth could be reached. The method enabled us for the first time to depict really the ^1H -protons of dental hard substances like enamel and dentin. The fast development of hard and software components in the near future is expected to lead to even more detailed pictures.

MARIS - Software Package for Spectroscopy and Imaging

M.Rydzy, T.Jakubowski, F.Hennel, A.Jasiński, P.Kulinowski, Z.Sulek, B.Tomanek
Niewodniczański Institute of Nuclear Physics, Laboratory of MR Tomography
Radzikowskiego 152, 31-342 Kraków, Poland

Imaging and spectroscopy systems may be controlled by many kinds of computers and software packages.

Our software package called MARIS (*Magnetic Resonance Imaging & Spectroscopy*) is written in "C" and it runs on an IBM-PC compatible computer (INTEL486). Computer is connected to the MR system via CAMAC interface. Communication with hardware devices is organised using high level functions.

The package enables using most of the standard procedures for professional imaging and spectroscopy: changing experiment parameters on line (like recovery time, sampling rate, number of accumulations), data acquisition, data processing (like: FFT, phase correction), etc.

Our package includes pulse program interpreter. The interpreter reads each line of pulse program written in a plain ASCII in the form of macro commands. Each command is interpreted, changed into specific internal language of pulse programmer and prepared in the computer memory to send to the controller via CAMAC.

The shapes of gradients as well as shapes of soft pulses are created in the form of separate files by a special program written in "C".

Data transfer to the computer is initialised by hardware interrupt from CAMAC, when data in the ADC memory is collected.

Single monitor is used both for user interface as well as for data presenting. The user interface is divided into five windows. Data is shown in data display window and the bar on the top of the screen contains names of data files actually loaded for display and processing. User can choose all possible commands either from menu or directly from the keyboard (command line window). Status window enables to change easily all accessible experiment parameters with a mouse and provides a quick way to display actual values of all parameters.

Special way of working with MARIS is using macros. Macro is a text file calling MARIS commands step by step using loops, logic conditions or special macro variables. This kind of work is particularly useful in more complex experiments, e.g. 2D spectroscopy.

MARIS can be adapted to many interfaces. This package was designed for spectrometer controlled via IEEE-488 (IEC-625) as well as CAMAC.

This work was supported by Committee of Scientific Research of Poland grant No. 2 2442 91 02.

Modular System for MR Microimaging

Z. Sulek, A. Jasiński, B. Tomanek, J. Kibiński, T. Skórka, S. Kwieciński
Niewodniczański Institute of Nuclear Physics, Laboratory of MR Tomography
Radzikowskiego 152, 31-342 Kraków, Poland

A home-build modular system for microimaging was constructed using CAMAC interface, PC compatible computer and a 6.4 T superconducting magnet with $\Phi 54$ mm bore.

Rf part of the system consists of:

- digitally controlled frequency synthesiser PTS 310,
- modulator with four orthogonal hard pulse channels (x, y, -x, -y) and fifth channel with $0-2\pi$ variable phase and possibility of linear modulation,
- converter for frequency shifting up to the desired band,
- two rf power amplifiers (selective for ^1H range and broad band for other nuclei) which can be switched to the hard pulse mode or linear amplification mode,
- both selective and broad-band preamplifiers with noise figure below 1 dB,
- receiver with 2π phase shifter, two-channel phase sensitive detection (in quadrature) and quadrature phase and amplitude correction,
- two-channel 6-pole antialiasing filter up to 300 kHz,
- two-channel 12-bits AD converter with maximum sampling rate 1 MHz and a buffer memory of 16 kpoints per channel.

Control blocks are localised in the CAMAC crate and work according to the CAMAC standard. These are:

- a programmable process controller, loaded from the main computer and running synchronously with the 10 MHz clock. It has 12 output lines which control timing of experiments. Its internal decoder of operation performs simple functions like time divisions, nested loops, etc.,
- a 4-channel generator of gradient waveforms and soft pulses envelopes - stored in digital form and clocked out to DA converters by pulses from the process controller,
- a controller of monochromatic image display with memory for 256×256 pixels of 8-bit scale of grey,
- an interface for control of rf system functions like receiver gain, filter bandwidth, phase of reference signal, etc.

The system operation is controlled from the PC computer by the software package called MARIS (MAGnetic Resonance Imaging and Spectroscopy) which contains control functions for hardware as well as acquisition and data processing procedures.

An integrated, temperature regulated microimaging probe consisting of the rf coil and shielded gradient coils was made. Gradient coils of 20 mm ID driven from Techron 7570 power amplifiers generate gradients up to 1 T/m in 100 μsec with very little eddy currents.

This work was supported by Committee of Scientific Research of Poland grant No. 2 2442 91 02.

NMR Imaging as an Indicator of Chemical Potential

A. E. Fischer, B. J. Balcom, T. A. Carpenter, and L. D. Hall

*Herchel Smith Laboratory for Medicinal Chemistry,
University of Cambridge School of Clinical Medicine,
University Forvie Site, Robinson Way,
Cambridge, CB2 2PZ United Kingdom*

NMR Imaging is widely used in medicine to visualize human anatomy. Applications in chemistry are hindered by low signal to noise of the NMR phenomenon, which is frustrating given the well known sensitivity of some NMR parameters towards chemical and physical properties.

Dissolved paramagnetic molecules increase the relaxation rate of the solvent protons proportional to their concentration. The proportionality constant differs widely between paramagnetic species and depends on the number of unpaired electrons, the electron spin relaxation, the rate of molecular tumbling and the exchange rate of inner sphere and bulk solvent. By choosing appropriate paramagnetic molecules these relations can be used to infer from the relaxation rate of the solvent protons chemical parameters like pH values (1), redox potential (2), temperature and viscosity to name just a few. By applying NMR imaging sequences the variation of these parameters can be mapped in space and time (3) and will be demonstrated for pH values and redox potential.

1. B. J. Balcom, T. A. Carpenter and L. D. Hall, *Can. J. Chem.*, 70, 2693 (1992)
2. B. J. Balcom, T. A. Carpenter and L. D. Hall, *J. Chem. Soc. Chem. Commun.* 312, 312 (1992)
3. B. J. Balcom, A. E. Fischer, T. A. Carpenter and L. D. Hall, *J. Amer. Soc.* 115, 3300 (1993)

Construction of Multiply Band-selective 180° Refocusing RF Pulses for Simultaneous Multi-slice Spin Echo Imaging

B. Newling, T. A. Carpenter, J. A. Derbyshire, and L. D. Hall

*Herchel Smith Laboratory for Medicinal Chemistry,
University of Cambridge School of Clinical Medicine,
University Forvie Site, Robinson Way,
Cambridge, CB2 2PZ United Kingdom*

The use of phase-tailored RF pulses to perform multiple slice excitation has previously been suggested (1, 2). Pulses for these sequences were developed by the Fourier transform method. We demonstrate here a generalization of the work of Roberts et al. (3) to generate multiply band-selective 180° refocusing pulses from phase-tailored self-focused 90° RF excitations. The resulting pulses allow multiple slice excitation sequences to be performed in combination with spin echo imaging.

1. J. Hennig and R. Schillinger, 9th Annual S.M.R.M Abstracts, p.163 (1990).
2. S. Muller, Magn. Reson. Med., 10, 145 (1989).
3. T. P. L. Roberts, T. A. Carpenter and L. D. Hall, J. Magn. Reson., 101, 78 (1993).

Fast Spin-Echo Techniques for High-Field Magnetic Resonance Microscopy*

Xiaohong Zhou, Gary P. Cofer, Steve A. Suddarth, and G. Allan Johnson

Center for *In Vivo* Microscopy, Department of Radiology
Duke University Medical Center
Durham, North Carolina 27710

Theoretical analyses conducted by many MR microscopists indicate that the spatial resolution of MR microscopy can reach a few microns or even submicrons (1). To realize this resolution, a large number of k-space sampling points is required to provide the necessary digital resolution. This requirement often results in prohibitively long data acquisition times. The recently developed fast spin-echo (FSE) technique (2, 3) provides a possible solution to this problem. Unlike most other fast imaging techniques based on gradient echoes, FSE minimizes the annoying magnetic susceptibility effects, making itself more suitable for high-field MR microscopy.

Application of FSE to MR microscopy is challenged by a number of technical problems. First, the strong magnetic field gradients required by MR microscopy cause considerable diffusion-related signal loss. Second, frequent gradient switching in conventional FSE pulse sequences induces mechanical vibrations and eddy currents, degrading the spatial resolution and causing phase errors. Third, the reduced T_2 relaxation times at high fields limit the number of echoes obtainable in an echo train and result in pronounced ringing artifacts, image blurring, and/or edge enhancement.

We have developed several techniques to address the aforementioned problems. Using a phase accumulation approach, we devised a new pulse sequence to reduce the required phase-encoding gradient amplitude by a factor of 16, and decrease the gradient switching frequency by a factor of 2. Images obtained using this pulse sequence exhibited comparable quality to those obtained with conventional techniques. We have also developed an artifact reduction algorithm to simultaneously reduce artifacts introduced by T_2 decays and phase errors. This algorithm requires only one extra excitation to obtain a set of non-phase encoded projections. Based on the projections, spatially resolved T_2 values and phase errors are estimated and used to correct the raw k-space data. Our results show that the artifact reduction algorithm can significantly improve the quality of FSE images.

With these technical developments, we expect that FSE techniques will be widely used in MR microscopy to reduce imaging time, or to improve the digital resolution, especially for 3D imaging with large data arrays.

- (1) For example, B. Blümich and W. Kuhn, "Magnetic Resonance Microscopy", VCH, Weinm, Germany, 1992.
- (2) Hennig, J., Nauerth, A., Friedburg, H., *Magn. Reson. Med.*, 3, 823, 1986.
- (3) Mulkern, R.V., Wong, S.T.S., Winalski, C., Jolesz, F.A., *Magn. Reson. Imaging*, 8, 985, 1990.

* This work was supported by an NIH Grant (P41-RR-05959-02) and an NIEHS Grant (R01-ES04187-04A1).

MRI and Determination of T_1 and T_2 of Solid Polymers Using a 1.5 T Whole-Body Imager

+*S. Widmaier, +*W.-I. Jung, *O. Lutz

+Max Grundig Klinik, 7580 Bühl 13, Germany

*Institute of Physics, University of Tübingen, 7400 Tübingen, Germany

Introduction

Imaging of polymers in the solid-state provides a great variety of new applications and a large number of approaches have been demonstrated but so far none can be considered to be routine since they all require very special instrumentation.

Nevertheless remarkable results can be obtained using spin-echo sequences with echo times TE as short as 4 msec and a standard 1.5 T NMR whole-body imager for ^1H imaging of polymers in the solid-state without any modification of the NMR hardware designed for clinical usage.

Imaging based methods to determine relaxation times offer the possibility to determine simultaneously the relaxation times of different polymeric materials within one set of measurements and local differences of relaxation times within an object by selecting different areas within the object. Since there are unneglectable signal contributions from the polymeric materials surrounding the actual object such as, for example, the receiver coil case or the interior covering of the tomograph it is necessary to distinguish the contributions, a point where conventional ^1H spectroscopy methods fail due to the large linewidth of the signals and the small chemical shift differences between them.

Methods and Experimental

The spin echo sequences used were implemented on a Siemens Magnetom 63 whole-body imager operating at 1.5 T, a commercial circularly polarized headcoil was used to transmit and to receive the signals. The gradient system is the commercial nonshielded system with maximum gradients of 10^{-2} T/m.

The spin echo sequence SE40 shown in Fig. 1 has an echo time TE of minimum 4 msec. 512 μsec Hamming filtered sinc pulses in presence of slice selection gradients (G_z) of $1.2 \cdot 10^{-3} \frac{\text{T}}{\text{m}}$ are used for slice selective excitation of a 20 mm slice. The phase-encoding gradient (G_y) is split into two parts, one applied after the 90° pulse and the other smaller one directly applied after the rephasing 180° pulse with inverted sign. Limited by the maximum gradients a maximum field of view (FOV) of 375 mm is obtainable.

Results and Discussion

Various polymers in the solid-state such as, for example, Polystyrene (PS), Acrylonitrile - Butadiene - Styrene (ABS), Polyoxymethylene (POM), Polyurethane (PUR), and Polyvinylchloride (PVC) can be imaged (1) despite of their short transverse relaxation times T_2 on the order of 2 ms and beside this fact in some cases interesting results occur, for example, unexpected inhomogeneities in a sample become visible in the image.

Based on sets of images the local relaxation times can be determined, giving longitudinal and transverse relaxation times of 100 - 1000 msec and 1 - 3 msec, respectively for the polymers mentioned above. The data sometimes indicate local differences and multiple compounds which occur in polymers for different reasons, for example amorphous and crystalline areas, different degrees of crosslinks or signal contributions from additives such as dyestuff or softening agents.

Furthermore, as a neat application a "self-portrait" of the polymeric materials of the receiver coil will be given. "Self-portrait" means that the headcoil acting as transmitting and receiving coil produces an axial ^1H NMR image of itself, that is, an image of the surrounding case which consists of polymeric materials.

Polymers in the solid-state with transverse relaxation times T_2 as short as 1-2 msec can be imaged using a whole-body imager which is advantageous for examinations of heterogeneous objects of a large extension. Besides new applications in materials science and production survey it offers opportunities *in vivo*, for example when imaging implants or whenever extreme short transverse relaxation times are present.

References

1. Widmaier S., Jung W.-I., Pfeffer K., Pfeffer M., Lutz O., *Magn. Reson. Imaging*, in press.

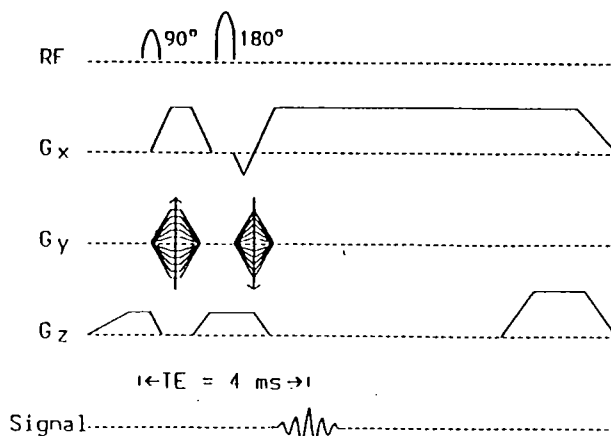


Fig. 1 Spin-echo sequence SE40 with an echo time of minimum 4 msec.

Optimization of RF coil parameters for microimaging applications

Knut Mehr, Peter Dejon, and Winfried Kuhn

Fraunhofer Institute for Biomedical Engineering
Ensheimer Str. 48, D-66386 St. Ingbert, Germany

The performance of the RF coil has a high influence on the quality of NMR measurements. Due to the different requirements of microimaging experiments compared to "classical" high resolution spectroscopy, the weighting of many experimental parameters is significantly changed. This has to be kept in mind when optimizing the RF coil configuration for microimaging systems.

Especially parameters as the active coil length and the distance between the RF coil and the tuning/matching network can be used to improve the system performance for Microimaging applications, mainly focused on voxel sensitivity, inplane homogeneity and power handling capability. This leads to significant changes compared to classical designs optimized for high resolution probes.

In this poster we discuss some test results obtained at 400 MHz with several different RF coil configurations based on a three turn coil design [1] for sample tubes with a diameter of 10 mm.

Reference:

- [1] K. Mehr, P. Dejon, E. Koeller, and W. Kuhn:
New RF coils for NMR Microscopy with increased B_1 -Homogeneity
33rd ENC, 1992, Asilomar, CA, USA

PLANAR MICROCOILS SENSORS FOR NMR MICROSCOPY

T.L. Peck^{1,3}, L. LaValle¹, R.L. Magin^{1,3}, I. Adesida^{1,2}, and P.C. Lauterbur^{3,4}

¹Department of Electrical and Computer Engineering, 1406 W. Green St., ²Center for Compound Semiconductor Microelectronics, 208 N. Wright St., ³Beckman Institute, 405 N. Mathews, and ⁴Biomedical Magnetic Resonance Laboratory, 1307 W. Park, University of Illinois, Urbana, IL 61801

Abstract - The goal of this research is the development of planar, microlithographically fabricated microcoils for biomedical applications. We have constructed and tested a series of microcoils (with diameters to less than 50 μm , trace widths of 1 μm - 5 μm , and 3 - 25 turns) and demonstrated that such coils can be used for NMR spectroscopy.

The signal detected by a radio frequency (RF) coil in a nuclear magnetic resonance (NMR) experiment is directly proportional to the volume of the sample and the sensitivity (B_1/i) of the RF coil^[1,2]. Optimal signal detection is achieved when the size of the RF coil is tailored to provide efficient magnetic field coupling between the coil and sample. The noise in an NMR experiment is predominantly thermal noise, and originates primarily within the conducting sample and the coil. When using submillimeter RF microcoils to examine small biological samples (with $d_{\text{sample}} < 1 \text{ mm}$), the resistance of the coil dominates the resistance of the sample^[3,4]. Therefore, an accurate electrical circuit model of coil resistance is required to accurately predict the signal-to-noise ratio (SNR) that can be achieved when using microcoils. The electrical circuit models used to characterize the resistance of larger coils cannot be directly applied to smaller coils, in which the wire diameter (d) approaches one skin depth (δ) at the frequency of operation. We have developed a circuit model for coil resistance that is based on a scaling parameter $z = d/\delta$. One advantage of using this scaling parameter is that experimental verification of the model is readily accomplished using larger scaled coils and sophisticated instrumentation available for accurate measurement of coil resistance at lower frequencies. Furthermore, this technique is not specific to solenoids, but can be applied to any coil geometry. In previous studies we have shown that an enhanced SNR is achieved when using wire-wound, solenoidal microcoils (50 mm - 1000 mm in diameter). Our resistance model suggests that further enhancement in the SNR may be realized with smaller microcoils^[5-7].

Presently, our efforts have been to further reduce the size of microcoils to less than 50 μm using microlithography. Using this technology, micro-miniature planar coil structures with feature sizes to less than 1 μm and aspect ratios of 2:1 can be realized. Further enhancement of the aspect ratios can be achieved using electroplating. A series of planar, spiral microcoils (10 μm - 200 μm diameter, 1 μm - 5 μm trace widths, and 3 - 25 turns) was constructed as multi-layered thin films of gold or aluminum photolithographically patterned onto a glass substrate, with a covering layer of photoresist for insulation. Electrical connection between the layers is made by plating holes ("vias") etched into the insulation. A center or core hole may be etched through all layers for sample placement. In preliminary studies, we have characterized the electrical behavior and SNR performance of the microcoils using a network analyzer (HP8751A, HP8510) with S-parameter test set (HP87511A, HP8516A), and a Cascade Microtech 42 microwave R&D probe station to measure the input reflection coefficient (S_{11}). The microcoils have typical inductance values of 1 - 10 nH and resistance values of several Ω . Microscopic (¹H) NMR spectroscopy experiments were performed using a GN-300 (7.05 T)/89 mm NMR spectrometer. NMR spectra at 7.05 T were obtained using a silicone rubber (RTV) sample (linewidth of 132 Hz) placed directly over the coils. The microcoils were used to both transmit RF energy to the sample and to receive the free induction decay. The measured SNR is approximately equal to theoretical predictions, and provides further support to our coil resistance model. These microcoils are well-suited to NMR microscopy experiments with biological samples as well.

Future microcoil designs based on these techniques could involve coil arrays, integrated impedance matching networks, and transceiver circuitry. These designs thus form the basis for a new family of integrated NMR biosensors.

References

1. Abragam, A., Principles of Nuclear Magnetism (Oxford University Press, Oxford, 1961).
2. Hoult, D.I. and Richards, R.E., *J. Magn. Reson.* 24, 71, 1976.
3. Hoult, D.I. and Lauterbur, P.C., *J. Magn. Reson.* 34, 425, 1979.
4. Cho, Z.H., Ahn, C.B., Juh, S.C., and Lee, H.K., *Med. Phys.* 15, 815, 1988.
5. Peck, T.L., Magin, R.L., and Lauterbur, P.C., *Abstracts*, 9th Annual Meeting of the SMRM, 207, 1990.
6. Peck, T.L., Ph.D. Dissertation, University of Illinois at Urbana-Champaign, 1992.
7. Peck, T.L., Magin, R.L., and Lauterbur, P.C., in preparation.

Acknowledgments:

The authors would like to recognize Richard Ficker for his technical assistance with the fabrication of the microcoils and Carl Gregory for his technical assistance with the GN-300. This work has been supported by NSF Grant DIR 91-02419, NIH Grant PHS 5 P41 RR05964, NSF DIR 89-20133 and the Servants United Foundation.

Use of Difference Propagators in the Measurement of Flow in the Presence of Stationary Fluid

Paul T Callaghan*, Walter Köckenberger† and James M Pope‡

*Department of Physics and Biophysics, Massey University, Palmerston North, New Zealand; †Botanische Institut, Universität, Bayreuth, Germany; ‡School of Physics, University of New South Wales, Kensington NSW 2033, Australia.

Abstract

In NMR angiography it is conventional to produce an image in which only the moving spins are visible. We address a somewhat different problem which is important in the measurement of water flow in plant vascular tissue. Here, the signal within a single pixel ($\sim 10 \mu\text{m} \times 10 \mu\text{m}$) may contain a contribution from both xylem (or phloem) vessels, as well as surrounding cells or inter-cellular space in which the water is stationary. This means that any attempt to measure delicate water flow rates can be frustrated by a dominant stationary water signal. The problem of suppressing the signal from stationary fluid is well-known in flow imaging by NMR. One common method is the use of subtraction methods based on two gradient pulses of differing sign. We have adapted this approach to Dynamic NMR Microscopy where the q -space encoding is performed with successively incremented gradient pulses of alternating sign. The propagators thus obtained are then subtracted to produce a difference propagator which arises from only the moving spins. This propagator is then analysed to reveal their velocity.

One special problem which arises is that the propagator for a pixel containing an entire xylem vessel or phloem sievetube will be characteristic of the entire Poiseuille velocity distribution. This leads to a difference propagator which consists of an asymmetric rectangular function. We demonstrate this experimentally using a phantom consisting of water flowing in microscopic capillaries surrounded by stationary water. A Poiseuille profile-fitting method is shown to work well both in this phantom and in the mapping of counterflowing xylem and phloem water motion in plant stems *in vivo*.

1. P T Callaghan, *Principles of NMR Microscopy*, Oxford University Press, 1992.
2. S Posse and W P Aue, *J Magn Reson* **88**, 473 (1990).
3. P T Callaghan, L C Forde and C J Rofe, *J Magn Reson*, submitted (1993).

High Gradient PGSE Experiments in a Superconducting Magnet

**Bertram Manz, Andrew Coy, Philip J Back and
Paul T Callaghan**

Department of Physics and Biophysics, Massey University,
Palmerston North, New Zealand.

Abstract

Pulsed gradient spin echo NMR is sensitive to the translational motional spectrum of molecular ensembles. This can be used to determine the diffusion coefficient of polymers in solution. Traditionally very high gradient PGSE experiments have been confined to electromagnets or to the stray field regions of superconducting magnets. We wish to take advantage of the spectral resolution available in the central region of a superconducting magnet and to that end we have designed and built a high gradient screened gradient coil (7.5 T/m). We show the design of the probe and some preliminary data for diffusion of high mass polymers.

Edge Enhancement Effects in Microcapillaries

Andrew Coy, Lucy C Forde, Craig J Rofe and
Paul T Callaghan

Department of Physics and Biophysics, Massey University,
Palmerston North, New Zealand.

Abstract

Resolution in NMR Microscopy is normally limited by signal-to-noise ratios, but when the molecules in sample are diffusing, additional effects must be considered. Such effects have been treated by considering the motional narrowing of the image spectrum due to diffusion in the presence of an imaging gradient^(1,2). However when realistic imaging parameters are used this effect can be shown to be negligible. Of far more significance in Fourier Imaging microscopy is the Stejskal-Tanner attenuation resulting from the k -space imaging gradients and the spin or gradient echoes that are necessary for this type of microscopy⁽³⁾.

As well as explaining image signal attenuation at high resolutions, diffusive relaxation also provides a contrast mechanism for observing variations in the local propagator. One fundamental restriction on molecular diffusion of any sample is the presence of boundaries or walls to molecular motion. In particular molecules near the walls of a sample container will diffuse shorter rms distances than molecules free to diffuse in the middle of the container. This effect can provide significant edge enhancement of NMR Imaging at high resolution.

Such experiments have been carried out on rectangular and circular microcapillaries. Significant edge enhancement can be seen in both samples. As well as explaining edge enhancement, this diffusive relaxation mechanism also provides a way to investigate directly the form of the local propagator in other restricted diffusion environments as well as indicating desirable ways to avoid such effects in the quest for higher NMR microscopy resolution.

1. W B Hyslop and P C Lauterbur, *J Magn Reson* **94**, 501 (1991).
2. B Pütz, D Barsky, and K Schulten, *J Magn Reson* **97**, 27 (1992).
3. P T Callaghan, A Coy, L C Forde, and C J Rofe, *J Magn Reson A* **101**, 347-350 (1993).

VECSY: Velocity Correlation Spectroscopy Using q -space Encoding

Bertram Manz and Paul T Callaghan

Department of Physics and Biophysics, Massey University,
Palmerston North, New Zealand.

Abstract

We introduce a new pulse sequence (VECSY) for velocity-encoding correlation spectroscopy. This sequence, which is chemical shift sensitive, is based on two pairs of gradient pulses which provide independent q -space encoding. The 2D Fourier spectrum then exhibits the velocity correlation in a manner akin to the chemical shift correlation in a NOESY experiment. We present some VECSY spectra of a rotating Couette system. The corresponding simulations show that the pulse sequence works very well.

This technique can be used to measure correlation lengths on a scale of 10 mm down to 0.1 mm for water flow, but the lower limit may be significantly reduced for more slowly diffusing molecules. We have applied this method to water flow through a porous medium, thus determining the relevant correlation length.

THE LOW FIELD NMR-IMAGING OF SMALL OBJECTS

V. Frolov

Institut of Physics, University of St.-Petersburg,
St.-Petersburg 198904

There is a tendency to work at the highest magnetic fields as possible for an imaging of small object. The advantages of the high fields is very good known. Neanmoins low fields have the preferences too. These are: the increasing of relaxation contrast for certain objects, simplicity of the execution, economy etc. Two low field imagers, one at 7 mT and another at 0.15T, were realized in Institut of Physics of University of St.-Petersburg.

The first is a multipurpose experimental installation designed for the test and the optimization of divers methods of NMR-imaging. The static magnetic field is created with a solenoid having two compensating coils and systems of gradients, prepolarization and field-cycling. Owing to the low level of magnetic field no cooling is needed and a good spatial resolution is attained by using enough faibles field gradients. A direct amplification and a homodyne digital phase-sensitive detector are used. The program-controlled sequencer allows to form series of radio- and gradient pulses at the operator's desire. The images of certain biological objects and of details of caoutchouc were obtained.

The another imager is designed for an analysis of specimens of oil-bearing rock. NMR-imaging allows to study the distribution of saturating water and oil, an process of displacing of water by oil and vice versa, the change of structure due to mecanical or chemical influences upon a specimen.

The static magnetic field for the imager is created with a permanent magnet made by institut for Scientific Research "DOMAIN" with the magnet poles spaced by 12 cm. This imager is distributed by "REGIONTECHNICA", JS Co, Ltd, St.-Petersburg.

Low Power Slice Selection and NMR Imaging with Noise Excitation H. Nilgens, B. Blümich⁺, J. Paff⁺, P. Blümmler

Max-Planck-Institut für Polymerforschung, Postfach 3148, 55021 Mainz

⁺Lehrstuhl für Makromolekulare Chemie, RWTH Aachen, Worringerweg 1, 52074 Aachen

Introduction

Excitation power is one of the major problems in medical and biomedical nuclear magnetic resonance imaging. The currents induced from fast switching gradients pose a risk for the patient as well as high rf excitation power. We have developed a method which reduces the excitation power substantially and allows slice selection. Moreover, gradients can be switched slowly.

Procedure

Stochastic rf excitation reduces the excitation power by a factor of the order of 10^3 . However, gradient modulation, the size of the data array to be acquired, systematic noise inherent to the method, and most importantly the lack of slice selection schemes have seriously degraded the attractiveness of the method. The use of pseudo-random noise excitation (Hadamard NMR) in combination with back projection for image construction promises to alleviate these shortcomings. In order to overcome the problem of slice selection, we have developed a new class of slice-selective presaturation sequences (SPREAD), with low peak-power requirements, easy adjustment of the slice parameters and excellent slice shapes.

Results

It can be shown, that the combination of stochastic rf excitation and SPREAD fulfils the following criteria:

1. Low excitation power to access large volumes at high frequencies
2. Good signal-to-noise ratio
3. Short acquisition times
4. Low peak power for slice selection
5. A minimum amount of hardware modifications necessary for implementation on commercial imagers.

Conclusion

The combination of Hadamard imaging and SPREAD is a very attractive possibility to do whole body imaging with low power noise excitation and slow gradient switching speeds for slice selection.

Measurement of Water Permeability of Diffusion-Barriers by NMR Signal Enhancement

Andreas P. Kiefer, Erwin Kuchenbrod, Axel Haase
Physikalisches Institut, Universität Würzburg, 97074 Würzburg, Germany

Introduction

For many biological studies the permeability of membranes is of decisive importance. We developed a technique to calculate the diffusion coefficient of membranes. Based on a two-compartment model, we simulated T1 and concurrent T2 weighted images. The results were verified in phantom study and in plant imaging.

Methods

The simulation describes a standard T1 weighted spin-echo sequence with long TE to get additional T2 weighting. We restricted the simulation to one dimension with no loss of generality. The Bloch - equations containing additional diffusion terms (1) were numerically solved for the two compartment model. The two compartments, having different T1 and T2 values were separated by a membrane with a defined water permeability. Using a finite difference method, the differential equation was substituted for a difference equation. This yields a tridiagonal system of equations which has to be solved for each timestep (2).

In the phantom studies, we used a 10 μ m membrane to separate the two compartments. One region consisted of pure water (A), the other one (B) of water plus contrast agent (Gd-DTPA-Polylysin, mol. weight 70kD from Schering). The contrast agent was encapsulated in liposomes because the pore size of the membranes is larger than the size of the contrast agent. The pulse sequence was a standard SE with shortened TR in order to obtain both, T1 and T2 weight. The images were carried out at a resolution of 7 \times 7 μ m² on a Bruker AMX 500 (11.7 Tesla) with a microimaging kit .Roots of several plants were tested for the biological application. We performed spin echos with varying TR and TE. Furthermore T1 and T2 maps were produced to calculate the permeability of the membrane by comparison the acquired image with the simulation.

Results and Conclusions

In the simulation, the phantom study and the biological application, a distinct signal enhancement at the membrane can be observed under special imaging conditions. This enhancement can be explained by spins with a short T1 value in compartment B diffusing to compartment A during the imaging sequence (see Figure 1) where they relax with a long T2. This effect depends strongly on the permeability of the membrane: the higher the diffusion coefficient, the higher the enhancement. These results were confirmed by phantom and plant studies. The latter showed, that not every plants root possess such a signal enhancement, corresponding to their different permeability.

Permeable membranes are enhanced in T1 - T2 - weighted imaging, if they separate compartments of different relaxivity. This effect can be used to calculate diffusion coefficients of biological membranes.

magnetization

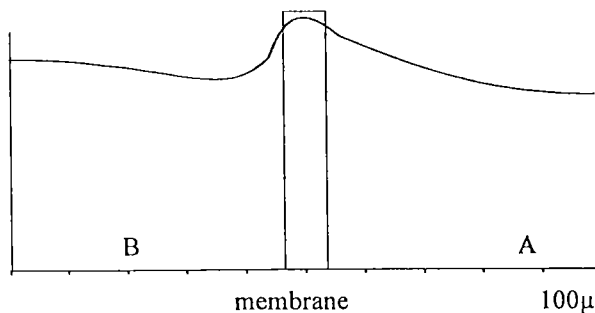


Figure 1:
Simulation of transverse magnetization in T1 - T2
weighted image. Separating membrane is in the middle

$$D_{\text{membrane}} = 50 \% D_{\text{Water}}$$

Compartment A : T1 = 4.5 sec; T2 = 1 sec

Compartment B : T1 = 1.5 sec; T2 = 0.03 sec

TE = 18 msec

Reference 1. H.C.Torrey *Physical Review*, **104**, 563,1956

2. D.Marsal, *Die numerische Lösung partieller Differentialgleichungen*, B.I., 1975

CONSTRUCTION OF MICRO-IMAGING GRADIENT COILS BASED ON A TARGET-FIELD-APPROACH

B. Kalusche, A. V \ddot{a} th, H. Adolf, A. Haase

Physikalisches Institut, Lehrstuhl f \ddot{u} r Biophysik, Am Hubland, 97074 W \ddot{u} rzburg, Germany

PURPOSE

In NMR-microscopy strong imaging gradients are needed with short rise times. Our goal was to develop a technique which allows an easy construction of coils with the postulated properties.

DESIGN

The design of the gradient coils is based on the Target-Field-Approach described by R. Turner [1]. The approach provides a current density on a cylinder which generates a target field B_z that is specified on the surface of an inner cylinder. From the continuous current distribution the locations of the discrete wires are calculated by integrating current contour lines.

For the z-gradient these contour lines are turned in a tube of glass fabric soaked in phenolic resins. In these grooves the wire is laid.

For the transverse gradients the contour lines are converted into a PostScript-file. The printout of this file is used as a mask for etching the conducting paths from a polyester foil coated on both sides with a copper layer of 100 μm . Sticking two foils on the surface of the tube with an insulating foil between them gives the x- and y-gradients.

EXPERIMENTAL

Using the technique described above we constructed a micro-imaging gradient coil with an inner diameter of 20 mm. The coil was built for a BRUKER AMX-500 widebore magnet (89 mm) with a magnetic field strength of 11.7 T.

The measured gradient rise time is shorter than 50 μs ($I=30\text{A}$) because of the low inductance of the coils ($L=8.7 \mu\text{H}$ for the z-gradient, $L=13.7 \mu\text{H}$ for the transverse gradients). The magnitude of the gradient field is 4.7 G/cm/A for the x- and y-direction and 5.3 G/cm/A for the z-direction. Deviations from linearity were measured to be less than 5 % over ± 4 mm along the transverse and longitudinal directions.

CONCLUSION

The described technique is fast and easy to perform. It requires no expensive milling machine for positioning the wires on the cylinder surface. Instead of this the current paths are etched on a flexible foil which will be fixed on the cylinder. With this technique we constructed also gradient coils with inner diameters of 40 mm and 120 mm.

The low inductance of the gradient coils allows a short switching time which is important for fast imaging methods.

Reference: [1] R. Turner, J. Phys. D. 19, L 147 (1986)

EPI Implementation with Conventional MRI Hardware

J. A. Derbyshire, T. A. Carpenter
and L. D. Hall

*Herchel Smith Laboratory for Medicinal Chemistry,
University of Cambridge School of Clinical Medicine,
University Forvie Site, Robinson Way,
Cambridge, CB2 2PZ United Kingdom*

The echo-planar imaging (EPI) technique is a desirable method for obtaining magnetic resonance images of dynamic processes due to its minimal acquisition time, and natural T_2 , or T_2^* contrast. Successful implementation of the technique is usually perceived to require specialized MR hardware. Eddy currents induced by rapidly switched, unshielded gradients may distort the field from the level of homogeneity required for direct Fourier reconstruction. This work demonstrates the implementation of EPI methods on a conventional MR system (without shielded gradients) and introduces a reconstruction algorithm which compensates for time-varying inhomogeneities in the primary (switched) gradient direction, substantially reducing the effects of eddy-currents. The algorithm has been implemented for a variety of NMR imaging systems demonstrating its robustness, and providing a low-cost means to perform EPI routinely on conventional MRI hardware.

ROTATING FRAME NMR MICROSCOPY*

Klaus Woelk, Jerome W. Rathke, and Robert J. Klingler

Chemical Technology Division, Argonne National Laboratory, 9700 South Cass Avenue, Argonne, Illinois 60439

A new type of NMR microscopy using the *Rotating Frame Imaging* (RFI) procedure in a toroid cavity detector has been developed to provide high-resolution chemical-shift information while simultaneously resolving distances on the micrometer scale. RFI was first established by D. I. Hoult¹ and implements a gradient in the radio-frequency field (B_1) instead of a gradient in the main magnetic field (B_0) to resolve distances. A major advantage of this method is that the resonance frequency of the nuclear spins is not manipulated to a measure of distance. Thus, chemical shift and distance can easily be resolved simultaneously. In the past, it has been reported to be difficult to create a B_1 gradient that is both accurate (i.e. mathematically well defined) and also strong enough to facilitate resolutions of distances below 0.1 mm. Therefore, RFI was found unsuitable for NMR microscopy. A toroid cavity resonator, however, satisfies *Rotating Frame Microscopy* (RFM) requirements and enables resolutions down to a few micrometers. Furthermore, improvements of the resolution are expected to reach the magic boundary of $1\mu\text{m}$.

The toroid cavity detectors consist of an inner wire (central conductor) and an outer cylindrical body. Thus, the B_1 field is completely confined within the cavity. It is strongest near the central conductor and drops off as the inverse of the distance toward the outer walls. Significantly, the toroid cavity is unique in the accuracy of its B_1 gradient, which has been proved by measurements of the NMR signal intensity as a function of the pulse width. Both sensitivity and distance resolution increase with the gradient in B_1 and, consequently, the toroid detector is especially suited for NMR microscopy of films that uniformly surround the central conductor. For example, a resolution of $20\mu\text{m}$ has been achieved by ^{19}F -NMR spectroscopy when the central conductor was coated with two different layers of Teflon.

The distance resolution of the presented method is in the first approximation independent from the NMR-frequency linewidth. Therefore, RFM seems to be especially attractive for investigations of solids and polymers, where broad lines usually limit the spatial resolution to $50\text{-}100\mu\text{m}$. A theoretical evaluation predicts a maximum resolution of $6.5\mu\text{m}$ when the present toroid cavity design is used. However, several refinements of the probe are in progress. An additional advantage of the toroid cavity is that even small signal intensities (as expected from the resolution of very small volumes on the surface of the central conductor) are observed due to an NMR sensitivity that increases linearly with the B_1 field.

As shown from results in ^1H -, ^{13}C -, and ^{19}F -NMR spectroscopy RFM is useful in determining the relationship between chemical structure and depth for coatings deposited on the surface of the central conductor. Furthermore, high-pressure and high-temperature capabilities of toroid cavities enable measurements of penetration rates in polymer or ceramic films *in situ* under various conditions. Additionally, electrochemical processes can be monitored, when the central conductor is used as a working electrode.

¹ D. I. Hoult, *J. Magn. Reson.* 33, 183 (1979)

* This work was supported by the U. S. Department of Energy, Division of Chemical Sciences, Office of Basic Energy Sciences, under Contract W-31-109-Eng-38.

ABSTRACT

SOLID-STATE NMR IMAGING WITH MAGIC-ANGLE SPINNING. Herman Lock, Marian Buszko, Yahong Sun and Gary E. Maciel, Department of Chemistry, Colorado State University, Fort Collins, CO Colorado 80523.

As one of the main attractive features of NMR imaging in the long term may be chemical selectivity or specification via the chemical shift, we have recently focussed on incorporating MAS in our solid-state NMR imaging strategies. ^1H and ^{13}C imaging probes that incorporate MAS and circuitry that generates rotating gradients constitute the hardware focus of this work.

^{13}C CP-MAS imaging experiments have been carried out with one transverse spatial dimension and a chemical shift dimension, and in two spatial dimensions (with or without chemical shift selection).

^1H NMR imaging under MAS has been carried out in one spatial dimension (along the rotor axis) and in two spatial dimensions (transverse to the rotor axis), with and without homonuclear dipolar line-narrowing by the TREV sequence, which has favorable characteristics for incorporation into ^1H CRAMPS imaging strategies.

Typical imaging characteristics and preliminary applications will be presented.

*International Conference on Magnetic Resonance Microscopy
Heidelberg, Germany September 5-10, 1993*

**NMR FORCE MICROSCOPY: Development of Cantilevers
and Polarized Samples for Nuclear Detection**

Gregory J. Moore and Laurel O. Sillerud

Biomedical NMR Facility, Division of Life Sciences

Los Alamos National Laboratory, Los Alamos, NM 87545

Recent theoretical work has shown that mechanical detection of magnetic resonance from a single nuclear spin is in principle possible. This theory has recently been experimentally validated by the mechanical detection of electron spin resonance (ESR) signals using microscale cantilevers. Currently we are extending this technology in an attempt to detect nuclear signals which are three orders of magnitude lower in intensity than electron signals. In order to achieve the needed thousand-fold improvement in sensitivity we have undertaken a two-fold approach: 1) the development optimized mechanical cantilevers and 2) the development of highly polarized samples.

To date, commercially available cantilevers designed for use in Scanning Tunneling (STM) and Atomic Force Microscopy (AFM) have been used in Magnetic Resonance Force Microscope (MRFM) instruments. However, the properties of these cantilevers are not optimized for MRFM experiments. We are currently designing cantilevers with optimal sensitivity by numerical simulation of the mechanical properties including length, mass, Q, resonant frequency, and spring constant. Fabrication of cantilevers via ion milling will be directed by the outcome of these simulations.

The second means of improving the sensitivity which we are pursuing is the development of highly polarized samples. To date, MR force detection experiments have been performed at room temperature and at low magnetic field strengths resulting in polarizations on the order of 10^{-6} . Our focus has been to improve the achievable nuclear polarizations using a three fold approach: 1) increased magnetic field strength (2.5T), 2) decreased temperature (100mK), and 3) use of samples polarized by Dynamic Nuclear Polarization (DNP). Our recent experiments have demonstrated nuclear polarizations in excess of 50% in molecules of toluene.

3D NMR Imaging of Water Invasion into a Chip

Siegfried Hafner and Winfried Kuhn

Fraunhofer Institut für Biomedizinische Technik IBMT
Arbeitsgruppe Magnetische Resonanz
Ensheimer Str.48 66386 St. Ingbert, Germany

The uptake of water and its distribution in the polymeric parts of a chip is of considerable interest because water influences the longtime reliability of the electronics.

Unlike in tissue water can show broad NMR lines if it is absorbed in materials, e.g. the polymeric body of a chip, where the lines broaden up to 3.5 kHz. This leads to severe problems for conventional imaging.

In the experiment a chip saturated with water in a water steam atmosphere was imaged. After this the chip was dried in six steps from each of which also images were taken. It was found that the best imaging method for this problem is 3D backprojection imaging. Due to the short T_2 value the spin echo time τ had to be chosen as short as 300 μs to achieve acceptable signal to noise.

From the results of this experiments it could be concluded that the water mainly invades the chip through the gap between metallic parts and the polymeric body whereas the surfaces seem to be relatively water tight.

Radial Distribution Function and other Statistical Evaluations of NMR Micrographs of Porous Media

H.-P.Müller, J.Weis, R.Kimmich

Sekt. Kernresonanzspektroskopie, Universität Ulm, D-89069 Ulm, Germany

Introduction

Porous materials were intensively studied by NMR microimaging methods. Generally the resulting distributions (spin-density, velocity, etc.) were found to have a heterogenous or random structure which is also typical for amorphous materials.

Method

The structure of porous materials has a certain analogy to the molecular microstructure of amorphous solids or liquids. Therefore the principles of radial distribution analysis, which originally were applied in the description of the short range order of amorphous materials, have been used.

By using this radial distribution and other correlation functions we processed spin density and flow velocity distributions of porous materials obtained by 3D and 4D methods of NMR microimaging and flow microimaging.

The statistical analysis was tested with a sample of densely packed glass beads (diameter 1 mm), which is known to have a very uniform distribution of pore size and serves as a good model.

Results

From our statistical treatment usefull informations, such as spin density and velocity fluctuations in a disordered pore network can be obtained. The goal is to reveal any correlation of these quantities.

Conclusion

Radial distribution functions have been evaluated for different porous systems. The glass bead model system reveals a short range order analogous to that of liquids in a molecular length scale.

NMR Magic Sandwich Echo Imaging of Rigid Polymers

F.WEIGAND, B.BLÜMICH*, H.W.SPIESS

Max-Planck-Institut für Polymerforschung, D-55021 Mainz, Germany

*RWTH Aachen, Makromolekulare Chemie, Worringerweg 1, D-52056 Aachen, Germany

A solid-state NMR imaging technique with protons is presented to obtain spatial resolution in rigid polymers. It is based on magic sandwich echoes (MSE). The modification of a multiple echo detection method was combined with short gradient pulses. This allows in a simple manner to overcome the strong dipolar couplings in solids up to 50 kHz. Therefore a fast gradient pulse driver was constructed with switching times between 550-910 nsec giving a maximum gradient strength of 330 mT/m. This approach fulfills essential demands for investigations in material sciences: Non-invasive experiments and short measuring times. With a new detection technique the spectral width was doubled and thus one-dimensional projections and spatially resolved spectra of rigid polymer phantoms were measured. The use of the dipolar coupling strength and the T_1 relaxation time as contrast parameter is demonstrated.

- [1] S. Matsui, *Chem. Phys. Lett.* **179**(1991)187
- [2] S. Hafner, D.E. Demco, R. Kimmich, *Meas. Sci. Technol.* **2**(1991)882
- [3] F. Weigand, B. Blümich, H.W. Spiess, *to be published*, 1993

Surface-Coil Parameter Imaging of Materials

Carsten Fülber, Bernhard Blümich*, H.W. Spiess

Max-Planck-Institut für Polymerforschung, Ackermannweg 10, 55021 Mainz, Germany

*RWTH Aachen, Makromolekulare Chemie, Worringerweg 1, 52056 Aachen, Germany

It has been demonstrated that the relaxation times T_2 , T_1 and $T_{1\rho}$ can act as versatile contrast parameters in NMR imaging. Hence not only the spin density information of conventional imaging, but also different regimes of the molecular motion on a microscopic scale are accessible by NMR imaging.

To this end not only whole-body coils but also surface coils can be employed. The use of surface coils as NMR receivers and transmitters enables investigations with a good filling factor of localized regions selected from large objects. The signal intensity across the image, however, is modulated and attenuated by a complex excitation and reception function caused by the field inhomogeneity of the surface coil. The signal intensity is also affected by the pulse sequence used in the experiment. This signal-intensity variation is converted into signal-to-noise variation by measurement of parameter images.

As T_1 and T_2 do not depend on the excitation field strength ω_1 , they are suitable parameters here. For signal excitation and detection with surface coils, saturation recovery and spin-echo techniques can be used. For the relaxation time $T_{1\rho}$ in the rotating frame the situation is more complicated, because $T_{1\rho}$ is dependent on ω_1 . Such a parameter-image, therefore, still contains the signal attenuation from the changing excitation field strength. But an ω_1 -independent parameter image can be calculated by combining a $T_{1\rho}$ and a T_2 image. The resulting image represents the correlation time of the molecular motion τ_c .

The method is illustrated by measurements on a phantom consisting of natural rubber and Proxon[®], a PVC based elastomer. A τ_c -profile is presented, which displays good contrast between the two substances. The method suffers from the uncertainty about the effective B_1 -field across the sample. This can be computed for simple coil geometries, as in our case, or can be determined by NMR imaging of homogeneous samples such as water filled cavities.

This technique is a first approach to the imaging of correlation times τ_c in special motional regimes. Applications of this technique are envisioned in surface coil imaging of large polymer and elastomer samples, where environmental stress and aging are often manifested in a change of molecular mobility corresponding to a change of the correlation time.

Pore Geometry Information Via Pulsed Field Gradient NMR

A. J. Lucas[†], S. J. Gibbs[†], M. Peyron[†], G. K. Pierens[†], L. D. Hall[†]
R. C. Stewart[‡] and D. W. Phelps[‡]

[†] *Herchel Smith Laboratory for Medicinal Chemistry
University of Cambridge School of Clinical Medicine
University Forvie Site, Robinson Way
Cambridge, CB2 2PZ United Kingdom*

[‡] *Amoco Production Company, Tulsa Research Center, 4502
East 41st Street, P.O.Box 3385, Tulsa OK74102, USA.*

Studies of echo attenuation at long diffusion times in pulsed field gradient NMR experiments (1) on a variety of rock core samples are interpreted in the light of recent theoretical analysis of the effect of pore geometry and surface relaxation (2). This study is motivated by the need to test the applicability of that theory to real rock systems.

1. P. T. Callaghan, A. Coy, D. MacGowan, K. J. Packer and F. O. Zelaya, *Nature*, 351, 467 (1991).
2. P. P. Mitra and P. N. Sen, *Phys. Rev. B* 45, 143 (1992).

Ingress of Water into Zeolite 4A Powder Plugs

B.Leone, M.R.Halse, J.H.Strange

Physics Laboratory, University of Kent, Canterbury, Kent
CT2 7NR, UK

A.R.Lonergan, P.J.McDonald

Dept of Physics, University of Surrey, Guildford, Surrey, GU2 5XH,
UK

E.Smith

Unilever Research, Port Sunlight Laboratory, Bebington, Wirral, L63
3JW, UK

Abstract

One dimensional profiles of the concentration of water absorbed from vapour diffusing into compacted type 4A zeolite powder have been obtained by broadline NMR imaging using sinusoidal field gradients at a frequency of 5kHz. T2 values were typically 300 μ secs. After an induction period of \sim 6 hours, a region of full hydration advances linearly with time into the zeolite plug. This behaviour is typical of Case II diffusion. A simple numerical simulation allowing for intra- and inter-grain diffusion gives good agreement with the experimental results.

Keywords: NMR imaging: Translational diffusion: Zeolites

**Quantitative NMR Flow Measurement in Systems of Complex Geometry:
Applications in Chemical and Petroleum Engineering.**

S. Yao, V. Rajanayagam and J. M. Pope

**School of Physics, The University of New South Wales, Kensington, NSW 2033
Australia**

The sensitivity of NMR imaging to fluid motion and flow has received widespread attention in biomedical applications of MRI, notably Magnetic Resonance Angiography. Recently a number of non-medical applications of flow imaging have emerged. These include studies of flow of water and nutrients in plants, permeation and flow of water and oil in porous media such as oil bearing rocks and applications in food processing and chemical engineering.

Techniques for the selective visualisation of flowing material and flow measurement may be classified into 'time of flight' techniques in which spins are magnetically tagged and their displacements monitored at some later time and 'phase' methods in which flow information is incorporated in the phase of the NMR signal. The latter methods appear to be particularly useful for quantitative flow measurement in systems of complex geometry [1].

In this paper we present results of quantitative flow measurements at microscopic resolution in (a) hollow fibre membrane filtration modules and (b) model porous media comprising compacted glass beads of various sizes down to 1mm diameter. The flow imaging technique employed was that of Callaghan and Xia [2], which allows for simultaneous mapping of both flow velocity and diffusion coefficient. In both types of system studied we compared volume flow rates calculated from the flow maps with values measured directly, to check quantitative accuracy of the flow rates obtained. Parameters influencing the accuracy of flow velocity determination include (i) efficiency of flow encoding and dynamic range considerations, (ii) intra-voxel velocity shear and (iii) partial volume effects. The first of these can be minimised by appropriate choice of the flow encoding gradient, while signal dephasing due to velocity shear may be minimised by flow compensating the imaging gradients. Our results show that for a given spatial resolution/matrix size, partial volume effects can be compensated by appropriate thresholding of the images prior to Fourier transform in the flow-encoding dimension.

References:

- [1] 'Quantitative NMR imaging of flow', J.M. Pope and S. Yao, Concepts in Magnetic Resonance, (in press).
- [2] 'Velocity and diffusion imaging in dynamic NMR microscopy', P.T. Callaghan and Y. Xia, J. Magn. Reson. 91, 326-341, (1991).

Methacrylic Acid Polymerization. Travelling Waves Observed by Nuclear Magnetic Resonance Imaging.

Bruce J. Balcom¹, T. Adrian Carpenter, Laurance D. Hall
Herchel Smith Laboratory for Medicinal Chemistry, University of Cambridge
School of Clinical Medicine, Cambridge, UK , CB2 2PZ

Nuclear Magnetic Resonance Imaging (NMRI) has been used to measure the velocity and reaction front structure of a travelling wave polymer system². The polymer precursor solution is neat methacrylic acid with benzoyl peroxide as the initiator³. Profiles were acquired as short t_e spin echoes. A series of 1D images of the long axis of the reaction vessel are acquired as a function of time to form a composite image. The reaction front is the transition point separating regions of high signal intensity (monomer) from regions of diminished intensity (polymer or monomer sequestered in polymer). The polymer/monomer interface is sharply defined (< 1.2 mm wide) and is characterized by an abrupt discontinuity in the nmr spin-spin relaxation time constant T_2 .

The travelling wave system is characterized by a variable length induction period with diminished, but erratic, front velocity and a sharp break point, with sudden acceleration of the wave front followed by steady propagation of the front at a rate of 0.61 ± 0.1 cm/min. The structure of the reaction front, its position and its velocity were measured directly from the composite NMRI image. NMRI measurements were predominantly ¹H, however some experiments with a ¹⁹F tracer were performed. No quantitative differences in the system behaviour were observed with the heteronuclear tracer.

The front velocity measured by NMRI was compared to an optical measure of the front velocity, outside the magnet, to delineate a possible magnetic field effect (MFE). A putative MFE would alter the kinetics of the free radical polymerization, which in turn would alter the rate of heat production of the reaction. The rate of heat production at the front controls the rate of front propagation because this system is thermally initiated (Flame Theory). Comparison of front velocities therefore provides a convenient, albeit indirect measure of an MFE.

References:

- (1) NSERC post-doctoral fellow Herchel Smith Laboratory 1990-1992.
Current Address: Department of Physics, The University of New Brunswick
Fredericton, New Brunswick, Canada, E3B 5A3.
- (2) Balcom, B. J., Carpenter, T. A., Hall, L.D. *Macromolecules* 1992, 25, 6818-6823.
- (3) Pojman, J. A. *J. Am. Chem. Soc.* 1991, 113, 6284-6286.

MICRO-IMAGING BY MAGNETIC RESONANCE ON FLEXIBLE POLYURETHANE FOAMS

R. Pirlot, B. Chauvaux and J.M. Dereppe

Departement of Chemistry CPMC, University of Louvain-la-Neuve, Belgium.

R. Huis

Chemical Research Center Shell, Louvain-la-Neuve, Belgium.

Abstract.

3-D NMR images of flexible polyurethane foam samples have been used as input data for mathematical modelling. Segmentation methods allow the identification of each individual cell. This cell is displayed by a different colour. All relevant cell parameters, like : distribution of cell dimensions, angles, distances, surfaces and volumes have been calculated. The behaviour of the foam under mechanical deformations has been simulated by finite element analysis software like "ALGOR", by using the real cell structure.

EFFECT OF BRINE INJECTION ON WATER DYNAMICS IN *POST MORTEM* MUSCLE : STUDY OF T_2 AND DIFFUSION COEFFICIENTS BY MRI.

L. FOUCAT, G. BIELICKI, S. BENDERBOUS, J. P. DONNAT, A. TRAORE and J. P. RENO
Structures Tissulaires et Interactions Moléculaires / SRV - INRA - Theix
63122 Ceyrat - FRANCE

Water-holding capacity is enhanced when meat is treated with salt. ^{31}P spectroscopy, ^1H and ^{23}Na NMR micro-imaging have been used to investigate the effects of brine injection (1,2). This study, reported here, deals with the *post mortem* evolution of the transverse relaxation time T_2 and the diffusion coefficients D_z and D_x (respectively parallel and perpendicular to the muscle fibres axis) of the water proton in rabbit muscle.

Rabbits were anesthetized, the *biceps brachii* muscle exposed and its axillary arteries and veins ligated and cut. Brines (0.5 ml, 3M or 5M NaCl at 0°C) were arterally injected. The muscle (3-4g) was then excised, wrapped in parafilm and transferred in the micro-imaging probe head maintained at 4°C . NMR experiments were recorded on a Bruker AM 400 spectrometer equipped with the AM imaging accessory. A multiecho spin-echo sequence were used to map T_2 and the PGSE method to map $D_{z,x}$. For all experiments the pixel resolution was $157\ \mu\text{m}$ with a slice thickness of 2 mm. From T_2 (or D) maps, the number of pixels in a given T_2 (or D) interval was plotted against T_2 (or D). These histograms have allowed the statistical measurements of mean value, peak width and asymmetrical parameters.

Important differences between intact and salted muscles have been demonstrated. For intact muscle, the T_2 distribution is symmetric, the values are relatively spatially homogeneous and increase with time *post mortem* from 29 ms to an equilibrium value of 37 ms. For injected muscles, the distributions are always asymmetric with a great spatial heterogeneity of T_2 values. At first, the mean values (40 and 44 ms for 3M and 5M NaCl) are greater than those for the intact muscle and decrease with time *post mortem* to reach the same value of 38 ms. A concomitant decrease in asymmetry occurs. But, T_2 is still largely variable at 1000 min, in particular for the muscle salted with 3M NaCl. Concerning the translational diffusion, the distributions have been proved to be of Gaussian form with very similar dispersions for all muscles. The D_z value is always greater than D_x . For intact muscle, the diffusion anisotropy, defined by the ratio D_z/D_x , is 1.8 and constant *post mortem* and can correspond to the oriented muscular structure in the magnetic field B_0 . For both salted muscles, this anisotropy is initially 1.3 and increases to about 1.4 and 1.5 for muscles injected with 5M and 3M NaCl. At about 11 hours *post mortem*, the D_z mean values (0.93 , 0.89 and $0.87 \times 10^3\ \text{mm}^2\text{s}^{-1}$) decrease with increasing the NaCl concentration (0, 3 and 5M) while the D_x mean values increase (0.52 , 0.58 and $0.61 \times 10^3\ \text{mm}^2\text{s}^{-1}$). This observation can be explained by changes in muscular structure such as swelling.

1 - ^{31}P NMR Studies : Effect of brine injection on energy catabolism in rabbit muscle. G. Bielicki, S. Benderbous, L. Foucat, J. P. Donnat, J. P. Renou. Meat Science, submitted.

2 - ^{23}Na Magnetic Resonance Imaging : Diffusion of brine in muscle. J. P. Renou, S. Benderbous, G. Bielicki, L. Foucat, J. P. Donnat. Accepted in Magn. Reson. Imaging.

NMR Microscopic study of new gadolinium complexes

M. Wagner, R. Ruloff*, E. Hoyer*, W. Gründer

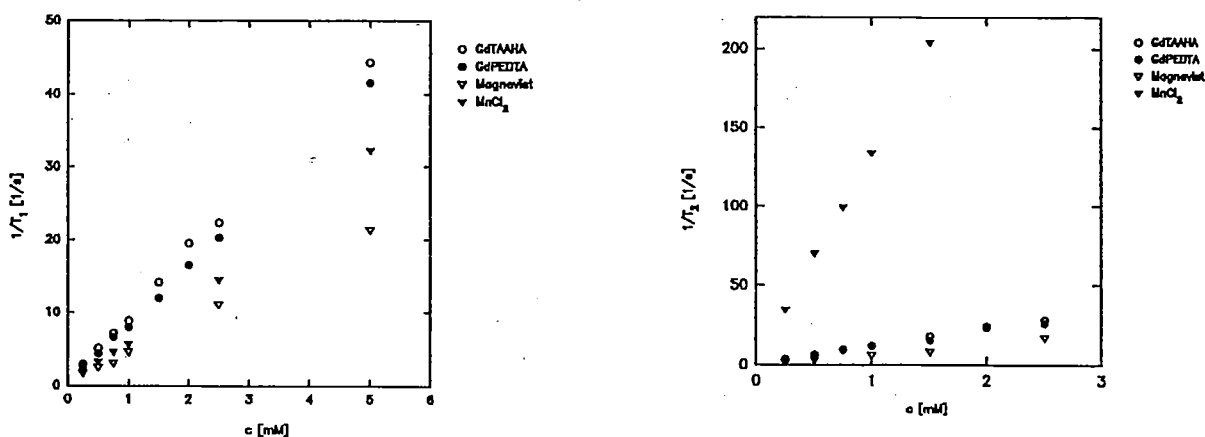
Institut für Biophysik und *Institut für Anorganische Chemie, Universität Leipzig,
D-04103 Leipzig, Germany

The main problems in an early diagnosis of arthrotic alterations are the visualization of the intactness of the surface and the determination of thickness of joint cartilage. The gadolinium complex of diethylenetriaminopentaacetat has been widely used to enhance contrast in NMR imaging. But it was shown, that free Gd-DTPA (Magnevist[®]) is taken up into the hyaline cartilage, so that surface and thickness of joint cartilage cannot be determined exactly. Application of liposome-entrapped GdDTPA (or MnCl₂) can improve essentially the representation of cartilage surface [1]. For application to MR arthrography, however, it is necessary to increase liposome stability and the relaxivity of the contrast agent. We have investigated new gadolinium complexes for the incorporation into liposomes with much larger relaxivities than those of Gd-DTPA.

The new synthesized contrast agents,

are soluble in water. All measurements were carried out at 300 MHz (Bruker AMX 300 equipped with a microimaging accessory). T₁ and T₂ relaxation times were determined using the inversion recovery technique and the Carr Purcell Meiboom Gill (CPMG) method, respectively. Intact knee joint of rabbits were imaged after intraarticular injection of 1 ml entrapped in egg yolk lecithin vesicles. MR microimaging was performed using spin echo sequences with TR = 300-500 ms and TE = 5,6-11 ms.

Relaxivities of these agents were measured to be much larger than those of Gd-DTPA.



On the other hand, the gadolinium complex of the ligand TAAHA was more stable than that of DTPA. This should result in a lower toxicity. Intraarticular injection of entrapped in lipid vesicles results in a good contrast between synovia and cartilage. The new contrast agents showed a good stability and a high relaxivity and were qualified for the incorporation into liposomes.

[1] W. Gründer, K.-H. Dannhauer, K. Gersonde, SMRM Abstracts, Vol.2, 881 (1991)

NMR Microscopic Representation of Joint Cartilage Degeneration by Liposome-Entrapped Ions

*W. Gründer, K.-H. Dannhauer, A. Werner, K. Gersonde**

Institut für Biophysik, Universität Leipzig, D-04103 Leipzig, Germany and
*Fraunhofer-Institut für Biomedizinische Technik (IBMT), D-66386 St. Ingbert, Germany

Introduction

For an early diagnosis of arthrotic alterations the visualization of abnormalities of the surface and thickness of joint cartilage is essentially. Although the intraarticular injection of Gd-DTPA improves the MRI arthroscopy, imaging of arthrotic changes is limited because of the diffusion of the contrast agent into the tissue. So, the roughness, intactness and thickness of the cartilage are not exactly depicted using free Gd-DTPA. Problems originating from the diffusion of the contrast agent could be avoided by employing non-diffusible contrast media, i.e. liposome-entrapped paramagnetics. In this paper we demonstrate, that intraarticular injection of liposome-entrapped $MnCl_2$ and Gd-DTPA (Magnevist^R) into the temporomandibular joint (TMJ) results in a considerably improved representation of the cartilage surface and the articular discus.

Material and methods

Intact TMJ of neonatal and four-week-old pigs were imaged after intraarticular injection of 0.1 ml 20 mM $MnCl_2$ and 0.1 ml 0.5 M Gd-DTPA (Magnevist) entrapped in egg yolk lecithine (20mg/ml) vesicles. By means of a needle, mechanical damages of the cartilage surface were set. To simulate degenerative arthritis, 0.1 ml papain and 0.05 ml cystein solutions were injected into the joint space at the third and the second day before sacrificing the animal. Spin-echo microimaging (TR = 500 ms, TE = 5.9 ms) was performed on a Bruker MSL 400 spectrometer (9.4 T). The pixel resolution and the slice thickness were 45 μm and 130 μm , respectively.

Results and discussion

Without contrast agent TMJ shows poor contrast between cartilage surface, joint cavity and surrounding tissue so that intactness and smoothness of the cartilage surface cannot be assessed. Degenerative arthrotic changes induced by the proteolysis with papain cannot be observed. Also after injection of free Gd-DTPA, the diffusion of this contrast agent hinders a clear distinction between cartilage surface and joint space. Intraarticular injection of $MnCl_2$, entrapped in lipid vesicles, results in a highly improved contrast of the joint space. The joint surface can be assessed and the papain induced cartilage degeneration is clearly observable. In the case of the mechanically damaged joint surface the microimages demonstrate invasion of lipid vesicles into the cartilage defects which so can be exactly localized.

Conclusions

Entrapping of diffusible paramagnetics in lipid vesicles results in a non-diffusible contrast medium which improves the presentation of details of joint surface and the visualization of the intactness or dislocation of the discus. The application of this type of contrast media can improve the early diagnosis of joint cartilage degeneration and increases the potential of the MRI arthroscopy.

High Spatial Resolution NMR Microscopy of Peripheral Joints of Man and Laboratory Animals

T. A. Carpenter[†], L. D. Hall[†], R. J. Hodgson[†], B. D. J. P. Munasinghe[†],
M. J. Nolan[†], J. A. Tyler[‡], and P. J. Watson[†]

[†] *Herchel Smith Laboratory for Medicinal Chemistry,
University of Cambridge School of Clinical Medicine,
University Forvie Site, Robinson Way,
Cambridge, CB2 2PZ United Kingdom*

[‡] *Strangeways Research Laboratory,
Worts Causeway,
Cambridge, CB1 4RN, United Kingdom*

Magnetic Resonance Imaging (MRI) of the major joints of man, such as the knee, now has a well-established clinical role. In contrast, relatively few studies have been made either of human finger joints, or of the peripheral joint of small laboratory animals such as the rat, or guinea pig. Working at 2.4 Tesla we have optimised data acquisition hardware to produce high spatial resolution images. In the distal interphalangeal joints slice thickness of 0.8mm and in-plane resolution of 0.075×0.15 mm has been achieved, with comparable resolution for guinea pig knee.

Using a range of image protocols we have visualised characteristic pathology in osteoarthritic fingers including damage to cartilage, ligaments and bone. In the guinea pig, sequential changes in the joint can be clearly followed, including cystic lesions in the bone.

This presentation will emphasise the technical requirements in this area, together with a summary of some of the results.

A Comparison of the Early Development of Ischaemic Damage Following permanent Middle Cerebral Artery Occlusion as Assessed using Histology and Magnetic Resonance Imaging.

N. G. Burdett[†], T. A. Carpenter[†], R. Gill[‡], L. D. Hall[†], R. Hatfield[†],
J. D. Pickard[‡], E. Shervill[‡], and N. R. Sibson[†]

[†] *Herchel Smith Laboratory for Medicinal Chemistry,
University of Cambridge School of Clinical Medicine,
University Forvie Site, Robinson Way,
Cambridge, CB2 2PZ United Kingdom*

[‡] *Academic Neurosurgery Unit,
Department of Surgery,
University of Cambridge School of Clinical Medicine,
Addenbrooke's Hospital,
Hills Road,
Cambridge, CB2 2QQ United Kingdom*

Permanent occlusion of the middle cerebral artery (MCA) in rats results in ischaemic damage in the dorsolateral cortex and in the caudate nucleus. The objective of this study was to compare the size of lesion using conventional histological techniques and diffusion weighted imaging.

The areas of ischaemic damage from the histology sections (n = 12/group) and MR images (n = 10) were mapped onto scale diagrams and measured using an image analyser. These areas were used to determine the total volume of ischaemic damage in each brain.

The study demonstrates (with good statistical correlation) that diffusion weighted MR images can be used to measure the early development of infarction following focal cerebral ischaemia and the time course of changes correlates well with those measured using conventional histology from 4 to 24 hours. At earlier times MRI appears to delineate an area larger than the area of ischaemic tissue seen by histology.

Diffusion Anisotropy and Size Restriction in the Rat Brain

A. BERG, F. GRINBERG, W. KUHN AND P. MESTRES#

*Fraunhofer-Institut für Biomedizinische Technik (IBMT),
W-6670 St. Ingbert, Germany*
*#Universität des Saarlandes, Fachrichtung Anatomie,
W-6650 Homburg/Saar, Germany*

Pulsed NMR spin echo-techniques in connection with static and pulsed field gradients are well established as valuable methods for measuring the translational self diffusion coefficient D of mobile molecules. Diffusion weighted MR imaging (DWI) appeared to be a useful method for the early detection of tissue damage due to cerebral ischemia in the rat brain. Nevertheless the link between the brownian motion of the water molecules the microscopic structure of the cerebral tissue and the macroscopic anatomy of the brain is still subject of modern research.

Investigations of the dependance of the NMR measured diffusion signal on the movement direction (diffusion anisotropy) might deliver useful information about dominant structural orientations. The observation of size restricted diffusion enables the aestimation of the dimension of the diffusion barriers. Thus both of the diffusion results deliver access to the microscopic cellular structure which cannot be spatially resolved in standard NMR microscopy.

It is the object of this presentation to offer diffusion images, to prove diffusion anisotropy and size restricted diffusion in the rat brain. We would like to present a simple physical model for the results and its biological counterpart.

2D and 3D Microimaging Studies of Tumor Spheroids

W. Gries, F. Grinberg, W. Kuhn, K. Gersonde

Fraunhofer-Institut für Biomedizinische Technik (IBMT), and Fachrichtung Medizintechnik,
Universität des Saarlandes, St. Ingbert, Germany

Introduction

Tumor spheroids are three dimensional cell systems (diameter 1 - 2 mm) with a necrotic center surrounded by a viable rim of proliferating and quiescent cells [1]. Tumor spheroids (a model for tumors without blood vessels) have been investigated by NMR microimaging [2-4]. In the present study T₂-weighted, parameter-selective and three-dimensional micro-imaging (spatial resolution of 23 x 23 μm²) allows a better characterization of the proliferation process in spheroids. With a new, 3mm rfcoil the acquisition-time can be reduced to about one hour. The NMR results are correlated by histological investigations.

Materials and Methods

Spheroid cultures: Spheroids of the WiDR human colon carcinoma (diameter: 1 - 2 mm) were cultured in a DMEM medium enriched with 10% fetal calf serum and equilibrated with 5% CO₂ in air. During the NMR measurements the spheroids were kept in quartz tubes (diameter: 2 mm) filled with isotonic saline phosphate buffer (pH 7.4).

NMR microscopy measurements were performed on a 9.4 T NMR spectrometer (MSL 400, Bruker) equipped with a microimaging unit. A 3 mm home made solenoidal coil and probehead improved the sensitivity. Data processing was performed in the software environment SUNRISE [5]. A spin-echo technique was employed. The inplane spatial resolution was 23 x 23 μm² and the slice thickness was 130 μm. T₂-weighted images were recorded with TR = 2 s and TE = 25 ms. T₁ images were obtained using an aperiodic saturation sequence by applying 90° hard pulses and a selective 180° Hermitian-shaped pulse (TE = 11 ms, TR from 0.4 s to 20 s). T₂-images were recorded employing CPMG pulse sequences and Hahn echo sequences (TR = 6 s, TE = 12-192 ms). Diffusion imaging was performed using the stimulated echo technique [6]. The diffusion time t_{diff} and the duration of the diffusion gradients δ were 39 and 2 ms, respectively, with an inplane resolution of 23 x 23 μm² and a slice thickness of 260 μm. The 128³ images were reconstructed with filtered backprojection and 3D FT techniques (TR = 1 s and TE = 20 ms).

Results

The microimages of spheroids exhibit a high - intensity rim corresponding to the viable cells and a low - intensity central region indicating the necrotic area. The apparent T₂ relaxation times are 41 ± 5 ms for the viable rim and 23 ± 2 ms for the necrotic center. The T₁ relaxation times are 2 ± 0.1 s for the rim and 2.7 ± 0.2 s for the necrotic center. The self-diffusion coefficients of water molecules are 0.56±0.16 x 10⁻⁵ cm²/s and 1.08±0.17 x 10⁻⁵ cm²/s for the rim and the necrotic center. The thickness of the viable rim varied between 150 and 260 μm. 3D images were obtained with an isotropic resolution of 23 x 23 x 23 μm³.

Conclusion

- Different histological areas in the spheroid can be visualized on the basis of relaxation times and diffusion coefficients.
- New coil and probehead technology improves signal to noise ratio and hence acquisition.
- Three-dimensional isotropic imaging with (23 x 23 x 23) μm³ spatial resolution allows a better characterization of the onset of necrosis or the beginning of angiogenesis.

References

- [1] R.M. Sutherland: Science **240**, 177 (1988).
- [2] O.L. Sillerud, J.P. Freyer, M. Neeman, M.A. Mattingly: Magn. Reson. Med. **16**, 388 (1990).
- [3] M. Neeman, K.A. Jarrett, L.O. Sillerud, J.P. Freyer: Cancer Research **51**, 4072 (1991).
- [4] M. Neeman, L.O. Sillerud, J.P. Freyer: SMRM, San Francisco, **1**, 943 (1991).
- [5] R. Brill, M. Staemmler: Proceedings of CAR'93, Berlin, 775 (1993).
- [6] F. Grinberg, P. Barth, W. Kuhn: 34th Experimental Nuclear Resonance Conference (ENC), St. Louis, 165 (1993).

***VISUALISATION OF SPINAL CORD DAMAGE BY A T-TUBE DRAINAGE
IN SYRINGOMYELIA.***

E. Beuls*/***, J. Gelan**, P. Adriaensens**, M. Vandersteen*, L. Vanormelingen*,
Y. Palmers*/**** and G.Freling (*****).

*Departement of Anatomy and ** Institute for Material Research at the Limburg University,
B-3590 Diepenbeek (Belgium); *** Departement of Neurosurgery, University Hospital,
Maastricht (The Netherlands); ****Departement of Radiology, St. Jansziekenhuis, B-3600
Genk; Departement of Neuropathology, University Hospital, Maastricht (The Netherlands).

This poster represents a postmortem study of the position of a T-tube inside a syringomyelic cavity. The position of a T-tube inside a syringomyelic cavity cannot be assessed neither during life nor postmortem. High Field MR microscopy at 9.4 Tesla offers a microscopic total spinal cord screening with a inplane resolution of 40 by 40 microns in the three spatial dimensions. The spinal cord of a syringomyelia patient was examined postmortem. The MR microscopic images show that correct positioning of a T- tube can hardly be achieved without damaging the parenchyma of the cord. Both the ends of the T-tube penetrate the walls of the syringomyelic cyst. The caudal end lies inside the ventral horn while the cranial end is seen lying inside the dorsal horn of the opposite side.

SCREENING OF SHORT TIME PRESERVATION METHODS FOR SPINAL CORD SPECIMENS TOWARDS OPTIMAL MRI CONTRAST.

P. Adriaensens** , M. Vandersteen* , E. Beuls*/*** , J. Gelan** , L. Vanormelingen* and Y. Palmers*/**** .

Departement of Anatomy and ** Institute for Material Research at the Limburg University, B-3590 Diepenbeek (Belgium); *** Departement of Neurosurgery, University Hospital, Maastricht (The Netherlands); ****Departement of Radiology, St. Jansziekenhuis, B-3600 Genk.

For fresh (physiological solution; 4°C) human spinal cord specimens, optimal high field MRI contrast in spin echo images is obtained by eliminating T1 and T2 weighting as much as possible, leaving essentially spin density weighted images. This requires short spin echo times (TE= 15-20 msec) and long repetition times (2-2.5 sec) , the latter being optimal employed by multiscrambling.

Experiments on bovine spinal however cord show that tissue degradation as a function of time cannot be ignored when studying a total human spinal cord (± 20 pieces of 2.5 cm; coil homogeneity)

Spin density as well as T2 calculations (multiecho pulsequence) demonstrate changes in both within 7 days, making it hard to compare and/or use these images as a reference for pathologic specimens.

A possible way to overcome these changes in contrast between gray and white matter and between neuroglial framework and white matter is to use other preservation techniques like freezing and formalin fixation. These techniques were checked on bovine spinal cord towards their impact on morphology, shrinkage and other deformation effects. Besides the well known shrinkages and other deformation effects of formalin, the main disadvantage was a decrease in neuroglial framework white matter contrast, leaving only gray white contrast.

Freezing on the other hand leads to significant increase contrast in general, making it the most favourable preservation technique for studying this tissue in a comparable way over a long period.

**REGIONAL OSSIFICATION DIFFERENCES IN THE HUMAN FETAL SPINE
BY HIGH FIELD MRI.**

L. Vanormelingen*, E. Beuls*/***, J. Gelan**, P. Adriaensens**, M. Vandersteen* and Y. Palmers*/****.

*Departement of Anatomy and ** Institute for Material Research at the Limburg University, B-3590 Diepenbeek (Belgium); *** Departement of Neurosurgery, University Hospital, Maastricht (The Netherlands); ****Departement of Radiology, St. Jansziekenhuis, B-3600 Genk.

The development of the vertebral column is a generally well know phenomenon in human embryology. Several studies about the timing of the appearance of ossification centres are published. But specifications about the further development during the fetal period are seldomly made. Moreover, regional ossification differences hardly are mentioned in literature. High Field MR imaging therefore is an excellent method to investigate entire specimen of human fetal vertebral columns. The resulting images have such a high resolution that they can be compared with low magnification light microscopy.

The entire spine of a human fetus, 6.5 months gestational age was removed and devided in cervical, thoracic, lumbar and lumbosacral parts, that were fixed in 2% formalin solution. MR investigation was done with a 9.4 Tesla Varian device, using a Multislice Spinwarp technique. TR= 2500 msec/ TE= 40 msec/ slice thickness= 1 mm./ NT= 24 to 40.

The first objective of this investigation is the study of the general MR appearance of the different structures of the spine. Secondly the spatial extent of these structures is minutly studied and described with the help from MR images in the three orthogonal planes. Finally regional differences in appearance and ossification of the vertebrae are described.

High Resolution Imaging of Growth and Gene Therapy of Gliomas Injected into Rat Brain.

R.Demeure, I.Mottet, J.F.Goudemant, Radiology Dpt.
A.Maron, T.Gustin, J.N.Octave, Neurochemistry Laboratory.
Catholic University of Louvain, Belgium

Introduction : In humans, gliomas are malignant and invasive tumors which are often inoperable and resistant to chimio- and radiotherapy. A way to solve this problem could be the development of a gene therapy of brain tumors. To evaluate this way of glioma therapy, an animal model has been developed. The purpose of the present study is the follow-up of the growth and regression after therapy in rat brain of this tumor kind using High Resolution Magnetic Resonance Imaging (HR-MRI).

Material and methods : Tumors were induced by injection into caudate nucleus of brain of 10 μ l (10mm³) of agarose gel containing cultured C6 glioma cells using stereotaxic guidance. This injection creates in brain a small spherical lesion of 1.5 mm radius. After anesthesia by intraperitoneal injection of chloral hydrate, rats were imaged in a 4.7 Teslas (200 MHz) superconductive magnet (Biospec/Bruker). Images were performed with a linearly polarized "bird cage" transmitter-receiver coil of 7 cm diameter. Magnetic field gradients of 38 Gauss/cm maximum gradient strength and a rise time of 512 μ s were generated by 152mm bore gradient coils. Series of 6 contiguous transversal slices were acquired using a T₂-weighted multislice rapid spin-echo pulse sequence called RARE (TR/TE/RARE factor ;3000ms/13ms/8) (1). The field of view (FOV), the slice thickness and the image matrix were respectively 5 cm, 1.25 mm and 256² pixels providing a spatial resolution of 130 μ m by image pixel. The tumor volumes were determined by summation of partial volumes measured in each slice where tumor was visible. These measurements were realized using an home made image processing software called MEDIMAN (2) implemented in a DEC-AXP workstation (Digital Co, USA).

Results : Immediately after glioma cells injection, the agarose gel microsphere generates a disk shape hypointense signal in MRI images. Seven days later, glioma begins to be visible as a thin hyperintense crown (0.11 mm thickness) around the agarose microsphere. HR-MRI allows a very good delineation of the tumor from agarose and normal brain tissue. The tumor volume and crown thickness increase versus time are presented in table I.

Conclusions : These preliminary results show that a non invasive and accurate measurement of tumor growth kinetics is possible with HR-MRI. Therefore, the follow-up of tumor regression after gene therapy will be also possible. A great advantage of HR-MRI

Time (days)	Tumor volume (mm ³)	Tumor thickness (mm)
7	0.91	0.11
9	4.87	0.44
11	7.59	0.65
14	9.05	0.73
21	30.9	1.39

Table I

with regard to classical tissue analysis techniques (histology) is the opportunity to follow the same rats throughout tumor growth and regression.

References :

- (1) B.Gallez, R.Debuyst, R.Demeure, F.Dejehet, C.Grandin, B.Van Beers, H.Taper, J.Pringot, "Evaluation of Nitroxyl Fatty Acid as Liver Contrast Agent for Magnetic Resonance Imaging", Mag.Reson.Med. (accepted for publication 05/1993).
- (2) A.Coppens, M.Sibomana, A.Bol, C.Michel, "MEDIMAN : an object oriented programming approach for medical image analysis", (submitted for publication 1993).

B. Shuter and J.M. Pope*

Radiology Department, Royal North Shore Hospital
and School of Physics, University of New South Wales*, Sydney, Australia

Introduction

Oxygen-dependent image contrast at field strengths higher than those in common clinical use has recently been demonstrated¹. Real-time changes in signal with anoxic respiration² offer strong corroborative evidence that deoxygenation of red blood cells is the cause. Deoxygenation is the immediate effect of sacrifice of experimental animals, an act which may be required on occasions in MRI research. However, the effect of sacrifice on MR characteristics of tissues, particularly relaxation times T1, T2 and T2*, does not appear to be well documented. We have attempted to assess these effects in a rat model.

Materials and Methods

Male Wistar rats (300g-350g) were anaesthetised (2%-3% Halothane in 100% oxygen at 1-2 litres/min) and a tail vein cannulated. Imaging was performed with the rat supine and snugly restrained in a plastic box at about 60° to the imaging table, a position which provided images least affected by motion and best reproducibility of organ relaxation times. T1, T2 and T2* were determined pre- and post-sacrifice (30mg Sodium Pentobarb via the tail vein cannula). The order of measurement was cycled post-sacrifice to ensure each relaxation time determination was made as close as possible to the act of sacrifice for at least three animals and to allow an estimate of trends.

A GE 1.5T MR imager was used to obtain slices through brain, kidney and liver (3mm, CSMEMP, 1NEX). T1 was determined from a (TE:25ms;TR:4,2,1,0.5,0.24, 0.18,0.12s) image series, T2 from a (TR:0.5s; TE:25,30,40,55,70ms) series and T2* from a (TR:0.5s; TE:11,15, 20,25,35,50,75ms) (MEMP, 1NEX, 45° flip angle). The T2 and T2* series were acquired as single echo images to ensure slice profiles were only affected by diffusion and not instrumental factors. Between images or sequences requiring long collection times (eg a TR:4s or a T2 sequence) and immediately before as well as after sacrifice, TR:240ms;TE:25ms images were acquired to monitor signal stability. Standard GE SIGNA software was used to perform T1 and T2 fitting. T2* was determined by fitting a single exponential to the signal decay using a simple least squares approach.

Results

The ratio of signal intensity on the TR:240ms;TE:25ms images immediately post-sacrifice (<3 min) to pre-sacrifice was <1 in the brain, liver and kidney cortex, not only in gradient-echo (GE) but also in spin-echo (SE) images (table below), although equivocally so in the brain. A slow return to pre-sacrifice levels was evident over a period of an hour post-sacrifice in the spin echo images. T2 fell after sacrifice (table below) in liver (p<0.001) but rose in brain (p<.005). Kidney regions trended to lower T2s without statistical significance. T2* fell without exception but was not significant in kidney papilla. Kidney T2* data showed oscillations which were probably chemical shift effects and which may have affected accuracy of T2* estimates. T1 increased on sacrifice (table below) in the liver (p<.001) and kidney cortex (p<.02), the latter only by a small amount. Other kidney regions had non-significant changes. Brain T1 was unaffected.

	T2 (ms)		T2* (ms)		T1 (ms)		Post/Pre Sacrifice Signal Ratio	
	Pre	Post	Pre	Post	Pre	Post	SE	GE
Brain:	63.5	67.2	57.4	52.8	1035	1042	0.98	0.91
Liver:	32.3	27.7	27.0	14.8	653	887	0.69	0.55
Kidney Cortex:	59.4	52.9	52.6	38.6	1045	1177	0.90	0.84
Kid Medulla:	67.6	58.5	43.8	33.1	1186	1290		
Kid Papilla:	123	104	96.4	64.6	2768	2328		

Discussion

At sacrifice image signal might be expected to rise. Motion and perfusion effects, which generally increase signal dephasing would cease, increasing T2*. If all of the observed increase in liver T1 occurred before the beginning of post-sacrifice image collection (about 1 min; T1 trend data suggested this unlikely), then a reduction of as much as 0.77 could be attributed to T1 effects. The much larger observed loss of image signal in liver gradient-echo images was consistent with magnetic field inhomogeneity effects caused by increased magnetic susceptibility of red blood cells on oxygen depletion. It is possible that deoxyhaemoglobin contrast may be exploited in liver at 1.5T, even though the major blood supply to this organ consists of venous blood.

Gradient-echo signal loss in brain could be ascribed to susceptibility effects as T1 did not change. Effects in kidney were suggestive of a similar mechanism, but less conclusive. Signal loss on spin-echo images could be explained by persistent proton diffusion in the presence of susceptibility-induced gradients. T1 increases observed may be accounted for by changes in water distribution or perhaps temperature effects.

References

1: Ogawa S. et al, *Magn. Reson. Med.* 14, 68 (1990). 2: Turner R. et al, *Magn. Reson. Med.* 22, 159 (1991).

INTERACTION OF PARAMAGNETIC METAL COMPLEXES WITH INTRACELLULAR WATER: A STUDY OF CYTOPLASM AND NUCLEI OF X. OOCYTES BY SPATIALLY RESOLVED T1-, T2-TIME MEASUREMENTS

S.Päuser, K.Keller*, C.Mügge, A.Zschunke
 Institut für Angewandte Analytik und Umweltchemie, FB Chemie der Humboldt-Universität zu Berlin, Hessische Str.1-2, 10115-Berlin,*Institut für Pharmakologie, Freie Universität, Thielalle 69-71, 14195-Berlin, Deutschland

Xenopus laevis oocytes (1 mm in diameter) were used as a convenient test model to study the membrane permeability of paramagnetic metal complexes by NMR-spectroscopy and NMR-microscopy [1,2].

Spatially resolved measurements of the relaxation times of the nuclei and different parts of the cytoplasm of X. oocytes by means of modified spin-echo sequences (SE) provided the information by which properties the different signal intensities (SI) within untreated oocytes are caused. The strong SI observed for the oocytes nuclei (see Fig.1) was caused by the highest proton density and T2-time as compared to other areas of the cell. The long T1 - time seems to confirm the assumption of mobile water molecules. Relatively low SIs of the vegetal pole (the dark pole of the cytoplasm in NMR-images) are explained by very short T2-times and a low spin density. We also observed the greatest deviations of the measured SIs, the T1-time values and spin densities in this part which is in line with the idea of a heterogeneous structure as can be aspected for the vegetal pole as a store for nutrition reserves. In order to study interaction of membrane permeable paramagnetic metal complexes with intracellular water relaxation time measurements were performed on oocytes, which were placed into a physiological solution containing the contrast agents in varying concentrations (see Fig.2). Into the oocytes nuclei a T1-time value similar to the T1-time of the surrounding medium was achieved. Independent of the complex concentration of the surrounding medium that of the dark cytoplasm was reduced by about $42 \pm 3 \%$. The very short T2-times does not qualify for analysis, since the changes observed are within the range of a natural deviation.

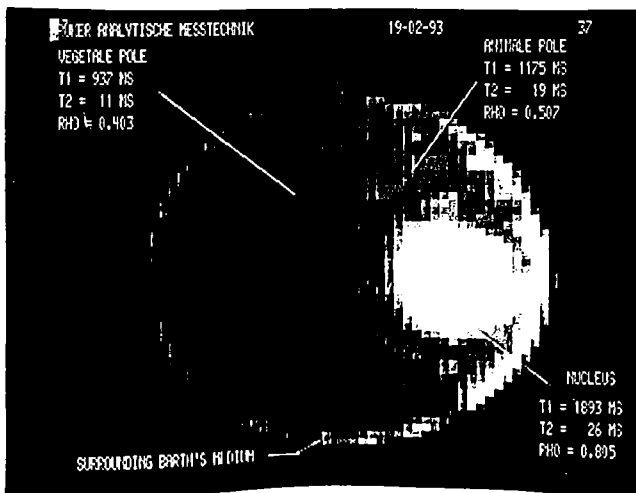


Fig.1: Zoomed SE image of a X. oocyte.
 Parameters: TR= 5027 ms, TE = 18.12 ms, SW = 25 kHz,
 read gradient: 100 mT/m, slice thickness: 832 µm.
 number of pixels: 256, number of experiments: 1

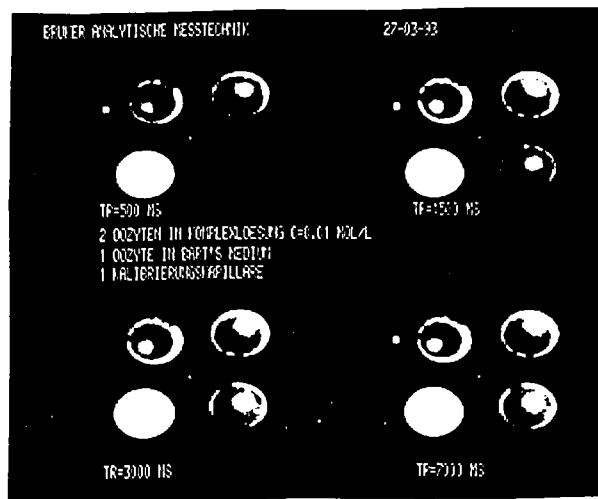


Fig.2: Two oocytes in a solution, dotted with a contrast agent, one untreated oocyte and a calibration capillary at different repetition times. The other parameters like Fig.1.

REFERENCES:

- [1] Päuser, H., Mügge, C., Zschunke, A.: Test of the Membrane Permeability of Paramagnetic Metal Complexes of Derivativon of 3-Acetylacetone Acid by NMR-Microscopy. Posterabstract I. International Conference on NMR-Microscopy Heidelberg 1993
- [2] Päuser, H., Keller, K., Mügge, C.: Study of the Membrane Permeability of a Paramagnetic Metal Complex on Single Cells. Magn. Imag. Vol.11, No.3, 419-424, 1993

High resolution NMR imaging and Microscopy of the rat ovarian cycle

Catherine Tempel, Gila Meir, Yael Steinfeld and Michal Neeman
Department of Hormone Research, Weizmann Institute of Science, Rehovot 76100 ISRAEL

The development of the ovarian follicle through the normal menstrual cycle involves a chain of fascinating hormonal events that lead to its growth, differentiation, maturation and luteinization. The preovulatory follicle of the rat reaches a diameter of approximately one millimeter, with no internal blood supply. Diffusion is the sole mechanism of nutrient and oxygen supply. Luteinization is accompanied by rapid invasion of blood vessels into the follicle.

The basic functional unit of the ovary, the follicle, was studied *in vitro* using high resolution on a BRUKER AMX400 spectrometer equipped with microscopy accessory. Diffusion and T_1 weighted images of a single perfused PMSG-primed follicle were acquired using an imaging version of the Stejskal-Tanner PGSE experiment with in plane resolution of 23 μm . The follicular fluid in the antrum appears as a dark region, almost iso-intense with the medium and the cell rim appears bright. The self diffusion coefficients for water were: $2.17 (\pm 0.019) \times 10^{-5} \text{ cm}^2/\text{s}$ for the medium, $0.46 (\pm 0.2) \times 10^{-5} \text{ cm}^2/\text{s}$ for the granulosa cells and $1.53 (\pm 0.45) \times 10^{-5} \text{ cm}^2/\text{s}$ for the follicular fluid. As expected, the medium and the antrum showed a single water compartment. On the other hand, the diffusion coefficient of water in the granulosa rim showed that water was segregated into at least two compartments with different diffusion coefficients, an extracellular one with fast diffusion and an intracellular one with slow diffusion ($D_g = 0.28 (\pm 0.16) \times 10^{-5} \text{ cm}^2/\text{s}$). The low diffusion coefficient of the granulosa region means that alimentation of the oocyte depends on nutrient permeability across the granulosa cell barrier, and that the oocyte and the cumulus cells could very well be in metabolic stress prior to ovulation.

Images of explanted super-stimulated ovarian follicles were acquired at different times after *in vivo* stimulation with luteinizing hormone (LH). Although the follicle volume increases by more than two fold during maturation, the thickness of its granulosa cell layer stayed constant ($0.137 \pm 0.007 \text{ mm}$). The diffusion coefficient of the granulosa cell layer stayed also unchanged ($0.47 \times 10^{-5} \text{ cm}^2/\text{s}$) while the diffusion coefficient of the follicular fluid increased by 75% during maturation because of absorption of fluids, thus facilitating nutrient transport across the antrum.

The female rat ovaries and uterus could be clearly resolved *in vivo* by NMR microimaging on a horizontal 4.7T Bruker-Biospec spectrometer. Rats were placed supine with the kidney and ovary positioned above a 2 cm surface rf coil. Gradient echo images and fat suppressed gradient echo images were acquired at different points along the rat menstrual cycle with an in plane resolution of 156 μm . Image resolution allowed differentiation between the oviduct, the graafian follicles, corpus luteum and blood vessels. We could see changes in NMR images of the ovaries and the uterus between the four days of the menstrual cycle, due to altered size and signal intensity and changes in the vascularization of the ovary and the uterus. At proestrus, the preovulatory stage, the ovary and the uterus were swollen with water and appeared bright in fat suppressed gradient echo images. Graafian follicles could be observed. During estrus the uterus and the ovary became highly vascularized and appeared dark in T_2^* weighted images. Some dark spots were detected in the ovary due to vascularized Corpus Luteum. At metestrus and diestrus, the ovaries and uterus were reduced to their minimal size. Moreover, we followed LH effect and ovulation in real time and saw direct effects of ovulation on image contrast.

In summary, the rat ovary provides a unique model for studying non invasively by NMR imaging hormonal control of differentiation at the levels of isolated organ culture as well as *in vivo*.

PRELIMINARY STUDIES on MOLLUSC SHELLS by ^{13}C CP/MAS and ^1H MICROSCOPY

Teresa Nunes , Gabriel Feio
ICTPOL, Av.Prof. Gama Pinto 2, 1699 Lisboa Codex , Portugal
and

Rolanda Albuquerque de Matos
Centro de Genética e Biologia Molecular, Av. Prof.Gama Pinto 2, 1699 Lisboa Codex, Portugal

The classification of the different species of snails found in Portugal is in progress.¹ Beyond all the information concerning the soft parts of the individual it is necessary to report the data on the shell characterization (size and shape, chemical analysis, etc.); for example, a detailed study of the shell spiral can be very useful to distinguish one species from another.

We present here a nuclear magnetic resonance study of several land and marine snails.

^{13}C CP/MAS spectra were obtained from powdered shells in order to simultaneously get a preliminary indication on ^1H relaxation times and to find any evidence for chitin content (a polysaccharide with N-acetylglucosamine repeating units, normally demanding a very expensive and time consuming chemical analysis). Until now we were not successful in this last proposal owing to severe spectral overlapping; however, we observed that the resonances of the carbonyl groups are easily seen and can provide an useful tool for ^{13}C microscopy and also that different ^1H relaxation times can be measured in the samples regarding the environment of the mollusc (much smaller relaxation times are assigned to marine snails in agreement with the presence of paramagnetic centers in sea water).

A ^1H microscopy study of the shell spiral is described. Using spin-echo or gradient-echo based sequences, depending on the spin-spin relaxation time of the sample, different projections of the shells were obtained. A tentative measurement of the different spiral parameters is performed. Obviously these data could be obtained by X-ray techniques but we are looking for a competitive method, since more than two hundred of different snail species have to be classified.

1. Albuquerque de Matos, R. - "Atlas of the Portuguese non-marine molluscs", in preparation.

MR Imaging of Degeneration and Self Repairing of Cartilage Contrast Enhanced by Mn²⁺-ions

Y. Morita‡, C. Raible, Y. Kusaka‡, K. Gersonde

Fraunhofer-Institut für Biomedizinische Technik, and Fachrichtung Medizintechnik, Universität des Saarlandes, St. Ingbert, Germany, ‡ Departement of Orthopaedics, Kyoto Prefectural University of Medicine, Japan

Introduction

High spatial resolution by NMR microscopy and contrast enhancement via Mn²⁺-proteoglycan interaction results in the visualization of fine structures in cartilage [1]. Furthermore local NMR-signal intensity correlates with the concentration of proteoglycans (PG's) which attract Mn²⁺-ions.

Degenerated cartilage is characterized by a loss of the PG's. In this presentation we show a model of degenerated cartilage which is based on chymopapain-induced digestion. The change of PG concentration due to chymopapain digestion results in changes of Mn²⁺-accumulation. Hence T₁-weighted images and T₁ and T₂ images of articular cartilage will reflect the degree of Mn²⁺-accumulation via changes of ¹H-relaxation times. It is the aim of the present study to identify differences between normal and degenerated cartilage and visualize the self repairing stage of cartilage by staining with Mn²⁺ and NMR microimaging.

Materials and Methods

For in vitro experiments cartilage of the knee of young chicken (broiler) were incubated at 37° C for 24 hours in 0.5 mg/ml activated chymopapain. For in situ experiments 10 mg/ml chymopapain solution were injected into the joint space of the right intact knee 2,7,14 and 21 days before sacrifice. For NMR microscopy a piece of the medial femoral condyles with articular cartilage, growth cartilage, and subchondral bone was dissected en block and combined in one NMR sample with the corresponding piece of the medial condyles of left knee as reference. All specimens were soaked for 10 min in an isotonic saline solution of 0.1 mM Mn²⁺ used as contrast agent. All measurements were performed on a 9.4 T NMR spectrometer (MSL 400, Bruker) equipped with a microimaging unit. T₁-weighted images (T_R = 500 ms, T_E = 9 ms) and spatially resolved T₁ and T₂ relaxation time measurements were done.

Results and Discussion

T₁-Weighted, T₁, and T₂ Images

Normal and degenerated cartilage without Mn²⁺ show no significant difference with regard to the signal intensity and the relaxation times. In the presence of Mn²⁺ normal articular cartilage shows higher intensity and shorter T₁ and T₂ relaxation times than degenerated cartilage. This reflects a higher concentration of PGs in normal articular cartilage rather than in degenerated cartilage, which accumulate more Mn²⁺.

Visualization of self repairing stages of cartilage

In the presence of Mn²⁺, articular cartilage in self repairing stage (21 days after injection of chymopapain) shows higher intensity and shorter T₁ relaxation times than degenerated cartilage (2 days after) and degenerate part and repairing part can be clearly distinguished in T₁ images.

Conclusion

- Losses of PG's in degenerated cartilage can be visualized in the presence of Mn²⁺.
- This noninvasive technique could be useful for the clinical diagnosis of degenerated cartilage.

References

- [1] Y. Kusaka, W. Gründer, H. Rumpel and K. Gersonde: Magn. Reson. Med. 24, 137 (1992)

Application of Nuclear Magnetic Resonance Microscopy for Studies of Lepidopteran Metabolism

John T Christeller*, William A Laing*, Craig D Eccles†,
Ute Skibbe† and Paul T Callaghan†

*The Horticulture and Food Research Institute of New Zealand, Batchelar Research Centre, Palmerston North, New Zealand; †Department of Physics and Biophysics, Massey University, Palmerston North, New Zealand.

Abstract

Lepidopteran larvae are a serious pest in New Zealand and international agriculture. To find a biological defense against these caterpillars, the metabolism has to be thoroughly investigated.

A remarkable property of these insects is a very high luminal pH in the gut, which is probably dependent on stage of development and on diet. Conventional measurement of intracellular pH involves the insertion of a pH microelectrode into the caterpillar⁽¹⁾. NMR imaging microscopy seems to be a better tool for the investigation of the insects' metabolism. There are two main advantages. The first is that NMR is noninvasive. Thus it is possible to feed the same caterpillar on different diets and to measure the pH. Furthermore NMR microscopy is able to resolve small pixels corresponding to the investigation of the pH in different regions of the caterpillar. High resolution up to 0.05 mm offers the possibility to study the modulation of pH gradients in time and space in living insects.

Two different nuclei are appropriate for this research. With proton NMR it is possible to illustrate the fluid transport through the insect and monitor the different regions within the caterpillar using T_1 - and T_2 -mapping and chemical shift imaging. With phosphorus NMR the pH of the gut can be investigated. The chemical shift of all ^{31}P resonances in natural phosphate compounds, including the inorganic phosphate peak is pH dependant. By comparing the chemical shift with a titration curve the pH can be determined⁽²⁾.

The model insect for the measurement is *Spodoptera Litua* Fabricius, the "tropical armyworm". Proton cross sections resolve the structure of the insect. By preceding the usual Fourier imaging pulse sequence with a chemical selective pulse, water and fat images could be received. The entire chemical shift spectrum was obtained by using three dimensional phase encoding. Thus the different regions, such as the dorsal vessel, the gut etc can be determined. Phosphorus measurement shows regions with different pH in the insect. ^{31}P chemical shift imaging seems to be a very effective method to provide information on the digestive regulation of these insects.

1. J A T Dow, *J Exp Biol* **172**, 355 (1992).
2. D G Gadian, G K Radda, R E Richards and P J Seelig, *In Biological Applications of Magnetic Resonance* (Ed R G Shulman), 463-535, Academic Press, New York, 1979.

QUANTITATIVE IMAGING of NMR RELAXATION in PLANTS.

Hommo T. Edzes, D. van Dusschoten and H. Van As

Wageningen Agricultural University

Department of Molecular Physics and Wageningen Agricultural NMR Centre

Dreijenlaan 3, 6703 HA Wageningen, The Netherlands

The information content of NMR images is increased considerably if nuclear magnetic relaxation times and diffusion constants are mapped in supplement to morphological details. So far qualitative 'T₂' plant images have generally been generated from single-exponential fits to a limited number of echoes with coarse time-resolution. It is our goal to obtain well-resolved relaxation curves in imaging experiments on a pixel-by-pixel basis.

On our SMIS imaging system we have implemented a CPMG-based multi-echo spin-warp sequence with which we are able to observe the transverse magnetization decay for over 2 s during which period 512 signal-containing image echoes of 64*64 pixels can be sampled. We were able to achieve this result by the use of a short echo interval (minimum of 2.5 ms) at a magnetic field strength of 0.47 Tesla (NMR frequency 20.35 MHz). A train of hard 180° refocussing pulses with (+--+) rf phase pattern is used. A probe with active shielded gradient coils (Doty Scientific) with fast rise- and fall times (<100 μs) enables us to use the short echo interval which is needed to minimize T₂ dispersion effects [1]. The measured transverse relaxation curves are a faithful representation of the relaxation behavior on a pixel-by-pixel basis. The deviation of the observed transverse relaxation times from the intrinsic ones is determined mainly by the diffusion attenuation which is inherent to the presence of the imaging gradients.

We are also able to measure sets of transverse relaxation images in combination with spin-lattice relaxation, diffusion measurements, 'true' CPMG transverse relaxation and magnetization transfer effects. The correlation between the different sets of images provides for improved quantification of the physical parameters and so increases our understanding of the origins of NMR image contrast in plants. Examples will be shown of relaxation and diffusion images of cherry tomatoes and of germinating fava beans.

[1] B.P. Hills and S.L. Duce, *Magn. Reson. Imaging* 8:321-331 (1990)

Exchange studied by combined diffusion and T₂ measurements.

D. van Dusschoten, J.B.M. Goense, H.T. Edzes, P.A. de Jager and H. Van As.
Agricultural University Wageningen
Department of Molecular Physics and Wageningen NMR Centre
Dreijenlaan 3, 6703 HA Wageningen, The Netherlands.

The investigation of water balance in biological systems has been one of the focus points of NMR research since its discovery. The water balance is maintained by diffusional processes which can be probed by both PFG NMR and CPMG measurements. The sensitivity of both types of measurements stems from distinct physical sources therefore giving a different type of information on water mobility. In a multi compartment system, even without exchange, the PFG S(T)E methods suffer from a lack of resolution, generally because of insufficient data points and diffusion constants resembling one another. Since multi exponential resolution in the time domain is more easily obtained, combining the above sequences into a PFG CPMG will result in an increased resolution in the b-domain [1]. Even more so when the acquired 2D data set is analysed in one stroke. This particularly enhances the accuracy of the diffusion constants so these can be separated when they differ less than a factor 1.5, the T₂'s being a factor 3 apart. In several Monte Carlo simulations and experiments this is demonstrated to work even with a SNR as low as 100.

When exchange between the compartments exists the above 2D analysis would result in erroneous T₂'s, amplitudes and D's. This gives a simple tool to check if exchange does occur. Because of the different probing in the time and b-domain the effect of exchange on the curvature in the two directions is rather distinct. By including exchange in the master equation of the 2D fit the original D's of the present compartments can be extracted even when exchange in the time domain is intermediate. Some results of the PFG CPMG sequence and the data analysis are shown in blood and apple tissue. This approach is similar to fitting a 2D data set as acquired by fluorescence decay [2].

The above methodology is novel for diffusion measurements by NMR and greatly increases its applicability in the (bio)physical field.

1. D. van Dusschoten, C.T.W. Moonen, H. Van As and P.A. de Jager, Book of Abstracts 11th SMRM, 1993.
2. J.M. Beechem, M. Ameloot and L. Brand, Chem. Phys. Lett. 120, 1985.

**SENESCENCE OF MUSHROOM (*AGARICUS BISPORUS*) STUDIED BY
T2 NMR IMAGING**

H.C.W. Donker, H.T. Edzes & H. Van As
Wageningen Agricultural University
Department of Molecular Physics and Wageningen Agricultural NMR Centre
Dreijenlaan 3, 6703 HA Wageningen, The Netherlands

The post-harvest senescence of mushrooms is predetermined, but strongly influenced by the storage conditions. The senescence can easily be observed by the appearance of the fruit-body. However the internal changes of the mushroom during storage can not easily be observed. They consist of the redistribution of water and other compounds caused by the development of specific parts of the fruit-body (1). We used quantitative NMR T2 and amplitude imaging to visualize the redistribution of water in the mushroom.

Three fruit-bodies, harvested simultaneously, were stored under different conditions. Two of them were stored for 5 days at 277 K, one in a closed box and one in an open box. The third mushroom was stored for 5 days at 295 K and 60% relative humidity in an open box.

A multi-echo imaging sequence was used to image these mushrooms during the storage period. At 0.47 T $T_e = 2.5$ ms was used to record 512 echo's with $T_r = 3$ s, resulting in a voxelsize of $0.47 \times 0.47 \times 2$ mm³. The T2 decay curve of each voxel was analysed mono-exponentially.

All mushrooms developed the gill and spores, where the mushroom stored at 295 K succeeded most, shown by a decrease of the T2 of the water in the gill.

The gill developed at the expense of the cap and the stipe. The stipe dries out almost completely, where the cap dries most just behind the gill and its outer surface.

The other two mushrooms do not dry as much as the one stored at room-temperature but do develop structure in the stipe.

These results demonstrate the contribution that NMR-imaging provides to the study of internal water balance of senescing mushrooms.

1) P.B. Flegg, D.M. Spencer and D.A. Wood, The Biology and technology of the cultivated mushroom, John Wiley & sons, Chichester, 1985.

THE UPTAKE OF WATER BY THE MUSHROOM (*AGARICUS BISPORUS*) VISUALIZED BY NMR IMAGING WITH THE AID OF Gd-DTPA CONTRAST ENHANCEMENT.

H.C.W. Donker, H.J. Snijder, H. Van As & A.W.H. Jans

Wageningen Agricultural University

Department of Molecular Physics and Wageningen Agricultural NMR Centre

Dreijenlaan 3, 6703 HA Wageningen, The Netherlands

In the post-harvest quality control of mushrooms interest exist in the uptake, transport and distribution of metabolites. Several mechanisms for the transport of metabolites were suggested, diffusion, cytoplasmic streaming, osmotic flow and transpiration, but the mechanism remains unknown (1). However, water is needed for transport through the fruit-body.

With NMR imaging we investigated the balance of water over a mushroom (see other poster of H.C.W.D.). However these experiments did not learn anything about the transportation of water and metabolites. Therefore we used Gd-DTPA as an example for the uptake of a salt by harvested mushrooms. The advantage of Gd-DTPA is the contrast enhancement which it induces in an NMR image, although the origin of the contrast is unknown.

We placed two different mushrooms with their stipe's in a Gd-DTPA solution and recorded eight T1-weighted magnetic resonance images over a period of 150 min. The first mushroom was freshly harvested, where the second mushroom was stored 24 hours at 295 K and 50% relative humidity. Because its storage regime the second mushroom was partly dried. The images were recorded on a 4.7 T imager with $T_e = 6$ ms and $T_r = 103$ ms, resulting in T1-weighted images.

The freshly harvested mushroom showed structured contrast enhancement that appeared at two small spots in the gill. The dried mushroom showed one broad contrast enhanced band in the stipe and a radial spreading of the contrast enhanced band in the cap and accumulated contrast enhancement in the complete gill.

The observed changes in the intensities (contrast enhancement) will be discussed in terms of the contrast mechanism of Gd-DTPA and the effect of Gd-DTPA on the local water balance of the cells.

1) P.B. Flegg, D.M. Spencer and D.A. Wood, The Biology and technology of the cultivated mushroom, John Wiley & sons, Chichester, 1985.

Development of fruits of blackcurrant (*Ribes nigrum*) revealed by NMR microscopy

B. Williamson^a, B.A. Goodman^a, G. Hunter^b, J.A. Chudek^b and J.A.B. Lohman^c

^a Scottish Crop Research Institute, Invergowrie, Dundee DD2 5DA, Scotland, U.K.

^b Department of Chemistry, University of Dundee, Dundee DD1 4HN, Scotland, U.K.

^c Bruker Spectrospin Ltd., Banner Lane, Coventry CV4 9GH, England, U.K.

Fruits of blackcurrant (*Ribes nigrum* L.) consist of tissues of different ontological origin, but these tissue types are difficult to discriminate by conventional histological techniques when the seeds are fully mature. This paper describes the use of NMR microscopy to follow the changes in differentiation of the pericarp, the locular tissue and the seeds through the various stages of development of the fruit. 3D surface-rendering techniques have been used in addition to the conventional image slices in order to display effectively the arrangement of the vascular supply to mature seeds.

Gradient-echo imaging techniques were found to provide better discrimination of tissue types than spin-echo sequences. With gradient-echo imaging there was a clear delineation of the pericarp from the locular parenchyma, a soft pulpy tissue within which the seeds are embedded. The early stages of differentiation of the gelatinous sheath, a single-cell layer investing each seed, was also identified by the gradient-echo method and at fruit ripening the gelatinous sheath surrounding each seed was clearly discernible. The vascular supply to developing seeds arising from two placentae at opposite sides of the pericarp and individual vascular traces to each seed were also revealed. The lipid-rich endosperm of mature seeds was localised by chemical shift selective imaging with spin-echo sequences.

Surface rendered 3-dimensional reconstruction of the image of ripe blackcurrant fruit revealed the spatial arrangement of the seeds in differing orientations within the locular cavity. The vascular traces departing from the opposing placentae in two star-like clusters were clearly visible in the rotated images of the reconstruction.

Development of grape (*Vitis vinifera* L.) fruits studied non-invasively by NMR microscopy

B.A. Goodman^a, B. Williamson^a, J.A. Chudek^b and G. Hunter^b

^a Scottish Crop Research Institute, Invergowrie, Dundee DD2 5DA, Scotland, U.K.

^b Department of Chemistry, University of Dundee, Dundee DD1 4HN, Scotland, U.K.

On a worldwide scale the grape (*Vitis vinifera* L.) is economically the most important of all fruit crops and control of the plant pathogen *Botrytis cinerea* represents a major production problem because of increasing resistance and consumer criticisms of pesticides in foods. In common with other fleshy fruits with hard seeds, it is difficult and extremely laborious to perform detailed histological studies on grapes using conventional destructive sampling techniques and it is impossible to follow developmental processes in a single specimen. We have, therefore, investigated the use of NMR microscopy to follow tissue differentiation in healthy fruit and that infected by *B. cinerea*.

The fruit of grape, in contrast to many soft fruits, is amenable to imaging with both spin and gradient echo sequences. It has been possible, therefore, to perform detailed histological investigations of fruits from formation through to maturity. The use of 3D data sets, in conjunction with surface rendered reconstruction routines, has allowed the development of the vascular architecture and the maturation of the seeds within the fruit to be examined in detail. By using chemical shift selective imaging it was possible to determine the distribution of sugars in the pericarp and lipid reserves in the endosperm.

Imaging parameters were determined for optimising the discrimination of healthy tissue from that infected by *B. cinerea* using both gradient and spin echo sequences and the progression of infection in single fruits observed over periods of up to 100 h.

Identification of freezing damage to flower buds of blackcurrant (*Ribes nigrum*) by NMR microscopy

R. Brennan^a, J.A. Chudek^b, G. Hunter^b and B.A. Goodman^a

^a Scottish Crop Research Institute, Invergowrie, Dundee DD2 5DA, Scotland, U.K.

^b Department of Chemistry, University of Dundee, Dundee DD1 4HN, Scotland, U.K.

In commercial plantations, severe crop losses of blackcurrant (*Ribes nigrum* L.) are frequently sustained as a result of frost damage during the flowering period. Breeding for frost tolerance is consequently a high priority in genetic improvement programmes. With conventional techniques, however, it is difficult to examine floral material in a meaningful way for the effects of internal structural damage that might have been caused by exposure to low temperatures. This paper describes the use of NMR microscopy to investigate *in vivo* the events which occur in blackcurrant flower buds of a frost-susceptible cultivar during and after freezing.

Modifications were made to a standard Bruker microimaging probe to allow measurements to be performed on flowers attached to a growing blackcurrant plant, the stem and root system of which were maintained outside of the spectrometer. Images were obtained of flowers before and after freezing, which was carried out inside the spectrometer by passing cold N₂ gas through the probe. After freezing, which was monitored by observing the disappearance of the FID, increases in the intensity of the water image were observed in specific areas of the flowers, most notably the stigma/style and ovarian regions. This suggests that these organs represent the main sites of damage during frost injury. Difficulties in observing detailed structural changes were encountered when using a series of planar slices because of subtle movements of the tissue as a result of the freezing process. These were overcome by using 3D image reconstruction techniques, which showed that the initial fluid build-up within the flower bud was followed by a progressive loss of signal intensity over a 48-hour period as a result of drying out of the dead tissue. It was only after such a period that physical damage to the flower buds could be seen visually.

NMR Microimaging of Capsule Development in the Moss *Dawsonia*.

#V. Sarafis and #*J.M. Tingle.

#Centre for Biostructural and Biomolecular Research.
University of Western Sydney, Hawkesbury.
Bourke Street, Richmond, NSW 2753
AUSTRALIA.

*School of Physics.
University of New South Wales.
PO Box 1, Kensington, NSW 2033 Australia.

The development of the capsule of the Australian giant moss *Dawsonia* has been followed in the species *D. superba*. The particular stages studied commenced with the fully expanded capsule, borne at the end of the seta, through the period of spore development to maturation. Optical microscopy of mature spores reveals that they contain globules of oil.

We are investigating the potential for NMR microimaging in studying the structure and development of the sporogenous layer and formation of mature oil-bearing spores. The drying of the capsule through maturation is accompanied by the structural transformation of the sporogenous layer into a 'bag' of dry, oil-bearing spores ready for dissemination (1).

The presence of air and the hetrogenous nature of the tissue create problems in imaging as a result of differences in the magnetic susceptibility. In an attempt to overcome this we have used slice selective spin echo imaging sequences with short echo times (TE, typically 11.5ms). We have also employed asymmetric echo acquisition allowing TE of 5.8ms to be achieved. Images at various developmental stages will be presented. These will be accompanied by NMR spectra indicating the gradual appearance of the oil peak and the reduction of water content.

(1) Goebel K. *Flora* 96, 1-202 (1906).

Axial Water Motion Within the Castor Bean Seedling Observed by Dynamic NMR Microscopy

Walter Köckenberger*, James M Pope† and
Paul T Callaghan‡

*Botanische Institut, Universität, Bayreuth, Germany; †School of Physics, University of New South Wales, Kensington NSW 2033, Australia; ‡Department of Physics and Biophysics, Massey University, Palmerston North, New Zealand.

Abstract

Waterflow plays an important role in nutrient uptake and translocation within plants. Flow over long distances occurs in two different types of specialized cells which are located in the tissue of the vascular bundles of the plant. In photosynthetic active plants the transpiration process sucks water from the soil through the vessels of the xylem to the leaves. Within the phloem waterflow is assumed to be driven by the differences in the osmotic pressure across the semipermeable membranes of the sieve tubes at the site where active loading of sucrose into the tubes takes place. In the present study water movement was measured simultaneously in both the sieve tubes of the phloem and the xylem vessel of Castor bean seedlings and transpiring plants, using an improved Dynamic NMR Microscopy method in which velocity and volume flow rates could be calculated. This method employed q -space encoding based on alternating sign, successively incremented gradients, thus yielding a difference propagator for each pixel.

The maximum velocity and the velocity distribution of both waterflows within the vessels of the xylem and within the sieve tubes of the phloem were analysed by fitting the difference propagators. Simultaneous flow in opposite directions was clearly observed. The shape of these propagators gives evidence for a Hagen-Poiseuille like velocity distribution of the waterflow. In case of the seedling the balance of phloem and xylem waterflow follows the law of mass conservation, consistent with the expected water circulation within the seedling. The balance for the plants with photosynthetically active green leaves shows a relatively stronger flow within the xylem vessels as expected for transpiring plants.

It is clearly demonstrated that the improved Dynamic NMR Microscopy method allows one to measure broad velocity distributions even when the fraction of moving water within each pixel is small.

Abstract for poster

Diffusion of cell-associated water in ripening barley seeds on NMR micro-imaging

N. Ishida*, H. Kano** and H. Ogawa***

* National Food Research Institute, Tsukuba, Ibaraki 305, Japan

** National Institute of Agrobiological Resources, Tsukuba, Ibaraki 305, Japan

***JEOL Datum Ltd., Akishima, Tokyo 196, Japan

Physical states of cell-associated water closely relate to sorts and rates of biological events. We intended to examine cell activity through detecting changes of amount and mobility of cell-associated water, and to measure sizes of water compartment in ripening barley seeds using an NMR microscope.

An NMR spectrometer with a superconducting magnet (JEOL GSX-270WB, 270 MHz for ^1H) and a micro-imaging system (JEOL JIM-270) were used for measurements. Diffusion-weighted images were measured by a spin-echo two dimensional Fourier-transform (90° - 180° pulses) or a stimulated echo (90° - 90° - 90° pulses) imaging technique combined with pulse field gradients. Resolution of images was a $0.05 \text{ mm} \times 0.05 \text{ mm}$ pixel and a 1.6 mm slice thickness (voxel 0.004 mm^3). The pulse field gradients (3 ms) were varied in magnitude (up to 278 mT/m) and in pulse interval (up to 500 ms) according to experiments.

Large amounts of water were located in the glume, the endosperm and vascular bundles in an early stages of seed development. Water in the endosperm was reduced with ripening of seeds, and those in the glume and the vascular bundles were maintained throughout the seed development though water cavity vicinal to the vascular bundles was reduced in size. Diffusion rate of water in the seeds at the early developmental stage, varying with tissues, was high, $1.5 - 2.1 \times 10^{-5} \text{ cm}^2/\text{s}$ corresponding to the diffusion rate of pure water. It fell to $0.6 - 1.0 \times 10^{-5} \text{ cm}^2/\text{s}$ at a milk-ripe stage and further declined before harvesting. Compartment sizes of cell-associated water were also reduced with growth stages, from $60 \mu\text{m}$ at the early developmental stage to $30 \mu\text{m}$ at the milk-ripe stage. Based on the results of experiments with varying magnitude of pulse field gradients, compartment size of cell-associated water varied with tissues and was not uniform in an individual tissue.

Sucrose Distribution in *Ricinus Communis* Seedlings observed by High Resolution Spectroscopic Imaging

A. Metzler, W. Köckenberger[†], M. von Kienlin Ph.D., E. Komor Ph.D.[†], A. Haase Ph.D.

Physikalisches Institut V., Universität Würzburg, 8700 Würzburg, Germany; [†]Botanisches Institut, Universität Bayreuth, 8580 Bayreuth, Germany

INTRODUCTION: Transport in plants is mainly located in two specialized types of cells organized in the vascular bundles of the plant. In the xylem region mainly water flow takes place. In the phloem region the conveyance of solutes is an important step in the distribution of assimilates in the plant. The major naturally transported compound in the sieve tubes of the phloem is sucrose.

Until recently (1) the common way to determine a distribution of carbohydrates and other compounds on microscopic scale was by cutting and biochemical analysis (2). The present study demonstrates the possibility to identify and quantify spatially localized compounds of plant chemistry by proton spectroscopic imaging (SI) *in vivo*.

METHODS AND MATERIALS: 6 day old castor bean seedlings were grown in special tubes, containing a 0.5 mM CaCl₂ solution aerated by a gentle flow of air bubbles through the bottom of the tube. In the experiment a seedling with its root still in the tube was put in a special teflon insert fitting in a modified BRUKER microimaging probe. The RF-coil was carefully fixed around the hypocotyl of the seedling. During all these experiments care was taken not to disturb the growing of the plant.

Short TE (7ms) spectroscopic imaging was accomplished using a Hahn echo pulse sequence running on a BRUKER AMX 500 WB NMR spectrometer with actively shielded gradient coils. A 64 x 64 data matrix with 6 mm x 6 mm FOV and 2 mm slice thickness was acquired in transverse orientation. Total time of acquisition was 3½ h (TR 3 s). Before Fouriertransform, a 10 Hz line broadening filter was applied in the spectral domain. In the two spatial domains no filter was used. The spectra were phased and shifted to obtain the water resonance at a constant position in all spectra.

In order to quantify concentrations, T₁- and T₂^{app}- values of the resonances in the selected slice were measured, using standard inversion recovery and Hahn echo pulse sequences without spatial encoding. Additionally a B₁- map was calculated from snapshot flash data with the intensity modulated by a rotating frame imaging preexperiment.

RESULTS: High signal intensities at the sucrose resonance frequencies (5.3 ppm, 4.1 ppm, 3.95 ppm, 3.7 ppm, 3.55 ppm, 3.45 ppm and 3.35 ppm) were observed in the phloem region of the hypocotyl. In the outer parenchyme region only low signal intensities at 5.3 ppm were seen. In the inner parenchyme center the signal intensity at 5.3 ppm was below the level of detection. The integral of a gaussian lineshape fitted to the signal at 5.3 ppm showed a gradient from this point to the phloem region. In the outer parenchyme the integral remained constant.

By calibration to an outer reference capillary and taking into account the measured T₁- and T₂^{app}- values and the B₁- map, a sucrose concentration of approximately 200 mM in the phloem was determined.

Besides these signals other background signals at 4.2 ppm - 3.0 ppm and at 2.5 ppm - 0.5 ppm could be detected.

DISCUSSION AND CONCLUSION: The SI-data allowed an identification of sucrose in plant. It showed, that a main amount of sucrose in plant is located in the phloem region of the hypocotyl. Compared to the outer parenchyme no significant reduction of sucrose concentration in the xylem region was detected. Resonance signals at 4.2 ppm - 3.0 ppm and at 2.5 ppm - 0.5 ppm could not be assigned, but may come from other carbohydrates and amino acids.

Chemical shift microscopy proved to be a versatile tool in plant histochemistry. Quantification is possible with additional knowledge of relaxation parameter. A shortening of the total experimental time can be achieved by reducing the data matrix size (voxel volume 17.5 nl) and further decrease of TR (T₁ of sucrose resonance at 5.3 ppm ≈ 700 ms). This will make it possible to monitor dynamic changes in plant metabolism caused by manipulation of environmental parameters.

REFERENCES:

- (1) H. Rumpel and J. M. Pope, *Magnetic Resonance Imaging* 10, 187-194 (1992).
- (2) J. Kallarackal, G. Orlich, C. Schobert and E. Komor, *Planta* 177, 327-335 (1989)

Gum Rheology: NMR Flow Imaging of Aqueous Polysaccharide Solutions

S. J. Gibbs[†], S. Ablett[‡], I. Evans[‡], D. E. Haycock[‡], T. A. Carpenter[†], and L. D. Hall[†]

[†] *Herchel Smith Laboratory for Medicinal Chemistry,
University of Cambridge School of Clinical Medicine,
University Forvie Site, Robinson Way,
Cambridge, CB2 2PZ United Kingdom*

[‡] *Unilever Research Laboratories,
Colworth House,
Sharnbrook,
Bedfordshire, MK44 1LQ United Kingdom*

Nuclear magnetic resonance (NMR) flow imaging is used to obtain the velocity distributions of aqueous solutions of 0.2% and 1% xanthan gum and 1% guar gum for flow in a 1.2 cm ID cylindrical pipe. These velocity distributions show little evidence of apparent wall slip; they are differentiated to obtain relationships between shear stress and shear rate which agree well with those obtained by cone and plate rheometry assuming no slip. The xanthan solutions are well described by a power-law dependence of shear stress on shear rate and the guar solution is better described by a Cross type relationship. The implications of these studies for future NMR flow imaging studies of more complex systems are presented.

Diffusion Imaging in the Presence of Static Magnetic Field Gradients

A. J. Lucas, S. J. Gibbs, E. W. G. Jones
M. Peyron, J. A. Derbyshire
and L. D. Hall

*Herchel Smith Laboratory for Medicinal Chemistry,
University of Cambridge School of Clinical Medicine,
University Forvie Site, Robinson Way,
Cambridge, CB2 2PZ United Kingdom*

Problems associated with large, static magnetic field gradients are reviewed and illustrated with pulsed field gradient NMR diffusion imaging experiments on two model systems. The model systems chosen are a water-filled cylinder and a water-filled annulus between two concentric cylinders both oriented transversely to the polarizing magnetic field. The latter system exhibits large magnetic field gradients ($\sim 5 \text{ G cm}^{-1}$), and the simplicity of the geometry permits an analytical description of the magnetic field distribution in the sample; calculations of the field distribution are consistent with direct measurements made using the chemical shift imaging technique. Diffusion imaging experiments based on either spin or stimulated echo sequences are reliable for the single-tube system in which static gradients are negligible. However, for the double-tube system, the large static gradients prevent reliable diffusion imaging by spin echo methods and cause artifacts in the results of standard stimulated echo techniques. A superior alternating pulsed field gradient technique, for which echo attenuation is less sensitive to the effects of the static background magnetic field gradients, provides reliable diffusion coefficient images for the double-tube system.

“Diffusion Imaging in the Presence of Static Magnetic Field Gradients”,
J. Magn. Reson. in press 1993.

Correlated Susceptibility and Diffusion Effects in NMR Microscopy Using Phase-Frequency Encoding

Lucy C Forde and Paul T Callaghan

Department of Physics and Biophysics, Massey University,
Palmerston North, New Zealand.

Abstract

Both susceptibility inhomogeneity and molecular self-diffusion are known to limit the resolution possible in NMR microscopy⁽¹⁾. The interplay between these phenomena can cause quite subtle intensity modulation and distortion in NMR images⁽²⁾. In particular where conventional phase-frequency encoding is employed this interplay can lead to sharply defined bright features. These arise because diffusional attenuation is nulled due to a cancellation of the read gradient by the local fields⁽³⁾. We describe these effects both from the standpoint of theory and experiment, illustrating both distortion and intensity modulation phenomena using a model system of glass rods surrounded by water and, where diffusional effects are to be suppressed, by a solution of high polymer.

1. P T Callaghan, *Principles of NMR Microscopy*, Oxford University Press, 1992.
2. S Posse and W P Aue, *J Magn Reson* 88, 473 (1990).
3. P T Callaghan, L C Forde and C J Rofe, *J Magn Reson*, submitted (1993).

PGSE NMR and Diffraction Effects

Andrew Coy and Paul T Callaghan

Department of Physics and Biophysics, Massey University,
Palmerston North, New Zealand.

Abstract

PGSE NMR is traditionally used to determine the broadening of the average propagator. Such an experiment would yield a self-diffusion coefficient for the molecules in the sample. However, in restricted environments, the local propagator is not always Gaussian and diffusing molecules do not always undergo Brownian motion⁽¹⁾. In such situations PGSE can be used to reveal the form of the propagator at high resolution and hence determine the nature of the restrictions affecting the molecules⁽²⁾.

Experiments have been carried out on molecules diffusing in various restricting geometries^(3,4). The PGSE results show diffraction-like features where a characteristic wave number is consistent with the length scales of the structure concerned. Structural parameters for rectangular, cylindrical, porous and fractal systems have been obtained using PGSE. Resolution can be as high as 0.1 μm and is restricted only by the size of the gradients applied.

1. P T Callaghan, D MacGowan, K J Packer and F Zelaya, *J Magn Reson* **90**, 177 (1990).
2. P.T. Callaghan, "*Principles of NMR Microscopy*", Oxford University Press, 1992.
3. P T Callaghan, A Coy, D MacGowan, K J Packer and F O Zelaya, *Nature* **351**, 467 (1991).
4. P T Callaghan, A Coy, T P J Halpin, D MacGowan, K J Packer and F O Zelaya, *J Chem Phys* **97**, 651 (1992).

Effect of Susceptibility and Diffusion Under Pure Phase Encoding

Craig J Rofe and Paul T Callaghan

Department of Physics and Biophysics, Massey University,
Palmerston North, New Zealand.

Abstract

In NMR microscopy signal to noise and hence resolution, improvements can be achieved with increasing B_0 field. However this occurs at the price of increasing image distortions due to susceptibility differences within a sample, an effect well demonstrated at low acquisition bandwidths where local gradients due to inhomogeneities are comparable with applied gradients. Severe signal attenuation due to molecular diffusion can also play an important role in this regime given an image resolution smaller than the distance moved by nuclei within an echo or acquisition period. This attenuation is avoided only at local null points where the susceptibility and applied gradients cancel each other.

We demonstrate that pure phase encoding can avoid both diffusive and susceptibility effects whilst retaining optimal signal to noise ratios. We have demonstrated this using an unscreened quadrupole gradient coil with gradients up to 200 G/cm.

Optimal Gradient Strength for Diffusion Experiments

(Stejskal - Tanner Pulsed Gradient Spin Echo Revisited)

S. T. Fricke*, L. Landini**, C. A. Veracini***, A. Benassi°, J. Nori°°

*FORMED Research Scientist, Via Trieste 41-PISA; ***Dipartimento di Chimica e Chimica Industriale, PISA; °Istitute di Fisiologia Clinica del CNR, Via Savi 8-PISA; **Dip. di Ingegneria dell'Informazione: EIT, Università di PISA, Via Diotisalvi 2-PISA; °°Dip. Radiologia, Ospedale Careggi, FIRENZE

The NMR Microscope offers the greatest hope for studying molecular motion be it in a pure sample or in the complex system of a biological sample. For many years NMR has been used to make diffusion measurements. For NMR diffusion experiments on pure samples there is little agreement (some of these results are reviewed in B-1). It is essential to minimize the experimental errors in order to delve further into the world of diffusion NMR. The optimization of the data acquisition process for the classic Stejskal and Tanner PGSE (Pulsed Gradient Spin Echo) experiment and CGSE (Constant Gradient Spin Echo) using a two point diffusion measurement is, in part, explored.

During a MRI session the scanning time should be kept as short as possible to assure accurate results. This inherently means that the number of images taken should be kept to a minimum. The study of diffusion is akin to measuring the velocity of an automobile in that one needs to find the vehicle at two points in space and time, hence, we need at least two images to measure diffusion. The variables generally exploited to make NMR diffusion measurements are time and gradient strength.

There are many factors hindering the diffusion experiment. Recent advances in the use of pulse sequences (C-3, G-1) promise to overcome bulk motion artifacts encountered during in-vivo experiments. Bulk motion has for a long time been a limiting factor for in-vivo measurements this problem being overcome it is now important to refine the diffusion experiment. Presented here is a simple analysis of errors due to gradients used for gradient spin echo diffusion measurement. With the proper choice of K equation 1 below may represent the standard error in the number calculated for the diffusion coefficient where A is a measured amplitude due to T₂; D the actual diffusion coefficient; G₁ and G₂ are the gradient strengths one and two used for the two point diffusion measurement and σ_A^2 is the standard deviation (which is assumed to be constant) of the measured of a peak height of a fourier transformed echo.

$$\sigma_D = \sqrt{\left[\left(\frac{\exp(KDG_1^2)}{AK(G_2^2 - G_1^2)} \right)^2 + \left(\frac{\exp(KDG_2^2)}{AK(G_2^2 - G_1^2)} \right)^2 \right] \sigma_A^2}$$

Equation 1. Error in diffusion measurement due to choice of gradient strengths G₁ and G₂.

From the equation above it is found that there is a calculable range of gradient strengths which are suitable for making an optimal "two point" diffusion measurement. Since the calculation is easily performed on a computer such calculations can be used as part of a diffusion measurement protocol. With the problem of which gradient strengths to use (for a two point measurement) out of the way, the experimenter realizes a usable range of gradients for multiple point measurements. It is noted that similar calculations can be made for any two varied parameters that contribute to the diminished signal intensity due to diffusion during a PGSE or CGSE experiment.

B-1. Beall P.T., NMR Data Handbook for Biomedical Applications, Pergamon Press (1984)

C-1. Callaghan P.T. and Eccles C.D., "Diffusion Limited Resolution in Nuclear Magnetic Resonance Microscopy", J. of Mag. Reson., 78 (1988), p. 1

C-2. Carr H.Y. and Purcell E.M., "Effects of Diffusion on Free Precession in Nuclear Magnetic Resonance Experiments", Phys. Rev., 94, 3 (1954); p. 630

C-3. Carney C., Analytical Treatment of Diffusion in Steady State Free Precession: NMR Techniques, Ph.D Thesis, Radiological Sciences Graduate Program, Department of Nuclear Engineering, Harvard Medical School, May 1991

F-2. Fricke S.T. *et al.*, Optimization of Data Acquisition for Diffusion Experiments, il Convegno Nazionale Pet e Rm in Oncologia Lulio1 (1993); p. 95-97.

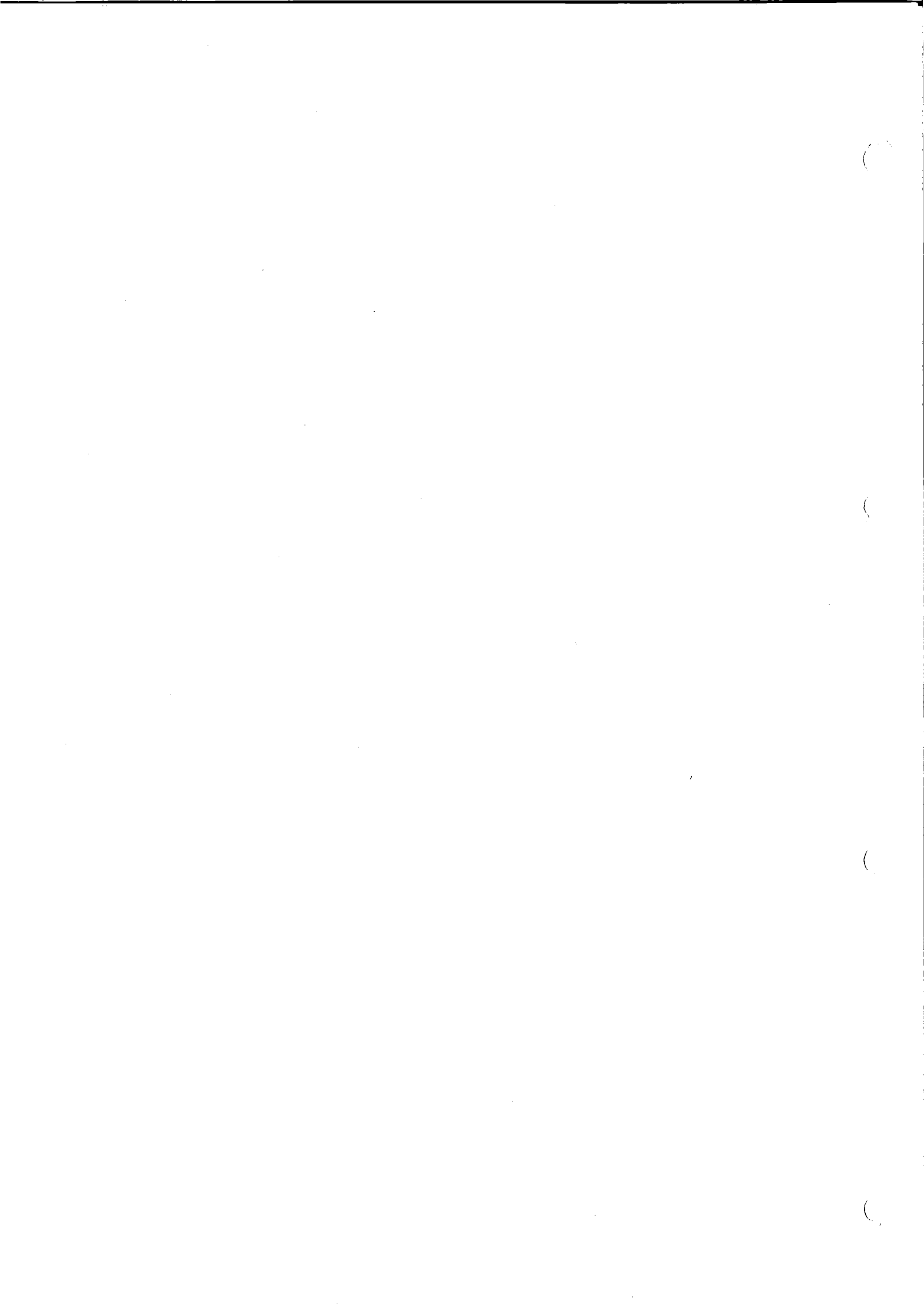
G-1. Van Gelderen P., *et al.*, "A Single -Shot Diffusion Experiment", J. of Mag. Reson., 103 (1993), p. 105-108

H-1. Hrovat M.I., Nuclear Magnetic Resonance Diffusion Studies, Ph.D Thesis. Department of Physical Chemistry, University of Texas at Austin, 1982

M-1. McCall D.W. *et al.*, "Self Diffusion Studies by Means of Nuclear Magnetic Resonance Spin-Echo Techniques", Ber. Bunsen Phys. Chem. 67, #3, (1963); p. 336

S-1. Stejskal E.O. and Tanner J. E., J. Chem. Phys. 42, 288 (1965)

Authors



Abel, E. W.	MAT 13
Ablett, S.	DIFF 9
Ackerman, J. L.	RAI 2
Adesida, I.	MET 18
Adolf, H.	MET 26
Adriaensens, P.	BIO 14, BIO 23, BIO 24, BIO 25, MAT 5
Amin, G.	DIFF 1
Antich, P. P.	BIO 7
Back, P. J.	MET 20
Balcom, B. J.	DIFF 1, MAT 23, MET 13
Barth, P.	DIFF 6, MAT 12, MAT 15, MET 9
Baumann, M. A.	BIO 11, MET 10
Baumgartner, P. A.	PLA 5
Becker, E. D.	after conference dinner talk
Benassi, A.	DIFF 14
Berg, A.	BIO 21
Berliner, L.	EPR 3
Beuls, E.	BIO 14, BIO 23, BIO 24, BIO 25
Bielicki, G.	BIO 16
Biesold, M.	BIO 13
Black, R. D.	BIO 8
Blackband, S. J.	opening lecture
Blümich, B.	MAT 4, MAT 18, MAT 19, MET 8, MET 24
Blümmler, P.	MET 24
Bodenhausen, G.	MET 5
Bourg, J.	EPR 2
Bowtell, R. W.	opening lecture
Brandl,	DIFF 4
Brennan, R.	PLA 16
Brondeau, J.	MET 4
Burdett, N. G.	BIO 20
Buszko, M.	MET 29
Callaghan, P. T.	DIFF 5, DIFF 7, DIFF 11, DIFF 12, DIFF 13, MET 6, MET 19, MET 20, MET 21, MET 22, PLA 9, PLA 18, DIFF 8, MET 4
Canet, D.	DIFF 3
Caprihan, A.	BIO 19, BIO 20, DIFF 1, DIFF 9, MAT 14, MAT 23, MET 13, MET 14, MET 27
Carpenter, T. A.	PLA 3
Chatson, K. B.	MAT 24
Chauvaux, B.	MET 31
Cho, Z. H.	PLA 9
Christeller, J. T.	MAT 8, MAT 13, PLA 6, PLA 7, PLA 14, BIO 8, MET 15
Chudek, J. A.	BIO 5
Cofer, G. P.	BIO 7
Cohn, M.	DIFF 12, MET 20, MET 21
Constantinescu, A.	PLA 4, PLA 20
Coy, A.	MET 1
Crestana, S.	BIO 3
Crozier, S.	BIO 18
Dai, H.	PLA 11
Dannhauer, K.-H.	MAT 7
de Jager, P. A.	BIO 30
de Luca, F.	
de Matos, R. A.	

de Vargas, L.	DIFF 7
Decorps, M.	MET 5
Dejon , P.	MET 17
Demeure, R.	BIO 26, MAT 6
Demsar, F.	MET 7
Denner, P.	MAT 12
Derbyshire, J. A.	DIFF 1, DIFF 10, MET 14, MET 27
Dereppe, J. M.	MAT 6, MAT 24
Devoulon, P.	MET 5
Di Nunzio, F.	MAT 7
Doddrell, D.	MET 1
Donker, H. C. W.	PLA 12, PLA 13
Donnat, J. P.	BIO 16
Dunham, M.	BIO 3
Eads, T. M.	PLA 2
Eaton, G. R.	EPR 1
Eaton, S. S.	EPR 1
Eccles, C. D.	PLA 9
Edzes, H. T.	PLA 10, PLA 11, PLA 12
Emsley,L.	MET 5
Ercken, M.	MAT 5
Evans, I.	DIFF 9
Feichtinger, E.	BIO 4
Feio, G.	BIO 30
Fischer, A. E.	DIFF 1, MET 13
Forde, L. C.	DIFF 11, MET 6, MET 21
Foucat, L.	BIO 16
Fricke, S. T.	DIFF 14
Frolov, V.	MET 23
Fujii, H.	EPR 3
Fukushima, E.	DIFF 3
Fülber, C.	MAT 4, MAT 19
Garrido, L.	RAI 2
Geilke, Th..	MAT 10
Gelan, J.	BIO 14, BIO 23, BIO 24, BIO 25, MAT 5
Gersonde, K.	BIO 10, BIO 18, BIO 22
Gibbs, S. J.	DIFF 1, DIFF 9, DIFF 10, MAT 20
Gill, R.	BIO 20
Glover, P. M.	opening lecture
Goense, J. B. M.	PLA 11
Goodman, B. A	PLA 6 , PLA 7, PLA 14, PLA 15, PLA 16
Goudemant, J. F.	BIO 26
Grabenwoger, M.	BIO 4
Gries, W.	BIO 22
Grimm, M.	BIO 4
Grinberg, F.	BIO 10, BIO 21, BIO 22, DIFF 6
Groß, D.	BIO 11
Gründer, W.	BIO 13, BIO 17, BIO 18
Grutzner, J. B.	DIFF 2
Gustiñ, T.	BIO 26
Haase, A.	DIFF 4, MET 25, MET 26, PLA 8, PLA 21
Hafner, S.	DIFF 6, MAT 12, MAT 15, MAT 16, MET 9
Hall, L. D.	BIO 19, BIO 20, DIFF 1, DIFF 9, DIFF 10, MAT 14, MAT 20, MAT 23, MET 13, MET 14, MET 27

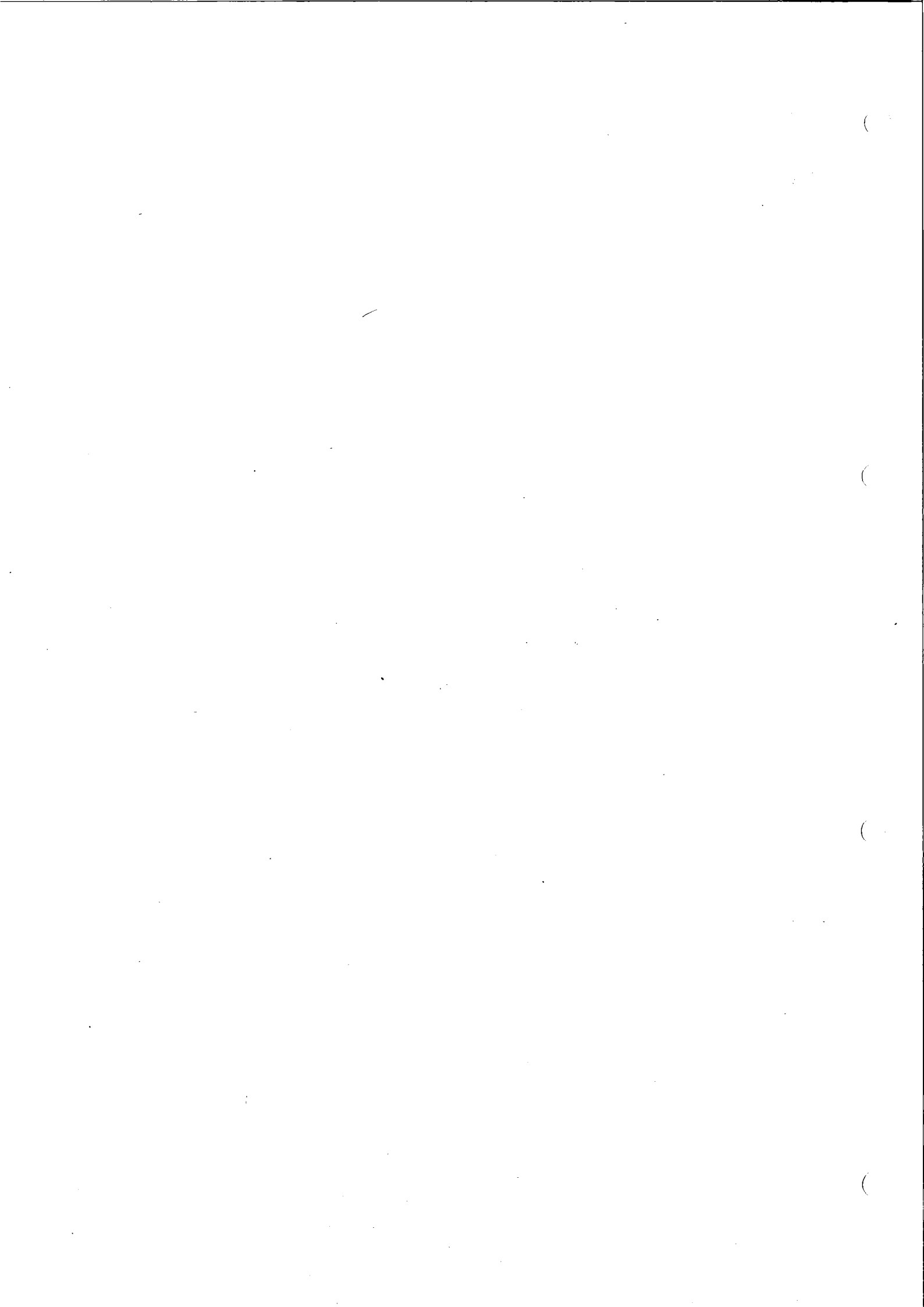
Halse, M. R.	MAT 1, MAT 21
Hatfield, R.	BIO 20
Haycock, D. E.	DIFF 9
Hennel, F.	BIO 12, MET 11
Hodgson, R. J.	BIO 19
Hoyer, E.	BIO 17
Huis, R.	MAT 24
Hull, W. E.	BIO 6
Humbert, F.	DIFF 8
Hunter, G.	MAT 8, MAT 13, PLA 6, PLA 7, PLA 14, PLA 15, PLA 16, MET 3
Hyslop, B.	PLA 19
Ishida, N.	MET 11
Jakubowski, T.	PLA 13
Jans, A. W. H.	MET 7
Jarh, O.	BIO 9, BIO 12, MET 11, MET 12
Jasinski, A.	BIO 8, MET 15
Johnson, G. A.	DIFF 10
Jones, E. W. G.	MET 16
Jung, W.-I.	MET 26
Kalusche, B.	PLA 19
Kano, H.	BIO 2
Kapadia, R. D.	PLA 4
Kauten, R.	BIO 28
Keller, K.	PLA 3
Kendall, E. J.	BIO 12
Kibinski, J.	MET 25
Kiefer, A. P.	MAT 3, MAT 17
Kimmich, R.	MET 28
Klingler, R. J.	PLA 8, PLA 18, PLA 21, MET 19
Köckenberger, W.	PLA 8, PLA 21
Komor, E.	EPR 3
Koscielniak, J.	BIO 9
Kozlowski, P.	EPR 2
Krishna, M. C.	BIO 12
Krzyzak, M.	MET 25
Kuchenbrod, E.	DIFF 6, MET 9, MAT 12, MAT 15, MAT 16, MET 17, BIO 21, BIO 22
Kuhn, W.P.	BIO 12, MET 11
Kulinowski, P.	MET 12
Kwiecinski, S.	MET 18
La Valle, L.	PLA 9
Laing, W. A.	DIFF 7
Lambert, R. K.	DIFF 14
Landini, L.	MET 3, MET 18
Lauterbur, P. C.	BIO 11
Lehmann, V.	MAT 21
Leone, B.	BIO 4
Leukauf, C.	DIFF 4
Link, A.	RAI 2
Liszak, M. J.	MAT 8, MAT 13
Lloyd, C. H.	MET 29
Lock, H.	PLA 6, PLA 14
Lohman, J. A. B.	

Lonergan, A. R.	MAT 21
Lucas, A. J.	DIFF 10, MAT 20
Lugeri, N.	MAT 7
Lutz, O.	MET 16
Maciel, G. E.	MET 29
MacKay, R. L.	PLA 7
Mackay, R. L.	MAT 13
Maffei, P.	MET 4
Magin, R. L.	MET 18
Mansfiel, P.	opening lecture
Manz, B.	MET 20, MET 22
Maraviglia, B.	MAT 7
Maron, A.	BIO 26
Maronpot, R. R.	BIO 8
Mason, R. P.	BIO 7
Mateescu, G. D.	RAI 3
Maylish, L.	MAT 2
McDonald, P. J.	MAT 21
McFarland, E.	BIO 3
Mehr, K.	MET 17
Meir, G.	BIO 5, BIO 29
Mestres, P.	BIO 21
Meszaros, S.	BIO 4
Metzler, A.	PLA 8, PLA 21
Meuli, R.	MET 5
Mischler, E.	DIFF 8
Mitchell, J. B.	EPR 2
Moore, G. J.	MET 30
Moreaux, C.	MAT 6
Morita, Y.	BIO 10
Morris, H. D.	MET 3
Mottet, I.	BIO 26
Mügge, C.	BIO 28
Müller, H.-P.	MAT 3, MAT 17
Munasinghe, B. D. J. P.	BIO 19
Muszynska,	BIO 12
Mutzenhardt, P.	MET 4
Neeman, M.	BIO 5, BIO 29
Nesbitt, G. J.	MAT 9
Neue, G.	MAT 10
Newling, B.	MET 14
Nielsen, D. R.	PLA 4
Nilgens, H.	MET 24
Nolan, M. J.	BIO 19
Nori, J.	DIFF 14
Nunes, T.	BIO 30
Octave, J. N.	BIO 26
Ogawa, H.	PLA 19
Paff, J.	MET 24
Palmers, Y.	BIO 14, BIO 23, BIO 24, BIO 25
Pananakis, D.	MAT 13
Panepucci, H. C.	PLA 20
Parker, A. D.	DIFF 1
Päuser, S.	BIO 28

Peck, T. L.	MET 18
Peters, A.	opening lecture
Peyron, M.	DIFF 10, MAT 20
Pfleiderer, B.	RAI 2
Phelps, D. W.	MAT 20
Pickard, J. D.	BIO 20
Pierens, G. K.	MAT 20
Pirlot, R.	MAT 24
	PLA 15, PLA 16
Pollers, I.	MAT 5
Pope, J. M.	BIO 27, MAT 22, MET 19, PLA 5 PLA 18
Posadas, D. A.,	PLA 20
Potter, K.	DIFF 1
Rahman, H. J.	MAT 1
Raible, C.	BIO 10
Rajanayagam, V.	MAT 22
Randall, E. W.	RAI 1
Rathke, J. W.	MET 28
Raulet, R.	MET 4
Renou, J. P.	BIO 16
Ritchey, W. M.	MAT 2
Rofe, C. J.	DIFF 7, DIFF 13, MET 21
Rugar, D.	MET 2
Ruloff, R.	BIO 17
Rydzy, M.	MET 11
Sarafis, V.	PLA 5, PLA 17
Sarkar, S. K.	BIO 2
Saunders, J. K.	BIO 9
Schauß, G.	BIO 15
Scheler, U.	MAT 4, MET 8
Schild, H.	BIO 15
Schneider, H.	MAT 15
Scrimgeour, S. N.	MAT 8, MAT 13
Seliger, J.	MET 7
Sersa, I.	MET 7
Sharp, J. C.	opening lecture
Shervill, E.	BIO 20
Shuter, B.	BIO 27
Sibson, N. R.	BIO 20
Sillerud, L. O.	BIO 1, MET 30
Simon, G.	MAT 12, MAT 15
Skibbe, U.	MAT 10, PLA 9
Skorka, T.	BIO 12, MET 12
Smith, E.	MAT 21
Smith, P.	MAT 2
Snijder, H. J.	PLA 13
Spiess, H. W.	MAT 4, MET 8, MAT 18, MAT 19
Stanley, D. W.	PLA 3
Steinfeld, Y.	BIO 5, BIO 29
Stewart, R. C.	MAT 20
Strange, J. H.	MAT 1, MAT 21
Subramanian, S.	EPR 2
Suddarth, S. A.	MET 15
Sueki, M.	EPR 1

Sulek, Z.	MET 11, MET 12, BIO 12
Sun, Y.	MET 29
Szayna, M.	BIO 9
Szeles, J. C.	BIO 4
Tannus, A.	PLA 20
Tempel, C.	BIO 5, BIO 29
Tessier, J. J.	MAT 14
Thelen, M.	BIO 15
Tingle, J.M.	PLA 5, PLA 17
Tomanek, B.	BIO 12, MET 11, MET 12
Traore, A.	BIO 16
Tyler, J. A.	BIO 19, MAT 14
Ugurbil, K.	MED 1
van As, H.	PLA 1, PLA 10, PLA 11, PLA 12, PLA 13
van Dusschoten ,D.	PLA 10, PLA 11
Vandersteen, M.	BIO 14, BIO 23, BIO 24, BIO 25
Vanderzande, D.	MAT 5
Vanormelingen, L.	BIO 14, BIO 23, BIO 24, BIO 25
Vath, A.	MET 26
Veracini, C. A.	DIFF 14
von Kienlin, M.	PLA 21
Wagner, M.	BIO 13, BIO 17
Wallner, A.	MAT 2
Wang, L. Z.	DIFF 3
Watson, P. J.	BIO 19
Weber, P.	MET 5
Weigand, F.	MAT 4, MAT 18
Weis, J.	MAT 3, MAT 17
Werner, A.	BIO 18
Widmaier, S.	MET 16
Williamson, B.	PLA 6, PLA 7, PLA 14, PLA 15
Woelk, K.	MET 28
Wu, Y.	RAI 2
Xing, D.	DIFF 1
Yao, S.	MAT 22
Zhao, B.	EPR 3
Zhou, X.	BIO 8, MET 15
Zick, K.	MAT 11, MET 10
Zschunke, A.	BIO 28

Participants



Prof. Ackerman, Jerry L.
Mass. Gen. Hospital
MR-Center
13th Street, Building 149
Charlestown, MA 02129
USA
Phone ++1-617-726 3083
Fax ++1-617-726 7422
E-Mail jerry@nmr-r.mgh.harvard.edu

Prof. Andrew, E. Raymond
Univ. of Florida
Dept. of Physics
215 Williamson Hall
Gainesville, FL 32611
USA
Phone ++1-904-392 6691
Fax ++1-904-392 8863
E-Mail

Dr. Bartuska, Victor J.
Otsuka Electronics Europe SARL
Parc d'Innovation
Les Scientifiques - Rue Tobias Stim
F-67400 Strasbourg-IIIkirch
Frankreich
Phone ++33-88-66 82 00
Fax ++33-88 66 82 04
E-Mail

Prof. Becker, Edwin D.
National Institute of Health
Lab. of Chem. Physics
Building 5, Room 124
Bethesda, MD 20892
USA
Phone ++1-301-496-1024
Fax ++1-301-496-0825
E-Mail tbecker@sunder.niddk.nih.gov

Prof. Berliner, Lawrence J.
The Ohio State Univ.
Dept. of Chemistry
120 W., 18th Avenue
Columbus, OH 43210-1173
USA
Phone ++1-614-292 0134
Fax ++1-614-292 1532
E-Mail berliner@livers.mps.ohio-state.edu

Prof. Blümich, Bernhard
RWTH Aachen
Inst. für Makromolekulare Chemie
Worringer Weg 1
D-52056 Aachen
Germany
Phone ++49-241-80 6421
Fax ++49-241-80 6980
E-Mail bluemich@rwth-aachen.de

Dr. Adriaensens, Peter
L.U.C.
Universitaire Campus
B-3590 Diepenbeek
Belgium
Phone ++32-11-268 300
Fax ++32-11-268 301
E-Mail

Prof. Balaban, Robert S.
National Institute of Health
NHLBI/LCE, Bldg. 10, Room B1D-161
9000 Rockville Pike
Bethesda, MD 20892
USA
Phone ++1-301-492 3658
Fax ++1-301-402 3289
E-Mail

Dr. Baumann, Michael A.
Klinikum der Johannes-Gutenberg-Universität
Klinik für Zahnerhaltung & Parodontologie
Langenbeckstr. 1
D-55131 Mainz
Germany
Phone ++49-6131-17 30 89
Fax ++49-6131-17 66 29
E-Mail

Dr. Bella, Juraj
Poly-Bios
Research Centre
Padriciano 99
I-34012 Trieste
Italy
Phone ++39-40-375 6611
Fax ++39-40-779 7091
E-Mail

Prof. Beuls, Emile
Universitair Hospital Maastricht
P. B. 5800
P. Debyelaan 25
NL-6202 Maastricht
Netherlands
Phone ++31-43-87 40 41
Fax ++31-43-87 78 78
E-Mail

Prof. Bodenhausen, Geoffrey
Universite de Lausanne
Section de Chemie
Rue de la Barre, 2
CH-1005 Lausanne
Switzerland
Phone ++41-21-316 3710
Fax ++41-21-316-3728
E-Mail

Dr. Alvila, Lella
University of Joensuu
Dept. of Chemistry
P. O. Box 111
SF-80101 Joensuu
Finland
Phone ++358-73-151 33 47
Fax ++358-73-151 33 90
E-Mail alvila@joyl.joensuu.fi

Dr. Balcom, Bruce J.
University of New Brunswick
Physics Department
P. O. Box 4400
Fredericton, N. B. E3B 5A3
Canada
Phone ++1-506-453 4723
Fax ++1-506-453 4581
E-Mail bjb@unb.ca

Mr. Baumeister, Edgar
Universität Tübingen
Inst. für Org. Chemie
Auf der Morgenstelle 18
D-72076 Tübingen
Germany
Phone ++49-7071-296 922
Fax ++49-7071-295 246
E-Mail

Dr. Berg, Andreas
Fraunhofer Institut für Biomed. Technik
Arbeitsgruppe Magnetische Resonanz
Ensheimer Str. 48
D-66386 St. Ingbert
Germany
Phone ++49-6894-980 253
Fax ++49-6894-980 400
E-Mail

Dr. Beynon, Peter J.
Kodak Ltd.
Research Division
Headstone Drive
GB-Harrow, Midd. HA1 1PF
England
Phone ++44-81-424-5626
Fax ++44-81-424-5750
E-Mail

Mr. Brandl, M.
Universität Würzburg
Physikalisches Institut
Am Hubland
D-97074 Würzburg
Germany
Phone ++49-931-8885868
Fax ++49-931-706297
E-Mail

Herrn Büttgen, Norbert
Techn. Hochschule
Inst. für Exp. Festkörperphysik
Hochschulstr. 6

D-64289 Darmstadt

Germany

Phone ++49-6151-165 130

Fax ++49-6151-162 833

E-Mail

Dr. Carpenter, T. Adrian
Univ. of Cambridge
Herchel Smith Lab.

University Forvie Site, Robinson Way

GB-Cambridge, CB2 2PZ

England

Phone ++44-223-336-805

Fax ++44-223-336-748

E-Mail

Prof. Cho, Z. H.
California College of Medicine
Depart. of Radiological Sciences

Irvine, CA 92717

USA

Phone ++1-714-856 5904

Fax ++1-714-856 8033

E-Mail

Dr. Crestana, Silvio
CNPDIA-EMBRAPA

P.O. Box 741

13560-970 Sao Carlos-Sao Paulo

Brazil

Phone ++55-162-725-741

Fax ++55-162-725-958

E-Mail

Dr. Delayre, John L.
Tecmag, Inc.

6006 Bellaire Blvd.

Houston, TX 77081

USA

Phone ++1-713-667 1507

Fax ++1-713-667 3180

E-Mail

Mr. Derbyshire, Andrew
University of Cambridge
Herchel Smith Laboratory
University Forvie Site

GB-Cambridge CB2 2PZ

England

Phone ++44-223-336 758

Fax ++44-223-336 748

E-Mail

Prof. Callaghan, Paul T.
Massey University
Dept. of Physics

Palmerston North

New Zealand

Phone ++64-63-690 99

Fax ++64-63 540 207

E-Mail p.callaghan@massey.ac.nz

Mrs. Chang, Inyong
Universität Mainz
Inst. für Physikalische Chemie
Jakob Welder Weg 15

D-55099 Mainz

Germany

Phone ++49-6131-395 733

Fax ++49-6131-394 196

E-Mail chang@vpcma.chemie.uni.mainz.de

Dr. Chudek, John A.
University of Dundee
Chemistry Dept.

GB-Dundee DD1 4HN

Scotland

Phone ++44-382-301 334

Fax

E-Mail

Dr. Crozler, Stuart
University of Queensland
Centre for Magnetic Resonance
St. Lucia

Brisbane, QLD 4072

Australia

Phone ++61-7-365 4100

Fax ++61-7-365 3833

E-Mail stuart@cmr.uq.oz.au

Dr. Demeure, Roger
Catholic University of Louvain
Neurochemistry Laboratory
Place L. Pasteur 1

B-1348 Louvain-la-Neuve

Belgium

Phone ++32-10-474 479

Fax ++32-10-472 774

E-Mail

Prof. Dereppe, J. M.
Univ. Cat. de Louvain
Lab. de Chimie Physique
Place Louis Pasteur 1, 3A

B-1348 Louvain-la-Neuve

Belgium

Phone ++32-10-472-775

Fax ++32-10-472-774

E-Mail

Prof. Canet, Daniel
Université de Nancy I
Lab. Méthod. RMN
BP 239

F-54506 Vandoeuvre-Nancy

France

Phone ++33-8391-2049

Fax ++33-83 91 2367

E-Mail

Mr. Chauvaux, Benoit
University of Louvain
Unite CPMC
Bat. Lavoisier, Pl. L. Pasteur 1

B-1348 Louvain-la-Neuve

Belgium

Phone ++32-10-472 775

Fax ++32-10-472 774

E-Mail

Dr. Coy, Andrew
Massey University
Dept. of Physics & Biophysics

Palmerston North

New Zealand

Phone ++64-6-3505 333

Fax ++64-6-3540 207

E-Mail a.coy@massey.ac.nz

Dr. de Bruyn, Andre
Universiteit Gent
Dept. of Organic Chemistry
Krijgslaan, 281 S4

B-9000 Gent

Belgium

Phone ++32-91-64 44 75

Fax ++32-91-64 49 98

E-Mail

Dr. Denner, Paul
Hochschule Erfurt/Mühlhausen
Fachbereich 04-Physik
Nordhäuser Str. 63

D-99006 Erfurt

Germany

Phone ++49-361-536 323

Fax

E-Mail

Mr. Donker, H. C. W.
Agricultural University
Dept. of Molecular Physics
Dreyenlaan 3

NL-6703 Wageningen

Netherlands

Phone ++31-83-7082 016

Fax ++31-83-7082 725

E-Mail

Prof. Eads, Thomas M.
Purdue University
Dept. of Food Sci.
Smith Hall
West Lafayette, IN 47907-1
USA
Phone ++1-317-494-1749
Fax ++1-317-494-7953
E-Mail eadst@mace.cc.purdue.edu

Dr. Edzes, Hommo T.
Wageningen Agricultural Univ.
Dept. of Molecular Physics
Dreyenlaan 3
NL-6703 Wageningen
Netherlands
Phone ++31-83-7084 326
Fax ++31-83-7082 725
E-Mail hommo@mac.mf.wau.nl

Dr. Feio, Gabriel
ICTPOL/INIC

Av. Prof. Gama Pinto 2
P-1699 Lisboa Codex
Portugal
Phone ++35-1-7950-790
Fax ++35-1-7965-622
E-Mail

Mrs. Forde, Lucy
Massey University
Dept. of Physics & Biophysics

Palmerston North
New Zealand
Phone ++64-6-3569 099
Fax ++64-6-3540 207
E-Mail

Dr. Frolov, Vacheslav
University of St. Petersburg
Inst. of Physics
Uljanovskaja 1/1
St. Petersburg 198 904
Russia
Phone
Fax ++7-812-428-7240
E-Mail

Mr. Gellke, Thomas
Universität Dortmund
Inst. für Physik. Chemie
Otto-Hahn-Str. 6
D-44221 Dortmund
Germany
Phone ++49-231-755 3932
Fax ++49-231-755 3771
E-Mail

Prof. Eaton, Gareth R.
University of Denver
Dept. of Chemistry
Denver, CO 80208
USA
Phone ++1-303-871 2980
Fax ++1-303-871 2254
E-Mail geaton@circe.cair.du.edu

Dr. Elgert, K.-F.
Institut für Textilchemie
DITF
Körschtalstr. 26
D-73770 Denkendorf
Germany
Phone ++49-711-3408 134
Fax ++49-711-3408 185
E-Mail

Dr. Fichtner, Klaus-Peter
DKFZ
Zentrale Spektroskopie
Im Neuenheimer Feld
D-69120 Heidelberg
Germany
Phone ++49-6221-42 4514
Fax ++49-6221-49461
E-Mail

Dr. Foucat, L.
INRA
STIM/SRV-INRA-Theix

F-63122 Cevrat
France
Phone ++33-73-624 175
Fax ++33-73-624 237
E-Mail

Mr. Fuelber, Carsten
Max-Planck-Institut für Polymerforschung
Postfach 3148
D-55021 Mainz
Germany
Phone ++49-6131-379 240
Fax ++49-6131-379 100
E-Mail

Prof. Gelan, Jan
Limburgs Universitair Centrum
Instituut voor Materiaal Onderzoek
Univ. Campus, Gebouw D
B-3590 Diepenbeek
Belgium
Phone ++32-1-122 99 61
Fax ++32-1-122 32 84
E-Mail

Prof. Eaton, Sandra
University of Denver
Dept. of Chemistry
Denver, CO 80208
USA
Phone ++1-303-871 3102
Fax ++1-303-871 2254
E-Mail seaton@circe.cair.du.edu

Mrs. Ercken, Monique
Limburgs Universitair Centrum
Department SBG
Universitaire Campus
B-3590 Diepenbeek
Belgium
Phone ++32-11-268 303
Fax ++32-11-268 301
E-Mail

Mr. Fischer, Alan
University of Cambridge
Herchel Smith Laboratory
University Forvie Site
GB-Cambridge, CB2 2PZ
England
Phone ++44-223-336 758
Fax ++44-223-336 748
E-Mail

Dr. Fricke, Stanley T.
University di Pisa
Istituto di Fisiologia Clinica del CNR
Via Savi 8
I-56100 Pisa
Italy
Phone ++39-50-583 111
Fax ++39-50-553 461
E-Mail

Prof. Fukushima, Eitichi
Lovelace Medical Foundation
2425 Ridgecrest Dr., SE
Albuquerque, NM 87108
USA
Phone ++1-505-262-7155
Fax ++1-505-262-7043
E-Mail

Dr. Gibbs, Stephen
University of Cambridge
Herchel Smith Laboratory
University Forvie Drive
GB-Cambridge, CB2 2PZ
England
Phone ++44-223-336 758
Fax ++44-223-336 748
E-Mail

Mr. Gries, Wolfgang
Fraunhofer Institut für Biomed. Technik
Arbeitsgruppe Magnetische Resonanz
Ensheimer Str. 48
D-66386 St. Ingbert
Germany
Phone
Fax
E-Mail

Dr. Gründer, Wilfried
Univ. Leipzig
Inst. f. Biophysik
Liebigstr. 27
D-04103 Leipzig
Germany
Phone ++49-341-7167 311
Fax ++49-341-7167 574
E-Mail

Dr. Hafner, Siegfried
Fraunhofer Institut für Biomed. Technik
Arbeitsgr. Magnetische Resonanz
Ensheimer Str. 48
D-66386 St. Ingbert
Germany
Phone ++49-6894-980 256
Fax ++49-6894-980 400
E-Mail

Mrs. Hauck, Daniela
RWTH Aachen
Inst. für Makromolekulare Chemie
Worringer Weg 1
D-52056 Aachen
Germany
Phone ++49-241-806 425
Fax ++49-241-806 980
E-Mail

Dr. Hirva, Pipsa
University of Joensuu
Dept. of Chemistry
P. O. Box 111
SF-80101 Joensuu
Finland
Phone ++358-73-151 33 33
Fax ++358-73-151 33 90
E-Mail hirva@joyl.joensuu.fi

Dr. Humbert, F.
Universite Nancy I
Lab. Method. RMN
B. P. 239
F-54506 Vandoeuvre-les-Nancy
France
Phone ++33-83-91 20 18
Fax ++33-83-91 23 67
E-Mail fh@meth-rmn.u-nancy.fr

Dr. Grinberg, Farida

Thüringenweg 22
D-89075 Ulm
Germany
Phone
Fax
E-Mail

Prof. Grutzner, John B.
Purdue University
Dept. of Chemistry
Brown Bldg 1393
West Lafayette, IN 47907
USA
Phone ++1-317-494 5247
Fax ++1-317-494 0239
E-Mail jja@mace.cc.purdue.edu

Prof. Hall, Laurie D.
Univ. of Cambridge
Herchel Smith Lab. for Med. Chem.
Robinson Way
GB-Cambridge, CB2 2PZ
United Kingdom
Phone ++44-223-336805
Fax ++44-223-336 748
E-Mail

Prof. Hennel, J. W.
Jagellonian University
Instytut Fizyki Jadrowej
Ul. Radzikowskiego 152
PL-31-432 Krakow
Poland
Phone ++48-12-370 222
Fax ++48-12-375 441
E-Mail

Dr. Hockings, Paul
SmithKline Beecham Pharmaceuticals

The Frythe, Welwyn
GB-Herts AL6 9AR
England
Phone ++44-438-782 744
Fax ++44-438-782 772
E-Mail hockingspd%frgen.dnet@smithkline.co

Dr. Hunter, Geoffrey
University of Dundee
Dept. of Chemistry

GB-Dundee DD1 4HN
Scotland
Phone ++44-352-307 305
Fax ++44-352-29190
E-Mail cy11@uk.ac.dundee.primea

Dr. Groß, Dieter
Bruker Analytische Meßtechnik

Silberstreifen
D-76287 Rheinstetten
Germany
Phone ++49-721-5161-167
Fax ++49-721-5161 297
E-Mail

Prof. Haase, Axel
Univ. Würzburg
Physikal. Institut
Am Hubland
D-97074 Würzburg
Germany
Phone ++49-931-888 5868
Fax ++49-931-706 297
E-Mail

Dr. Halse, Morley R.
University of Kent
Physics Laboratory
Giles Lane
GB-Canterbury, Kent CT2 7NR
England
Phone ++44-227-764 000/3277
Fax ++44-227-475 423
E-Mail mrh@ukc.ac.uk

Dr. Hermann, Gerard
SMIS France

C.A.I.R.E., 84 Route de Strasbourg
F-67500 Haguenau
France
Phone ++33-88-931 503
Fax ++33-88-633 901
E-Mail

Dr. Hull, William E.
DKFZ
Zentrale Spektroskopie
Neuenheimer Feld 280
D-69120 Heidelberg
Germany
Phone ++49-6221-424 515
Fax ++49-6221-401 271
E-Mail bio281@dhddkfz1

Dr. Ishida, Nobuaki
National Food Research Institute

Kannon-dai 2-1-2
Tsukuba, Ibaraki 305
Japan
Phone ++81-298-38 8035
Fax ++81-298-38 7996
E-Mail

Mr. Jacques, Alain
University of Louvain
Dept. of Chem.
Place Louis Pasteur 1
B-1348 Louvain-la-Neuve
Belgium
Phone ++32-10-47 27 73
Fax ++32-10-47 27 74
E-Mail

Dr. Jonsen, Paul
Chemagnetics

7, Claro Court Business Center, Claro Road
GB-Harrogate, HG1 4BA
England
Phone ++44-423-531 645
Fax ++44-423-531 647
E-Mail

Dr. Kibinski, Jacek
Jagellonian University
Institute of nuclear Physics
Radzikowskiego 152
PL-31-342 Krakow
Poland
Phone ++48-12-370 222/254
Fax ++48-12-375 441
E-Mail

Mr. Klinkenberg, M. P. C. J.
RWTH Aachen
Inst. für Makromolekulare Chemie
Worringer Weg 1
D-52056 Aachen
Germany
Phone ++49-241-806 430
Fax ++49-241-806 980
E-Mail

Prof. Krebs, Joachim
Eidg. Techn. Hochschule
Dept. of Biochemistry
Universitätsstr. 16
CH-8092 Zürich
Switzerland
Phone ++41-1-256 3005
Fax ++41-1-2526 323
E-Mail

Prof. Lauterbur, Paul C.
University of Illinois

1307 West Park Street
Urbana, Illinois 61801
USA
Phone ++1-217-244 0600
Fax ++1-217-244 1330
E-Mail bmrl@bmrl.med.uiuc.edu

Dr. Jasinski, A.
Jagellonian University
Institute of Nuclear Physics
Radzikowskiego 152
PL-31-342 Krakow
Polen
Phone ++48-12-370 222/254
Fax ++48-12-375 441
E-Mail jasinski@vsb02.ifj.edu.pl

Mr. Kalusche, B.
Universität Würzburg
Physikalisches Institut
Am Hubland
D-97074 Würzburg
Germany
Phone ++49-931-888 5868
Fax ++49-931-706 297
E-Mail

Mr. Klefer, A.
Universität Würzburg
Physikalisches Institut
Am Hubland
D-97074 Würzburg
Germany
Phone ++49-931-888 5868
Fax ++49-931-706 297
E-Mail

Dr. Köckenberger, Walter
Universität Bayreuth
Botanisches Inst.
Universitätsstr. 30
D-95440 Bayreuth
Germany
Phone ++49-921-552-638
Fax ++49-921-552-642
E-Mail WALTER.KOECKENBERGER@uni-Bayr.de

Prof. Kuhn, Reinhard
Fachhochschule Reutlingen
Inst. für Biochemie
Alteburgstr. 150
D-72762 Reutlingen
Germany
Phone ++49-7121-271 477
Fax ++49-7121-271 224
E-Mail

Mr. Lehmann, Volker
Bruker Analytische Meßtechnik

Silberstreifen
D-76287 Rheinstetten
Germany
Phone ++49-721-5161 225
Fax ++49-721-5161 297
E-Mail

Prof. Johnson, G. Allan
Duke University Medical Center
Dept. of Radiology/Box 3302
Box 3302
Durham, N. C. 27710
USA
Phone ++1-919-660 2711
Fax ++1-919-681 8648
E-Mail

Dr. Kendall, E. J.
National Research Council of Canada
Plant Biotechnology Institute
110 Gymnasium Road
Saskatoon S7N 0W9
Canada
Phone ++1-306-975-6335
Fax ++1-306-975 4839
E-Mail ekendall@pbi.nrc.ca

Prof. Kimmich, Rainer
Universität Ulm
Sektion Kernresonanz
Albert Einstein Allee 11
D-89069 Ulm
Germany
Phone ++49-731-502 3140
Fax ++49-731-502 2038
E-Mail

Prof. Komoroski, Richard A.
University of Ark. for Med. Sci.

4301 West Markham Street, Slot 582
Little Rock, AR 72205
USA
Phone ++1-501-686 6105
Fax ++1-501-686 5406
E-Mail

Dr. Kuhn, Winfried
Fraunhofer Institut für
Biomedizinische Technik
Ensheimer Str. 48
D-66386 St. Ingbert
Germany
Phone ++49-6894-980 250
Fax ++49-6894-980 400
E-Mail wpk@mt.izfp.fhg.de

Dr. Lloyd, Charles M.
Univ. of Dundee
Dent. School, Dept. of Dent. Sci.
Park Place
GB-Dundee DD1 4HN
Scotland
Phone ++44-382-26041
Fax ++44-382-201-604
E-Mail

Dr. Lock, Herman

Landsteiner Bocht 23

NL-2614 Delft

Netherlands

Phone ++31-15-120 126

Fax ++31-15-120 126

E-Mail

Prof. Mansfield, Peter

University of Nottingham

Dept. of Physics

University Park

GB-Nottingham NG7 2RD

Scotland

Phone ++44-602-514 740

Fax ++44-602-515 166

E-Mail

Prof. Mateescu, Gheorghe D.

Case Western Reserve University

Dept. of Chemistry

10900 Euclid Avenue

Cleveland, OH 44106

USA

Phone ++1-216-368 2589

Fax ++1-216-368 3006

E-Mail

Mr. Mehr, Knut

Fraunhofer Institut für

Biomedizinische Technik

Enshelmer Str. 48

D-66386 St. Ingbert

Germany

Phone ++49-6894-980 254

Fax ++49-6894-980 400

E-Mail

Dr. Middleton, David

SmithKline Beecham

Pharmaceuticals

The Frythe

Welwyn, Herts, AL6 9AR

England

Phone ++44-438-782 345

Fax ++44-438-782 772

E-Mail middletonda%frgen.dvet@smithkline.c

Dr. Moreaux, C.

Univ. Louvain

Place L. Pasteur 1, 3A

B-1348 Louvain la Neuve

Belgium

Phone ++32-10-478 638

Fax ++32-10-472 774

E-Mail

Dr. Lohman, Joost A. B.

Bruker Spectrospin Ltd.

Banner Lane

GB-Coventry, CV4 9GH

England

Phone ++44-203-855 200

Fax ++44-203-46 53 17

E-Mail

Mr. Manz, Bertram

Massey University

Dept. of Physics & Biophysics

Palmerston North

New Zealand

Phone ++64-6-3505 333

Fax ++64-6-3540 207

E-Mail b.manz@massey.ac.nz

Dr. McCain, Douglas

Wageningen Agricultural Univ.

Dept. of Molecular Physics

Dreyenlaan 3

NL-6703 Wageningen

Netherlands

Phone ++31-83-7082 044

Fax ++31-83-7082 725

E-Mail

Dr. Meszaros, Sandor

Hungarian Academy of Science

Inst. of Nuclear Science

Koszméte U. 19

H-4030 Debrecen

Hungaria

Phone ++36-52-17 266

Fax

E-Mail

Mrs. Miller, Jeanette

Multisana Med.-Technik GmbH

Barmherzigengasse 16/39

A-1030 Wien

Austria

Phone ++43-222-4087 159

Fax

E-Mail

Dr. Morita, Yasushi

Fraunhofer Institute for Biomedical Eng.

Magnetic Resonance Division

Enshelmer Str. 48

D-66386 St. Ingbert

Germany

Phone ++49-6894-980 240

Fax ++49-6894-980 400

E-Mail

Dr. Lugerì, Nicola

Univ. La Sapienza

Dept. of Physics

P. Aldo Moro 2

I-00185 Roma

Italy

Phone ++39-6-499-3484

Fax ++39-6-446-3158

E-Mail

Prof. Mason, Ralph P.

University of Texas

Southwestern Med. Center, Radiology

5323 Harris Hines Blvd.

Dallas, TX 75235-9058

USA

Phone ++1-214-648 8926

Fax ++1-214-648 2991

E-Mail

Prof. McFarland, Ph.D., Eric

Univ. of California

Dept. of Chem. & Nucl. Eng.

Santa Barbara, CA 93106-5080

USA

Phone ++1-805-893 4343

Fax ++1-805-893 4731

E-Mail mcfar@enrhub.ucsb.edu

Mr. Metzler, Alexander

Univ. Würzburg

Physikal. Inst.

Am Hubland

D-97074 Würzburg

Germany

Phone ++49-931-888-5860

Fax ++49-931-706297

E-Mail

Mr. Mischler, E.

Universite de Nancy I

Lab. Method. RMN

B. P. 239

F-54506 Vandoeuvre-Nancy Ce

France

Phone ++33-83-91 20 18

Fax ++33-83-91 23 67

E-Mail em@meth-rmn.u-nancy.fr

Dr. Müller, Hans-Peter

Universität Ulm

Sektion Kernresonanzspektroskopie

A. Einstein-Allee 11

D-89069 Ulm

Germany

Phone ++49-731-502 3130

Fax ++49-731-502 3150

E-Mail

Dr. Neeman , Michal
Weizmann Institute of Science
Dept. of Hormone Research

Rehovot 76100

Israel
Phone ++972-8-34 2487
Fax ++972-8-34 4116
E-Mail LHNEEMAN@WEIZMANN.weizmann.ac.il

Dr. Neue, Günther
Univ. Dortmund
Inst. für Physikal. Chemie
Otto-Hahn-Str. 6
D-44221 Dortmund

Germany
Phone ++49-231-755-3932
Fax ++49-231-755-3771
E-Mail uch018@unidozr.hrz.uni-dortmund.de

Dr. Nunes , Teresa
ICTPOL/LNETI

Av. Prof. Gama Pinto 2
P-1699 Lisboa Codex

Portugal
Phone ++351-1-797 3325
Fax ++351-1-796 5622
E-Mail

Mrs. Päuser , Sabine
Humboldt-Universität
Inst. für Chemie
Hessische Str. 1-2
D-10115 Berlin

Germany
Phone ++49-30-28468 283
Fax ++49-30-28468343
E-Mail

Dr. Platsch, Herbert
BASF AG
ZHV/B - B 9

D-67056 Ludwigshafen

Germany
Phone ++49-621-60 47310
Fax ++49-621-60 20914
E-Mail

Prof. Randall, Edward W.
Queen Mary and Westfield College
Dept. of Chemistry
Mile End Road
GB-London E1 4NS

England
Phone ++44-71 975 5555
Fax ++44-81 981 8745
E-Mail

Dr. Nesbitt , Geoffrey J.
Shell Research

Badhuisweg 3
NL-1003 AA Amsterdam

Netherlands
Phone ++31-20-630 3522
Fax ++31-20-630 8025
E-Mail nesbitt1@ksla.nl

Mr. Newling, Benedict
University of Cambridge
Herchel Smith Laboratory
University Forvie Site
GB-Cambridge CB2 2PZ

England
Phone ++44-223-336 758
Fax ++44-223-336 748
E-Mail

Dr. Paff, Jürgen
RWTH Aachen
Inst. für Makromolekulare Chemie
Worringer Weg 1
D-52056 Aachen

Germany
Phone ++49-241-806 425
Fax ++49-241-806 980
E-Mail paff@rwth-aachen.de

Dr. Pavesi, Laura
University of Pavia
Dept. of Physics "A. Volta"
Via Bassi 6
I-27100 Pavia

Italy
Phone ++39-382-392 466
Fax ++39-382-392 563
E-Mail

Prof. Pope , James M.
University of N.S.W.
School of Physics
P.O. Box 1
Kensington, N.S.W. 2033

Australia
Phone ++61-2-697 4557
Fax ++61-2-663 3420
E-Mail jmp@newt.phys.unsw.edu.au

Prof. Ritchey, William M.
Case Western Reserve University
Dept. of Chemistry
10900 Euclid Avenue
Cleveland, OH 44106-2

USA
Phone ++1-216-368-3668
Fax ++1-216-368-3006
E-Mail

Mr. Nestle, Nikolaus
Universität Ulm

Holdergasse 10
D-89271 Holzheim

Germany
Phone
Fax
E-Mail nestle@rzmain.rz.uni-ulm.de

Mr. Nilgens , Helge
MPI für Polymerforschung

Postfach 3148
D-55021 Mainz

Germany
Phone
Fax ++49-6131-379 100
E-Mail

Dr. Pakkanen , Tuula
University of Joensuu
Dept. of Chemistry
P. O. BOX 111
SF-80101 Joensuu 10

Finland
Phone ++358-73-151 33 40
Fax ++358-73-151 33 44
E-Mail

Dr. Peck, Timothy L.
University of Illinois
Dept. of Electrical and Computer Eng.
1406 West Green Street
Urbana, IL 61801

USA
Phone ++1-217-333 7480
Fax
E-Mail tpeck@

Mr. Raible, Christoph
Fraunhofer Institut
Magnetische Resonanz
Ensheimer Str. 48
D-66386 St. Ingbert

Germany
Phone
Fax
E-Mail

Dr. Rofe, Craig
Massey University
Dept. of Physics & Biophysics

Palmerston North

New Zealand
Phone ++64-6-3505 333
Fax ++64-6-3540 207
E-Mail c.rofe@massey.ac.nz

Dr. Rugar, Dan
Almaden Research Center IBM Research Division
Dept. K65/802
650 Harry Road
San Jose, CA 95120-6099
USA
Phone ++1-408-927-2027
Fax ++1-408-927-3025
E-Mail rugar@almaden.ibm.com

Dr. Sarkar, Susanta K.
Smithkline Beecham
L-940
109 Swedeland Road
King of Prussia, PA 19406
USA
Phone ++1-215-270 6652
Fax ++1-215-270 6608
E-Mail sarkar@smithkline.com

Dr. Schelner, Stefan
Multisana Medizintechnik GmbH
Gustav-Tschermak-G. 3A
A-1190 Wien
Austria
Phone ++43-222-4087 159
Fax ++43-222-3102 197
E-Mail

Dr. Scrimgeour, Sheelagh N.
Univ. of Dundee
Chemistry Dept.
Nethergate
GB-Dundee DD1 4HN
Scotland
Phone ++44-382-23181
Fax ++44-382-29190
E-Mail cy17@uk.ac.dundee.primea

Dr. Sillerud, Laurel O.
Los Alamos National Laboratory
Life Science Division
Los Alamos, NM 87545
USA
Phone ++1-505-667-1622
Fax ++1-505-665-3024
E-Mail

Mr. Skorka, Tomasz
Jagellonian University
Institute of Nuclear Physics
Radzikowskiego 152
PL-31-342 Krakow
Poland
Phone ++48-12-370 222/257
Fax ++48-12-375 441
E-Mail skorka@vsb02.ijf.edu.pl

Dr. Rydzy, M.
Jagellonian University
Institute of Nuclear Physics
Radzikowskiego 152
PL-31-342 Krakow
Poland
Phone
Fax
E-Mail

Dr. Schaumburg, Kjeld
Univ. of Copenhagen
Dept. of Chemical Physics
H.C. Ørsted Inst.-Universitetsparke
DK-2100 Copenhagen Ø
Denmark
Phone ++45-3532 0300
Fax ++45-3135 0609
E-Mail

Mr. Scheler, Ulrich
MPI für Polymerforschung
Postfach 3148
D-55021 Mainz
Germany
Phone ++49-6131-379 219
Fax ++49-6131-379 100
E-Mail

Dr. Sersa, Igor
Ljubljana University
Jozef Stefan Institute
Jamova 39
61111 Ljubljana
Slovenia
Phone ++38-61-159 199
Fax ++38-61-161 029
E-Mail igor.sersa@ijs.si

Dr. Simon, Gerald
Martin-Luther-Universität Halle
Physik. Inst.
Friedemann-Bach-Platz 6
D-06108 Halle
Germany
Phone ++49-3461-462 757
Fax ++49-3461-462 743
E-Mail

Prof. Spiess, Hans-Wolfgang
MPI - Polymerforschung
Postfach 3148
D-55021 Mainz
Germany
Phone ++49-6131-379 120
Fax ++49-6131-379 100
E-Mail

Mr. Sarafis, Vassilios
University of Western Sydney - Hawkesbury
School of Science
Bourke Street
Richmond, NSW 2753
Australia
Phone ++61-45-70 1436
Fax ++61-45-70 1621
E-Mail

Dr. Schauß, Gunther
Univ.-Klinik Mainz
Klinik für Radiologie
Langenbeckstr. 1
D-55131 Mainz
Germany
Phone ++49-6131-17 2295
Fax ++49-6131-17 6633
E-Mail

Prof. Schneider, Horst
Martin-Luther Universität Halle
Fachbereich Physik
Friedemann-Bach-Platz 6
D-06108 Halle
Germany
Phone ++49-345-37761
Fax
E-Mail schneider@physik.uni-halle.dbp.de

Herrn Sichelschmidt, Jörg
Techn. Hochschule
Inst. für Exp. Festkörperphysik
Hochschulstr. 6
D-64289 Darmstadt
Germany
Phone ++49-6151-165 130
Fax ++49-6151-162 833
E-Mail

Dr. Skibbe, Ute
Massey University
Dept. of Physics & Biophysics
Private Bag
Palmerston North, 5301
New Zealand
Phone ++64-6-3540 062
Fax ++64-6-3540 207
E-Mail uskibbe@massey.ac.nz

Mrs. Steinfeld, Yael
The Weizmann Institute of Science
Dept. of Hormone Research
Rehovot 76100
Israel
Phone ++972-8-342 487 / 3736
Fax ++972-8-344 116
E-Mail yael@imago.weizmann.bitnet

Prof. Strange, John H.
University of Kent at Canterbury
Physics Laboratory

GB-Canterbury, Kent CT2 7NR
England
Phone ++44-227 764 000X3321
Fax ++44-227-475 423
E-Mail jhs2@ukc.ac.uk

Mrs. Szayna, Matgorzata
Jagellonian University of Krakow
Inst. for Mining & Metallurgy

PL-31-342 Krakow
Poland
Phone
Fax
E-Mail

Mrs. Tempel, Catherine
The Weizmann Institute of Science
Dept. of Hormone Research

Rehovot 76100
Israel
Phone ++972-8-34 2487 / 3736
Fax ++972-8-344 116
E-Mail cathe@imago.weizmann.bitnet

Dr. Tingle, Jerry
University of Western Sydney-Hawkesbury

Bourke Street
Richmond, NSW 2753
Australia
Phone ++61-45-701 625
Fax ++61-45-701 621
E-Mail

Prof. Ugurbil, Kamil
University of Minnesota
Center for Magn. Res. Research
385 East River Road
Minneapolis, MN 55455
USA
Phone ++1-612-626-7007
Fax ++1-612-626-7005
E-Mail

Mr. van Dusschoten, D.
Agricultural University of Wageningen
Dept. of Molecular Physics
Dreyenlaan 3
NL-6703 Wageningen
Netherlands
Phone ++31-83-7082 026
Fax ++31-83-7082 725
E-Mail

Prof. Subramanian, Sankaran
National Institute of Health
Radiation Biology Section
Build. 10, Room B3/B69
Bethesda, MD, 20892
USA
Phone ++1-301-496 7511
Fax ++1-301-480 5439
E-Mail subu@helix.nih.gov

Dr. Szeles, J. Constantin
2. Chirurgische Univ.-Klinik Wien
E 500
Spitalgasse 23
A-1090 Wien
Austria
Phone ++43-222-319-7852
Fax ++43-222-310-2197
E-Mail

Mr. Tessier, Jean
University of Cambridge
Herchel Smith Laboratory
University Forvie Site
GB-Cambridge CB2 2PZ
England
Phone ++44-223-336 758
Fax ++44-223-336 748
E-Mail

Dr. Tomanek, Boguslaw
Jagellonian University
Institute of Nuclear Physics
Radzinowskiego 152
PL-31-342 Krakow
Poland
Phone ++48-12-370 222/257
Fax ++48-12-375 441
E-Mail tomanek@vsb02.ifj.edu.pl

Dr. van As, Hendrik
Agricultural University Wageningen
Dept. of Molecular Physics
Dreijenlaan 3
NL-6703 HA Wageningen
Netherlands
Phone ++31-8370 82034
Fax ++31-8370 82725
E-Mail henk.vanas@water.mf.wau.nl

Mrs. Vandersteen, Marie-Anne
Limburgs Universitaire Centrum
Department MBW
Universitaire Campus
B-3590 Diepenbeek
Belgium
Phone ++32-11-26 85 12
Fax ++32-11-26 81 99
E-Mail

Dr. Sulek, Zenon
Jagellonian University
Inst. of Nucl. Physics
ul. Radzikowskiego 152
PL-31-342 Krakow
Poland
Phone ++48-12-370-222/261
Fax ++48-12-375 441
E-Mail

Prof. Tegenfeldt, Jörgen
Uppsala University
Inst. of Chemistry
Box 531
S-75121 Uppsala
Sweden
Phone ++46-18-183 774
Fax ++46-18-508 542
E-Mail Tegen@kemi.uu.se

Dr. Timonen, Juha
University of Joensuu
Dept. of Chemistry
P. O. Box 111
SF-80101 Joensuu
Finland
Phone ++358-73-151 33 74
Fax ++358-73-151 33 90
E-Mail jtimonen@joyl.joensuu.fi

Dr. Tyler, Jenny A.
Strangeways Research Laboratories
Herchel Smith Laboratory
Worts Causeway
GB-Cambridge CB1 4RN
England
Phone ++44-223-243 231
Fax ++44-223-44609
E-Mail

Dr. van Cauteren, Marc
SMIS LTD
Surrey Research Park
10 Alan Turing Road
Guildford, Surrey GU2 5YF
England
Phone ++44-483-506 611
Fax ++44-483-63114
E-Mail

Mrs. Vanormelingen, Linda
Limburgs Universitaire Centrum
Department MBW
Universitaire Campus
B-3590 Diepenbeek
Belgium
Phone ++32-11-26 85 11
Fax ++32-11-26 81 99
E-Mail

Dr. Voelkel, Rüdiger
BASF AG
Kunststoff-Laboratorium
ZKM - Bau G 201
D-67056 Ludwigshafen
Germany
Phone
Fax ++49-621-609 2281
E-Mail

Dr. Wells, T. K.
SMIS LTD
Surrey Research Park
10 Alan Turing Road
Guildford, Surrey, GU2 5YF
England
Phone ++44-483-506 611
Fax ++44-483-63114
E-Mail

Mrs. Williamowski, Silke
Universität Dortmund
Inst. für Physik. Chemie
Otto-Hahn-Str. 6
D-44221 Dortmund
Germany
Phone ++49-231-755 3932
Fax ++49-231-755 3771
E-Mail

Mr. Wurz, Gerald
Universität Wien
Inst. für Organische Chemie
Währingerstr. 38
A-1090 Wien
Österreich
Phone ++43-1-31367-2253
Fax ++43-1-319 6312
E-Mail a8401dad@awiuni11.edvz.univie.ac.at

Mr. Weigand, Frank
MPI für Polymerforschung

Postfach 3148
D-55021 Mainz
Deutschland
Phone
Fax ++49-6131-379 100
E-Mail

Dr. Welti, Dieter
Nestle AG
Nestec SA Research Centre
Vers-chez-les-Blanc/Postfach 44
CH-1000 Lausanne 26
Switzerland
Phone ++41-21-785 89 08
Fax ++41-21-785 85 54
E-Mail

Dr. Williamson, Brian
Scottish Crop Research Institute
Mycol. & Bact. Dep.
Invergowrie
GB-Dundee DD2 5DA
Scotland
Phone ++44 382 562 731
Fax ++44 382 562 426
E-Mail

Dr. Zick, Klaus
Bruker Analytische Meßtechnik GmbH

Silberstreifen
D-76297 Rheinstetten-4
Germany
Phone ++49-721-5161 0
Fax ++49-721-5171 01
E-Mail

Dr. Weis, Jan
Universität Ulm
Skktion Kernresonanzspektroskopie
A. Einstein-Allee 11
D-89069 Ulm
Germany
Phone ++49-731-502 3133
Fax ++49-731-502 3150
E-Mail

Mr. Widmaler, Stefan
Universität Tübingen
Physikalisches Institut
Auf der Morgenstelle 14
D-72076 Tübingen
Germany
Phone ++49-7071-296 290
Fax ++49-7071-296 296
E-Mail

Dr. Woelk, Klaus
Argonne National Laboratory
CMT B-156
9700 South Cass Ave.
Argonne, IL 60439
USA
Phone ++1-708-252 6016
Fax ++1-708-252 9373
E-Mail woelk@cmt.anl.gov